2038-5625

Italian Journal of Agrometeorology

Rivista Italiana di Agrometeorologia

n. 2 – 2021

Poste Italiane spa - Tassa pagata - Piego di libro
Aut. n. 072/DCB/FI1/VF del 31.03.2005

FIRENZE UNIVERSITY PRESS

Cover photo by Graziano Lampa

Italian Journal of Agrometeorology

n. 2 - 2021

Firenze University Press

The ***Italian Journal of Agrometeorology*** (***IJAm - Rivista Italiana di Agrometeorologia***) is the official periodical of the Italian Association of Agrometeorology (AIAM) and aims to publish original scientific contributions in English on agrometerology, as a science that studies the interactions of hydrological and meteorological factors with the agricultural and forest ecosystems, and with agriculture in its broadest sense (including livestock and fisheries).

SUBSCRIPTION INFORMATION
IJAm articles are freely available online, but print editions are available to paying subscribers. Subscription rates are in Eur and are applicable worldwide.
Annual Subscription: € 50,00 Single Issue: € 25,00

CONTACT INFORMATION
Please contact ordini@fupress.com, if you have any questions about your subscription or if you would like to place an order for the print edition. Information on payment methods will be provided after your initial correspondence.

Published by
Firenze University Press – University of Florence, Italy
Via Cittadella, 7 - 50144 Florence - Italy
http://www.fupress.com/ijam

Italian Journal of Agrometeorology
Rivista Italiana di Agrometeorologia

Firenze University Press
www.fupress.com/ijam

OPEN ACCESS

Citation: A. Eruola (2021) Response of yam varieties to soil moisture regime in Southwestern Nigeria. *Italian Journal of Agrometeorology* (2): 3-14. doi: 10.36253/ijam-1324

Received: May 31, 2021

Accepted: July 18, 2021

Published: December 27, 2021

Data Availability Statement: All relevant data are within the paper and its Supporting Information files.

Competing Interests: The Author(s) declare(s) no conflict of interest.

Response of yam varieties to soil moisture regime in Southwestern Nigeria

Abayomi Eruola

University of Agriculture, Abeokuta,Nigeria
E-mail: layosky@yahoo.com

Abstract. A field experiment was conducted on varietal response of white yam to moisture regime in Abeokuta. The experiment comprised three varieties of yam (Efuru, Ise-osi and Oniyere), three mulching options (grass, polythene and unmulched), and two planting dates (early and late). Treatments were replicated three times using RCBD lay-out. Model for selecting planting date involved relating potential evapotranspiration (PE) to precipitation (P) in the form of 0.1PE<P < 0.5PE, partitioned for attaining optimal planting date into early $\{T_1 = \Sigma(\text{P-0.1PE}) \leq 0\}$ and late $\{T_2 = \Sigma(\text{P-0.5PE}) \leq 0\}$, respectively. For humid period defined by P> PE, the physiological parameters and moisture agro-climatic indices measured during phenological stages of yam grown were analyzed with respect to treatments. Result showed that T_1 defined as Σ(P-0.1PE) ≤ 10 mm appeared as the best model that significantly (P < 0.05) influenced emergence rate, phenological growth and tuber yield. All yam varieties evaluated were suitable for planting with respect to yield. Efuru and Ise-osi synchronized perfectly with Actual Water Availability and produced good vegetative growth with LAI of 1.08 and 0.91 leading to higher tuber yield of 12 and 11.64 tonnes ha^{-1}, respectively. Grass mulch had tuber yield, 4-6 tonnes ha^{-1}greater than the polythene and unmulched plots in all varieties. Mulching significantly (P< 0.05) increased tuber yield, 6-8 tonnes ha^{-1}than the unmulched. Conclusively, early planting with grass mulch increased tuber yield.

Keywords: crop, evapotranspiration, Penman formula, yield, Actual Water Availability.

INTRODUCTION

Water supply in terms of annual rainfall total is not a constraint to crop production in Southwest Nigeria (Ofori, *etal*. 2014). However, the seasonal and spatial variations in rainfall to a great extent have effects on agricultural activities (Um *et al.*, 2017; Gidey *et al.*, 2018), as most farmers find it extremely difficult to accurately determine the reliable beginning of the rain vis-à-vis favorable weather condition to commence their agricultural activities because rainfall plays a crucial role in determining agricultural yields (Audu, 2012; Bhandari, 2013; Shiru *et al.,* 2018). It is therefore necessary to implement methods of soil water conservation in farming operation to improve crop production and reduce food insecurity in Africa and in particular Nigeria (Tiamiyu *et al.*, 2015). The soil water conservation provides the means of minimizing the amount of water lost from the soils through evaporation and transpiration or the combination, the evapotranspiration.Most of soil moisture conservation strategies are relatively low cost and complex in their approach, based on the presence of required materials and technical capacity locally. Many of the methods rely on providing some kind of cover for the soil to minimize evapotranspiration and direct soil exposure to heat and sun. Examples of methods for reducing excess soil moisture loss include spreading manure or compost over the soil, Mulching, conservation tillage, crop rotation, Green manuring, among others. The selection of a specific variety largely depend on the way in which planting date is managed to prevent incidence of failure of agricultural crops, replanting and ultimate low yield that have characterized the agricultural food crops production in Nigeria.

Yam is a tropical crop which has as many as 600 species, of which six are economically important staple species. Out of the six, *Dioscorea rotundata* (white yam) and *Dioscorea alata* (water yam) are the most common species in Nigeria (IITA, 2009; Zaknayiba and Tanko, 2013). Yam is in the class of roots and tubers that is a staple of the Nigerian and West African diet, which provides some 200 calories of energy per capita daily. Bearing in mind that soil moisture is essential for the survival of yam (*Dioscorea rotundata)* setts before the rain is established, it is imperative to determine accurately the reliable onsets and cessation of the rain vis-à-vis planting date of yam. Furthermore, the occurrence of wet- season- dry spells which may last for a few days to more than three weeks particularly during the full vegetative stage when evaporative demand is high is another serious limiting factor to yam production (Mulebeke*et al*., 2010). However, for location with good soil moisture retention, yam may manage to utilize soil moisture reserve contained in the pores of the soil, or upon the very limited reserve contained in its own tissue during dry spells between rains. Yam may also adapt physiologically or behaviorally to prevent temporary depletion of the stored tissue moisture in other to prevent impairment of normal physiological function that may cause irreversible damage and plant death. This is more so that yam is highly susceptible to dry spells that occur during the onset of the rains and particularly before the rain has fully established. Therefore, since yam is planted between the periods extending from around the cessation of the rains in a given year to the time of onset in the succeeding year, it implies therefore that as soon as germination starts, soil moisture become critical. To alleviate the problem of soil moisture, there is need for efficient soil moisture conservation strategy in other to optimize soil physical condition affecting the crop yield (Susha *etal*. 2014). Various techniques used by traditional farmers in modifying the on- farm microclimate and efficiency of such techniques in West Africa have been studied and reported (Kutugi, 2002; Okoh, 2004; Gbadebor, 2006; Maikasuwa and Ala, 2013; and Yanmin Yang *et al*. 2015). As reported by International Institute of Tropical Agriculture (IITA, 1995; IITA, 2013), mulching is very important in yam cultivation. Nahanga and Věra (2015) reported that majority of the traditional yam farmers in West Africa use different mulching materials for yam cultivation. These materials range from dry grass, palm front to wood shaving. Of recent however, the IITA and some less conservative farmers were already using polythene plastic mulch in production of seed yam. However, research into the use of polythene plastic mulch in yam production is not widespread in Nigeria. Hence, for successful cropping, it is pertinent to relate the period of effective water availability to the phonological characteristic of yam variety in other toinvestigating the response of white yam to soil moisture variation. The investigation was based on assessment of planting dates, mulching options and mulching materialson the growth and yield of white yam.

MATERIALS AND METHODS

Description of study area

This study was conducted at the Teaching and Research farm of University of Agriculture along Alabata road, Abeokuta (7°15'N, 3°25'E) in Odeda Local Government Area of Ogun State, South Western Nigeria (Fig. 1) during the 2017 and 2018 cropping seasons. The study area is characterized by a tropical climate with distinct wet and dry seasons with bimodal rainfall pattern and mean annual air temperature of about 30°C. The actual rainfall totals during the 2017 and 2018 cropping season were 1177.2 and 1201.6 mm, respectively. The mean annual air temperature during the experimental years is 30°C. The soil at the experimental site was categorized as a well-drained tropical ferruginous soil. The A horizon of the soil is an Oxic Paleudulf of the Iwo series with 83% sand, 5% silt and 12% clay with a pH 6 considered tolerable for yam cultivation (Olasantan, 2007).

Experimental design and field measurement

A 3 years (from 2014-2016) fallowed piece of land was prepared as experimental site before the study

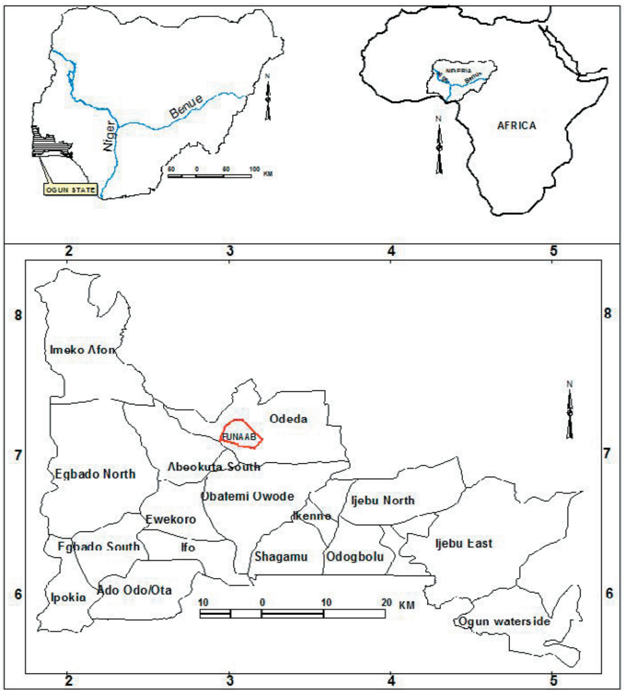

Fig. 1. Location of University of Agriculture, Abeokuta within Odeda Local Government Area in Ogun State, Southwestern Nigeria, Africa.

began. The site was cleared manually using cutlass in November 2016, in preparation for the 2016-2017 cropping following the popular practice by the farmers in the study area. This period marks the preparatory period for the cultivation of early yam planting in the study area. Yam mounds of height 60 cm and spaced 1.5 m x 1.5 m a walk way of 1 m between adjacent rows were made manually using African hoe to improve the soil aeration and hydrothermal conditions for crops emergence, root development, crop growth and yield (Kutugi, 2002). Three most important edible local white yam, *Dioscorea rotundata* cultivars (Efuru, 'A_1; Ise-osi 'A_2; and Oniyere 'A_3) were used. During each of the phenological stages, daily observation of air temperature (°C), wind speed at a height of 2 m (ms^{-1}), rainfall (mm) were made at meteorological enclosure adjacent to the experimental field. Other climatic parameters measured were open water evaporation (E_O) in mm determined according to Penman-Monteithformula using CROPWAT, 2009 model, actual water availability (AWA, mm) and consumptive water used by the crop (ET_{crop} or water requirement 'WR) in mm was computed as follow:

$$ET_{crop} = K_C \times E_O \text{ mm}$$

where K_C = Crop coefficient

K_C otherwise referred to as the relative evaporation is expressed as ET. E_O^{-1}, where ET and E_O were measured parameters. The crop coefficients (Kc) values, represent the crop type and the development of the crop. The Kc values for this study were adopted from FAO (1977) for crops. AWA according FAO (1977) was taken as the difference between actual precipitation and crop water requirement,

$$AWA = P\text{-}ET_{crop}$$

AWA is equivalent to available rainfall (P) plus change in stored water and this in turn correspond to actual evaporation. Therefore, for periods when P is less than potential Evapotranspiration (PE) AWA = ET_{crop} but for periods where P is greater than $ET_{crop,}$ AWA = P, since in this case actual Evapotranspiration (AE) = ET_{crop} while there is virtually no depletion of soil moisture. The quotient of AWA and ET_{crop} or WR enable a determination of the degree of humidity which is tolerable by a cultivated plant during the growing season, and allow sub-division to be applied between arid and humid environments. Deichmann and Eklundh (1991) set an aridity limit at 1.0 and a critical humidity limit at 2.0. Therefore the moisture supply for yam in this study was regarded as supra- optimum for an AWA:WR ratio above 2.0, optimum for a ratio between 1.0 and 2.0 and deficient for a ratio below 1.0. Climatic parameters were not measured directly at the experimental site but were estimated using meteorological tables (Doorenbos and Pruitt, 1984).

Furthermore, the rainfall-potential evapotranspiration (P and PE) model according to the procedure of Cocheme and Franquin, (1967) were followed to determine start and end of planting. The model used in this study was formulated to incorporate farmer's conventional calendar for yam cultivation. Consequently, planting date (T) was selected based on the following general model

$$0.1PE < P < 0.5PE$$

The time of planting is taken as the as period when accumulated difference between rainfall P and one tenth PE is zero ($\Sigma(P-0.1PE) \leq 0$). It follows that the two specific planting dates (T_1 & T_2) in each experimental years were generated from the general model above as follows:

$T_1 = \Sigma(P-0.1PE) \leq 24$ = March 22 which fell in the 9^{th} decade of 2017

$T_2 = \Sigma(P-0.1PE) \leq 259$ = June 5 which fell in the 16^{th} decade of 2017

$T_1 = \sum(P\text{-}0.1PE) \leq 10$ = January 21 which fell in the 3rd decade of 2018
$T_2 = \sum(P\text{-}0.1PE) \leq 182$ = April 6 which fell in the 10th decade of 2018

And the conventional farmer's planting date adopted from Ogun state Agricultural Development Program (OGADEP) records as follows:

$F_1 = \sum(P\text{-}0.1PE) \leq 0$ = January 7 which fell in the 1st decade of 2017 and 2018
$F_2 = \sum(P\text{-}0.1PE) \leq 150$ = April 15 which fell in the 10th decade of 2017 and 2018

The planting dates for the two cropping seasons (2017 and 2018 respectively) are as presented. The yam cultivar were cut into yam setts weighing an average of 550g and planted at a depth of 15cm on mounds. After sprouting, the yams were staked to about 3m high and the vines were trained regularly. No fertilizer and insecticide were applied and all plots were regularly hand weeded. Bush rat was controlled by regular clearing of the surroundings of the project site. The climatic requirements of yam from planting to harvesting were measured according to developmental stages of yam growth cycle form the time scale for which the collected data have been processed.The leaf area was calculated from leaf area of plant multiplied by total number of plant. While the leaf area index (LAI) according to Hunt (1978) formula is given as

$$LAI = \frac{\text{Leaf area}}{\text{Land area}} = \frac{\text{Total area / plot x No.of leaves / plot x No.of stand / plot x \% emergence /plot}}{\text{Land area / plot}}$$

Method of soil moisture conservation

Grass mulch (M_1) of 40 cm diameter, and 70 cm x 50 cm perforated polythene nylon mulch (M_2) with side covering the mound as black surface and white surface facing the atmosphere wereused for evaporation suppression. Mulching was done after planting between 6.30-7.30 in the morning and removed from the mound at humid period [($\sum(P\text{-}0.1PE) = 0$]experienced at 25th July (21 decade) for 2017 experimental year and 25th June (18thdecade) for 2018 experimental year.In addition to the mulched plot, un-mulch treatment was included in the experiment which served as control (C). This period coincided with the early tuber formation stage of yam. This period is the time when most traditional farmers in West Africa normally remove mulch materials. According to his work, it revealed that if the mulch materials are not removed during the tuber formation stage, it will prevent the infiltration of rainwater to encourage good tuberization.

Apart from the daily observation of meteorological parameters measured and estimated during the phenological stages, phenological crop growth parameter and yield characters were also measured. Data collected were subjected to analysis of variance (ANOVA) using Genstat statistical package discovery edition 3 to evaluate the effects of variety, planting date (season) and "mulching and mulching materials" on the growth and yield of white yam. The significant difference of treatment means were determined using least significance difference (LSD) 5% level of probability. The result of yield from experiment using model planting date (T_1 & T_2) and the yield obtained from Ogun State Ministry of Agriculture and Ogun state Agricultural Development Program [Farmer's conventional planting period (F_1 & F_2)]were compared to ascertain the effectiveness of model.

RESULTS AND DISCUSSION

The relationship between AWA and WR during the phenological stages, presented in figures 2 and 3 shows that though annual total water supply was adequate for the growth of yam for both experimental years, a long term moisture stress (AWA: WR < 1) resulting from short fall in AWA encountered before the onset of rainfall, perticulary during the emergence period was pronounced for the 2017 experimental year. This was noticed to cause loss of setts and disparity in emergence which led to growth retardation and reduction in tuber yield. The moisture stress was badly felt by most farmers in the area that depended solely on the yam calendar for planting (F1). However, the P-PE model prediction of planting date T1 (9th decade) was able to reduce this problem to a bearable level. Furthermore, excessive moisture which appeared to be supra optimal (AWA: WR > 2) was experienced during the moisture critical stages of late vegetative growth, the tuber initiation and tuber bulking period in the 2017 experimental year. This could be attributed to part of high AWA which occurred during the period when P was consistently greater than PE. The high AWA experienced at this period could also cause leaching of plant nutrient which reduced harvested tuber yield (Bello, 2000). It was also observed that earlier planting {$T_1 = (\sum(P\text{-}0.1PE) \leq 24$ which marked the 9th decade of 2017 and $T_1 = (\sum(P\text{-}0.1PE) \leq 10$ which marked with 3rd decade of 2018} so that the entire phenological stages coincided with period of AWA led to relatively longer period of complete plot emergence and the vege-

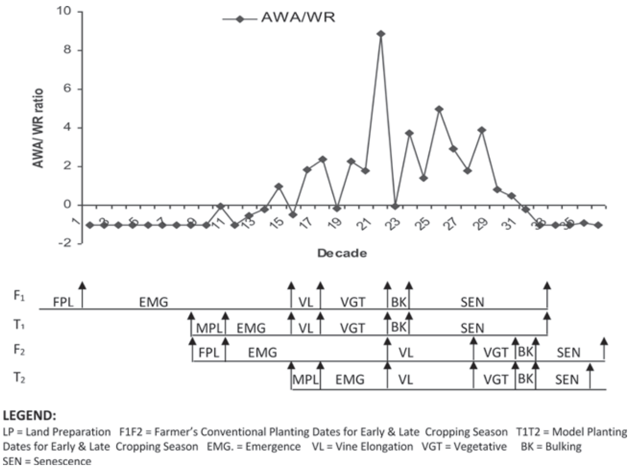

Fig. 2. Ratio between AWA and crop's water requirement (WR) for the two planting dates and conventional planting data at yam phenological stages in Abeokuta in 2017.

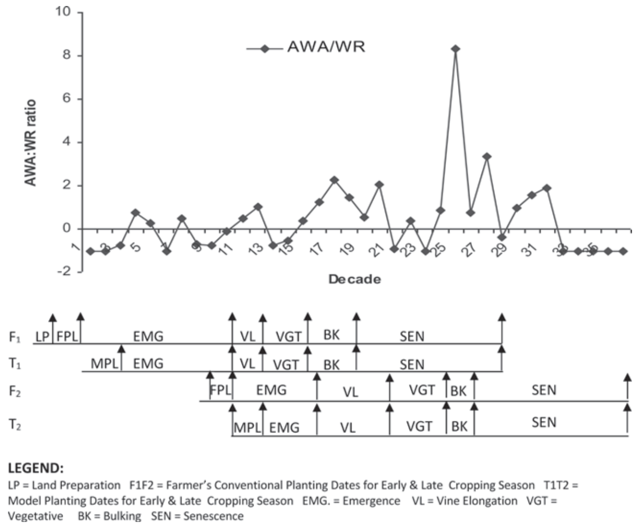

Fig. 3. Ratio between AWA and crop's water requirement (WR) for the two planting dates and conventional planting data at yam phenological stages in Abeokuta in 2018.

tative growth and consequently higher final yield whereas, late planting {$T_2 = (\Sigma(P\text{-}0.1PE) \leq 259$ which marked the 16th decade of 2017 and $T_2 = (\Sigma(P\text{-}0.1PE) \leq 182$ which marked the 10th decade of 2018} led to a situation whereby the AWA was not able to satisfy the moisture requirement of crop at the critical moisture requirement period of bulking before the cessation of rains which could lead to delay tuber initiation in yams and consequently causing considerably low tuber size and yam yield, this agreed with Maikasuwa and Ala (2013).

According to Odjugo (2008), the most critical stages for water requirement for yam are the tuber initiation and bulking. However, yam still requires water throughout its active growth period for vine and leaf development. It was not surprising to see that early planting designated T_1 [i.e $\Sigma(P\text{-}0.1PE) \leq 24$] in 2017characterized unpredictable distribution of rainfall significantly influencing emergence rate, vine length, number of leaves, number of branches, number of roots, root length, LAI, tuber length, tuber diameter, tuber weight, number of tuber and harvest yield (Tables 1 and 2). The variability of rainfall, characterized by late onset of rainfall (i.e. the accumulated difference between P and 0.5PE was very high), prolonged dry spell after planting during sprouting and emergence period and unbroken succession of wet days during the critical water requirement stage of bulking resulted in low growth and yield. Whereas, in the 2018 experimental year early planting was characterized by low accumulated difference between P and 0.5PE gave no significant difference ($P > 0.05$) between early planting T_1 and late planting T_2 on the emergence rate, vine length, number of branches, number of roots, vine diameter, root length, branch length, tuber length, tuber diameter, tuber weight, number of tuber and harvest yield (Table 3 and 4). However, for the 2018 experimental year, the P-PE model date of early planting T_1 had significantly influenced number of leaves and LAI. The higher leave area and LAI during the early season can be attributed to the adequate moisture availability. The high LAI was due to high leaves production and retention of leaves during the early planting than the late planting. The amount of leaf area available during tuber bulking period largely determines tuber yield in yam. Generally, the early planting particularly when the value of accumulated difference between P and 0.5PE were low as in 2018 cropping season was observed to have more yield when compared to early planting of 2017 cropping season that had high accumulated difference between P and 0.5PE. Furthermore, the early planting T_1 was observed to have more yield than late planting T_2 in both experimental years. The high yield from the early planting than the late planting for both experimental years related to the higher LAI which ensures higher bulking rate for a longer period and can also be attributed to phosphorus and mineralized nitrogen which are naturally high during the early rains absorbed by yams during growth (Zaknayiba and Tanko, 2013). While the significant low yield arising from delayed planting until the 9th decade of 2017 experimental year using model and even lower yield when farmer's conventional method (yield data collected from OGADEP) was used as shown in Figures 4 and 5 indicated that natural nutrient were largely missing as a result of leaching.This is moreso that the accumulated difference between P and 0.1PE at the

Table 1. Effect of variety, planting dateand mulching and mulching materials on growth of yamduring 2017 cropping season.

Factor	Emergence (%)	Vine elongation (cm)	No. of branches	No. of leaves	No of roots	Vine diameter (cm)	Branch length (cm)	Root length (cm)	LAI
Yam varieties									
Efuru A_1	41.7±7.21	83.9±26.20	20.8±2.42	499.5±121.14	21.1±2.96	1.511±0.07	71.8±7.76	31.1±3.12	1.078±0.42
Ise-osi A_2	44.0±6.45	74.4±24.69	15.5±2.40	571.8±129.32	21.4±2.28	1.358±0.07	65.3±6.02	29.1±2.61	0.911±0.28
Oniyere A_3	43.8±6.93	70.8±23.83	19.2±2.61	380.7±72.89	18.3±2.63	1.294±0.04	55.3±6.29	25.7±2.93	0.439±0.12
Prob. Level P	0.838	0.805	0.253	<0.001*	0.637	0.026**	0.186	0.411	0.002*
Planting season									
T_1	54.6±5.57	137.6±22.9	21.8±2.04	776.3±98.74	24.3±2.33	1.424±0.06	68.7±5.66	32.8±2.58	1.396±0.32
T_2	31.7±4.83	15.3±4.38	15.2±1.92	191.6±29.76	16.2±1.67	1.352±0.05	59.6±5.60	24.5±1.94	0.141±0.04
Prob. Level P	<0.001*	<0.001*	0.017**	<0.001*	0.009*	0.266	0.217	0.016**	<0.001*
Mulching material									
UnmulchC	14.8±2.71	31.1±15.54	14.3±1.41	239.6±42.56	20.2±2.90	1.272±0.08	58.8±6.82	23.8±3.15	0.044±0.02
Grass mulch M_1	68.4±5.33	150.4±30.21	24.3±2.98	757.2±125.68	23.7±2.97	1.447±0.05	74.9±6.34	32.2±2.84	1.650±0.42
Nylon mulch M_2	46.2±5.20	47.7±16.22	16.9±2.43	455.2±117.99	16.9±1.80	1.444±0.05	58.7±7.21	28.9±2.53	0.611±0.21
Prob. Level P	<0.001*	<0.001*	0.010*	<0.001*	0.190	0.049**	0.124	0.079	<0.001*

*Significant at P<0.01. **Significant at P< 0.05.

Table 2. Effect of variety, planting dateand mulching and mulching materials on yield and yield characteristic of yamduring 2017 cropping season.

Factor	Tuber length (cm)	Tuber diameter (cm)	Tuber weight (kg)	No of tuber	Harvest yield (ton/ha)
Variety					
Efuru	17.0±3.81	4.89±1.05	1.67±0.37	0.778±0.24	5.38±1.47
Ise-osi	23.3±3.87	6.03±0.98	1.56±0.31	0.750±0.12	4.97±1.03
Oniyere	18.8±4.18	5.41±1.21	1.54±0.36	0.556±0.12	4.54±1.39
0.235	0.502	0.891	0.378	0.214	
Planting date					
T1	30.0±2.73	8.30±0.73	2.60±0.25	1.019±0.13	8.04±1.17
T2	9.4±2.48	2.59±0.67	0.58±0.16	0.370±0.95	1.42±0.41
Prob. Level P	< 0.001*	< 0.001*	< 0.001*	< 0.001*	< 0.001*
Mulch material					
Unmulch C	10.60±3.91	2.89±1.01	0.84±0.29	0.556±0.23	1.11±0.41
Grass mulch M1	27.7±2.19	8.30±0.70	2.37±0.30	0.972±0.06	8.74±1.50
Nylon mulch M2	20.8±4.58	5.14±1.45	1.56±0.38	0.556±0.12	4.35±1.14
Prob. Level P	< 0.001*	< 0.001*	< 0.001*	< 0.028**	< 0.001*

*Significant at P< 0.01. **Significant at P< 0.05.

9th decade of 2017 had become significantly high (14-28mm). The period was observed to extend to the late planting at 16th decade. It is noteworthy that in the case of late onset of rains, farmers may become apprehensive of a planting date that fails to ensure that the crop matures by the end of the rains. Consequently, they may tend to plant immediately after the value of accumulated difference between P and 0.5PE approaches zero in other to avoid possible incidence of drought at critical moisture period of bulking.

It follows in the same vein that significant declined in yield occurred when accumulated difference between P and 0.1PE was in excess of 10mm. Thus planting can be done when accumulated difference between P and

Table 3. Effect of variety, planting dateand mulching and mulching materials on growth of yamduring 2018 cropping season.

Factor	Emergence (%)	Vine elongation (cm)	No. of branches	No. of leaves	No of roots	Vine diameter (cm)	Branch length (cm)	Root length (cm)	LAI
Yam varieties									
Efuru	A172.2±6.66	462±56.75	22.2±3.17	439.9±46.6	25.8±3.19	1.528±0.07	83.2±13.23	32.3±2.92	1.035±0.21
Ise-osi A_2	71.3±4.78	326±32.82	21.4±3.58	484±85.05	26.8±3.08	1.369±0.08	72.8±7.60	31.1±2.36	0.917±0.24
Oniyere A_3	70.3±4.97	319±26.59	23.2±3.69	435.2±46.67	23.7±3.34	1.322±0.05	79.0±7.64	32.2±3.46	0.823±0.14
Prob. Level P	0.935	<0.001*	0.927	<0.001*	0.808	0.059	0.746	0.956	0.061
Planting date									
T_1	74.0±4.13	381±40.29	25.1±2.97	568.1±57.22	29.4±2.82	1.465±0.05	94±9.13	35.5±2.60	1.230±0.17
T_2	68.5±4.6	357±28.03	19.4±2.58	332.6±28.65	21.5±2.19	1.348±0.06	62.7±5.92	28.2±2.02	0.628±0.10
Prob. Level P	0.205	0.424	0.121	<0.001*	0.05**	0.109	0.008*	0.044**	<0.001*
Mulching material									
UnmulchC	51.6±3.81	271±34.29	12.6±1.13	255.0±16.7	23.8±4.22	1.261±0.07	68.1±7.09	28.9±3.22	0.339±0.06
Grass mulch M_1	94.0±1.56	476±37.0	32.4±3.72	680.3±65.80	27.8±3.13	1.508±0.06	101.1±12.67	34.7±2.73	1.706±0.17
Nylon mulch M_2	68.1±4.30	360±41.91	21.7±3.20	415.8±42.49	24.8±1.98	1.450±0.06	65.9±7.60	32.0±2.87	0.751±0.10
Prob. Level P	<0.001*	<0.001*	< 0.01*	<0.001*	0.700	0.019 **	0.023**	0.408	<0.001**

*Significant at P< 0.01. **Significant at P< 0.05

Table 4. Effect of variety, planting dateand mulching and mulching materials on yield and yield characteristic of yam during the 2018 cropping season.

Factor	Tuber length (cm)	Tuber diameter (cm)	Tuber weight (kg)	No of tuber	Harvest yield (ton/ha)
Yam variety					
Efuru	34±2.63	10.09±0.76	3.33±0.34	1.056±0.07	11.94±1.71
Ise-osi	34.2±1.91	12.05±0.54	3.36±0.22	1.139±0.04	11.64±1.18
Oniyere	40.3±2.00	11.81±0.59	3.33±0.25	1.178±0.04	11.53±1.40
Prob. Level P	0.066	0.028**	0.993	0.567	0.936
Planting date					
T137.7±2.13	11.49±0.644	3.55±0.24	1.133±0.06	12.70±1.16	
T2	34.7±1.56	11.14±0.43	3.13±0.18	1.115±0.03	10.71±1.14
Prob. Level P	0.223	0.575	0.098	0.764	0.043**
Mulch material					
Unmulch C	31.8±2.87	9.52±0.75	2.54±0.29	1.078±0.08	6.24±0.87
Grass mulch M1	39.1±1.71	12.36±0.53	3.97±0.17	1.150±0.03	17.59±0.88
Nylon mulch M2	37.6±1.87	12.08±0.50	3.52±0.21	1.144±0.04	11.28±0.94
Prob. Level P	0.043**	<0.001*	<0.001*	0.567	<0.001*

*Significant at P<0.01. **Significant at P< 0.05.

0.1PE is less than 10mm (i.e Σ(P-0.1PE) ≤ 10mm). The implication for the schedule of farm operations for yam cultivation in the area is that land preparation should commence as soon as the accumulated difference between P and 0.1PE approaches zero while mound construction and planting could be done simultaneously immediately the difference reaches the zero value. Under no circumstance must farmer delay planting until the accumulated difference exceed 10 mm. This schedule is to ensure that adverse effects of high AWA are avoided or minimized while, at the same time, precautions are taken against possible shortfall in the duration of the rains, particularly if such an early onset of the rains is flawed by an abnormal early or sudden cession. In a situ-

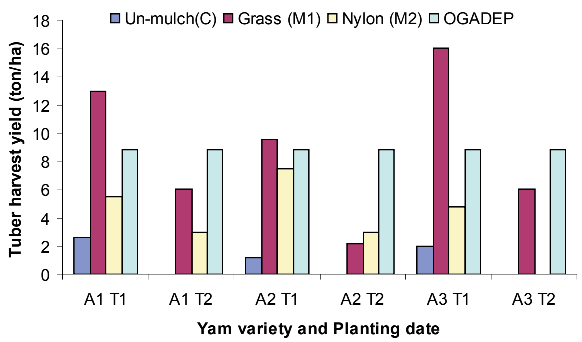

Fig. 4. Effect of planting date, mulching and mulching materials and varietyon tuber yield of three white yam grown at Abeokuta in 2017.

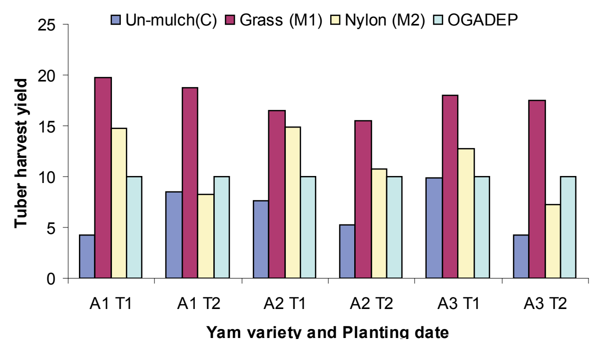

Fig. 5. Effect of planting date, mulching and mulching materials and varietyon tuber yield of three white yam grown at Abeokuta in 2018.

ation where the onset of the rains is extremely late such that incidence of drought is imminent and the duration of the rains might possibly fall short of 240days (24dacades- growing days of yam), then variety with phenology that synchronize perfectly with the pattern of AWA should be selected.

The importance of mulching in yam cultivation cannot be overemphasized particularly in the study area (Western Nigeria) where severe moisture deficit had been known to cause loss of setts and disparity in emergence. The water deficit is also known to reduce growth and tuber yield which normally contributed to economic loss. The study showed that mulching altered the microclimate favourably and resulted in improved yam growth, development and tuber yield in the study area as observed in the effect of mulching and mulching materials on the phenological crop growth of yam which was noticed to similar in both experimental years Tables 1 and 3. Generally, the yams planted under mulched plot were significantly higher in emergence rate, vine length, number of stem branches, and number of leaves and LAI of yam than for un-mulched plot. It was also found that mulching increased tuber yield by about 6-8 tha^{-1}than the unmulched. This finding agreed with previous report that the emergence and growth rate of yam seedling were observed to be significantly higher in mulched plots than the un-mulched plot by Olasantan 1999 and Odjugo,2008. Increased emergence and more rapid development of setts in mulched yams could be attributed to an increase in soil moisture content and the consequent modification of soil temperature under mulched plot (Okoh, 2004; Iyang, 2005). Furthermore, there was significant difference in these parameters with different type of mulching material used for the two experimental year. The grass mulched significantly improved the growth, development and yield of yam than the perforated white surface up and black surface facing down polythene nylon.Grass mulch had tuber yield of about 4-6 tha^{-1} greater than the polythene mulch and the unmulched plots. The beneficial effects of grass mulch on yam growth could be attributed to the nutrients released by decomposing mulch (Olasantan, 1999), and its physical effect on the possible reduction of nutrient losses by surface erosion and leaching. Furthermore, the beneficial effect of polythene nylon was also discussed by Odjugo, (2008). It is interesting to note that there were no significant difference between number of roots, vine diameter and root length of yam planted under mulched and unmulched plot, and also with different type of mulching material used during the two experimental year.

The effect of mulching and mulching material on the yield and yield components of yam were also similar in both experimental years. Generally, irrespective of planting date and variety of white yam planted, the yam planted under mulched plot were significantly higher in tuber length, tuber diameter, tuber weight and yield of yam than for un-mulched plot. This finding also agreed with previous report that the yield and yield components of yam were observed to be significantly higher in mulched plots than the un-mulched plot by Anthony and Ben, 2018. However, the significant reduction in the tuber length, tuber diameter, tuber weight and yield of yam as experienced in the 2017 experimental year as compared to 2018 year could be attributed to the moisture stress that marked the arid period of the 2017 year as earlier mentioned above thereby causing disparity in yam setts sprouting in all varieties under all mulched and un-mulched plots. Furthermore, there was significant difference in these parameters with different type of mulching material used for the two experimental years. The grass mulched plots were observed to be significantly higher than the perforated white surface up and black surface facing down polythene nylon. The beneficial effects of mulch on tuber yield particularly during the 2018 experimental year were probably due to favourable hydrothermal regimes of the soil for emergence and early development of yam plants. The mulch was also observed to increase the growth and tuber yield of yams possibly by reducing nutrient losses through controlling runoff and leaching in the raining season. The high yield as experienced in the grass mulch was also attributed partly to the possible influence of decomposed mulch material on increase in soil nutrient status and availability since the grass mulch is known to contain some element of Nitrogen, magnesium, calcium, phosphorus and potassium (Hulugalle etal., 1986), and these nutrients, particularly P, N and K are important in the growth and bulking of yam tubers, and consequently in the tuber yield (Hulugalle etal, 1986). Since fertilizer was not used in the study, the higher growth and tuber yield observed in the grass mulched plots compared to both the perforated white surface up and black surface facing down polythene nylon mulch and the un-mulched plots in the two experimental years was attributed to the effect of decomposed mulch on the nutrient content and in ameliorating soil physical conditions. It is also interesting to note that there was no significant difference between number of tuber of yam planted under mulched and un-mulched plot and with different type of mulching material used during the two experimental year.

The selection of cultivar (variety) is among the factor that contributes to the realization of a successful cropping (Bello, 2000 and Olasntan, 2007). Hence, the study further confirmed the agro-climatic potential of the study area for three white yam varieties. The fact that the total rainfall (1177.2 and 1201.6 mm for 2017 and 2018 experimental years respectively) recorded at the study site fell within the range of optimum annual rainfall (1000-1500 mm) reported for yam growth is not enough criteria for suitable crop variety selection in the study area. This was obvious in the high total rainfall received is as a result of one or two sporadic downpours, widely separated by periods of dry spells, experienced in the 2017 experimental year (Figure 2) which does not contribute meaningfully to the yam growth, rather, it the downpours generated flash floods while the little amount of rainfall evaporated rather than effectively recharging the soil for subsequent use by plant. It follows therefore that adequacy for good plant growth does not depend solely on total rainfall but a combination of rainfall and evaporation.

Since soil and thermal factors are not constraints though the duration of rains is appreciably longer and more reliable in Southwest than elsewhere in Nigeria. Selection of yam variety with appropriate phenologies that will synchronize the crop growth cycle with the period of effective water availability is required. For instance, it was observed from study that though there were no significant difference in most of the yam growth parameters measured like the emergence rate, vine length, number of stem branches, number of stem roots, branch length, tuber length, tuber diameter, tuber weight, number of tuber and the yield for the different yam variety planted during the 2017 and 2018 experiments, there were still some significant difference in some major parameter like the number of leaves, vine diameter and the LAI. It was observed that the Efuru and Ise-osi has the higher number of leaves and LAI followed by the Oniyere. Efuru and Ise-osi synchronized perfectly with the pattern of Actual Water Availability (AWA) and produced good vegetative growth with Leaf Area Index LAI, of 1.08 and 0.91 thereby leading to high tuber yield of 12 tonnes ha^{-1} and 11.64 tonnes ha^{-1}, respectively. Oniyere had LAI of 0.44 resulting in a lower tuber yield of 11.53 tonnes ha^{-1}.This implies that though all selected yam are suitable for planting in the study area. There are still some early maturing and moisture tolerant varieties that could have a larger canopy (LAI) and produce more yields even if the difference is little.

Generally, there was no significant interactive effect of planting date and mulching method, planting date and variety, mulching method and variety and planting date, mulching method and variety on growth parameters such as emergence rate, vine length, number of branches, number of roots, vine diameter, branch length and roots length (Tables 5 and 6) and also in yield and yield components (Tables 7 and 8) in both trials. However, there was an exceptional significant interaction ($P< 0.001$) between planting date and mulching method on vine length of yam irrespective of variety. Furthermore, significant interaction ($P< 0.001$) was observed between planting date and variety; mulching method and variety; and planting, mulching method and variety on number of leave and LAI of yam in both trials. All three varieties responded in the same way to planting date and/or mulching treatment, hence factorial effects of planting date x mulching method, planting date x variety, mulching method x variety and planting date x mulching method x variety were generally not statistically significant.

CONCLUSION

From this study, it is obvious that partitioning of the growing season into different phenological stages for investigating crop – water relationship using rainfall – potential evapotranspiration model will allow the determination of the extent to which the water availability

Table 5. Interactive effect of variety , planting date and mulching method on growth on yam during the 2017 cropping season.

Factor	Emergence (%)	Vine elongation (cm)	No. of branches	No. of leaves	No of roots	Vine diameter (cm)	Branch length (cm)	Root length (cm)	LAI
Prob. Level P									
Date x mulch	0.086	<0.001*	0.579	<0.001*	0.380	0.392	0.068	0.696	<0.001*
Datex variety	<0.001*	0.915	0.426	<0.001*	0.749	0.163	0.298	0.969	0.007*
Mulch x variety	0.611	0.465	0.999	<0.001*	0.468	0.514	0.304	0.429	<0.001*
Date x Mulch x variety	0.073	0.613	0.152	< 0.001*	0.601	0.053**	0.284	0.750	< 0.001**

*Significant at P< 0.01. **Significant at P< 0.05

Table 6. Interactive effect of variety , planting date and mulching method on growth of yamduring the 2018 cropping season.

Factor	Emergence (%)	Vine elongation (cm)	No. of branches	No. of leaves	No of roots	Vine diameter (cm)	Branch length (cm)	Root length (cm)	LAI
Prob. Level P									
Date x mulch	0.344	<0.001*	0.786	<0.001*	0.895	0.593	0.551	0.425	<0.001*
Date x variety	0.664	0.095	0.626	<0.001*	0.888	0.508	0.468	0.605	0.211
Mulch x variety	0.970	0.048	0.869	<0.001*	0.865	0.523	0.827	0.703	<0.001*
Date x Mulch x variety	0.621	0.252	0.694	<0.001*	0.538	0.904	0.963	0.508	0.043**

*Significant at P< 0.01. **Significant at P< 0.05.

Table 7. Interactive effect of variety , planting date and mulching method on yield and yield characteristic of yamduring the 2017 cropping season.

Factor	Tuber length (cm)	Tuber diameter (cm)	Tuber weight (kg)	No of tuber	Harvest yield (ton/ha)
Prob. Level P					
Date x mulch	0.132	0.330	0.316	0.032**	<0.001*
Date x variety	0.871	0.665	0.693	0.077	0.066
Mulch x variety	0.224	0.150	0.080	0.100	0.025**
Date x Mulch x variety	0.441	0.719	0.950	0.596	0.758

*Significant at P< 0.01. **Significant at P< 0.05.

Table 8. Interactive effect of variety , planting date and mulching method on yield and yield characteristic of yam during the 2018 cropping season.

Factor	Tuber length (cm)	Tuber diameter (cm)	Tuber weight (kg)	No of tuber	Harvest yield (ton/ha)
Prob. Level P					
Date x mulch	0.296	0.094	0.329	0.261	0.077
Date x variety	0.313	0.047**	0.268	0.213	0.266
Mulch x variety	0.407	0.305	0.257	0.605	0.266
Date x Mulch x variety	0.305	0.501	0.156	0.291	0.183

*Significant at P< 0.01. **Significant at P< 0.05.

will satisfy water requirement of crops during the different phenological stages. Such information helps in the design of appropriate technological/ agronomical devices that will maximize beneficial effects. For instance, a balanced water supply during critical water requirement such as active growth period of vine and leaf development, tuber initiation and bulking; the most critical stages being at tuber initiation and bulking will lead to an effective yield. On the other hand, too little or excess water supply is detrimental, as it might lead to poor development and growth of the crop and consequently low yield. Generally early planting particularly when accumulated difference between P and 0.5PE where comparatively low {Σ(P-0.1PE) ≤ 10mm} gave a better yield as compared to later. Hence, for effective yam production in Southwestern Nigeria, farmer's must not delay planting until the accumulated difference between P and 0.1PE exceed 10mm.Furthermore, there was every indication that mulching significantly improved the emergence and development of yam setts and increased tuber yield and also grass mulch has significantly lower produced higher yield than the polythene mulch. However, both mulches have the physical effect of reduction of nutrient losses by surface erosion and leaching and also checks weed growth.

Also judging from the duration of the period of effective water availability, rainfall during the moist period, extreme lateness of onset of rainfall and water requirement by each of selected yam varieties, the production potential of some variety such as Efuru and Iseosi can be encouraged in the study area.

REFERENCES

Anthony, A. M and Ben K. B., 2018. Yam plant growth and tuber yield response to ex-situ mulches of moringa oleifera, chromolaena odorata and panicum maximum under three natural fallow aged systems. *Annals of Ecology and Environmental Science*, 2(3): 7-14.

Audu, E.B., 2012. A Descriptive Analysis of Rainfall for Agricultural Planning in Lokaja Local Government Area of Kogi State, Nigeria. *Interternational Journal of Science Technology* 2(2): 850-854.

Bello, N.J., 2000. Application of rainfall- potential evapotranspiration model for the determination of optimum planting date of maize (*Zea mays*) in a tropical wet and dry climate.*Journal of Agricultural sciences*. 70 (7): 437-400.

Bhandari, G., 2013. Effect of Precipitation and Temperature Variation on the Yield of Major Cereal in Dadeldhura District of far Western Development Region, Nepal, *International. Journal of Plant Animal Environmental Science* 3(1): 247-255.

Cocheme, J. and Franquin, P., 1967. An agroclimatological survey of a semi arid area in South of the Sahara. *WMO Technical note No. 86*, Geneva.

CROPWAT., 2009. CROPWAT for windows, An FAO software, version 8.0. http://www.fao.org/nr/ water / infores databases cropwat.html

Deichmann, U., and Eklundh, L., 1991. "Global Digital Data Sets for Land Degradation Studies: A GIS Approach." GRID Case Study Series 4. United Nations Environment Programme, Global Environmental Monitoring System and Global Resource Information Database, Nairobi.Accessed February 2006. [http://geodata.grid.unep.ch/].

Doorrenbos, J. and Pruitt, W.O., 1984. Guidelines for predicting crop water requirements. *Food and Agricultural Organization. Irrigation and Drainage paper No. 24*. Rome: FAO.

FAO., 1977. Food and Agriculture Organization. Irrigation and Drainage Paper No 24, Rome: FAO

Gbadebor, P.V., 2006. The climate, the soils and the West African traditional farmers. *AgroEcosystem Bull*. 4: 12-17.

Gidey, E., O. Dikinya, R. Sebego, E. Segosebe, and A. Zenebe., 2018. Analysis of the long-term agricultural drought onset, cessation, duration, frequency, severity and spatial extent using vegetation health index (VHI) in Raya and its environs, northern Ethiopia. *Environmental Research System* 7 (13). https://doi.org/10.1186/s40068-018-0115-z.

Hulugalle, N.R. and Lal, R., 1986. Soil water balance in intercropped maize and cowpea grown in a typical hydromophic soil Western Nigeria. *Agronomy Journal* 77: 86-90.

Hunt, R. 1978. Plant Growth Analysis. The Institute of Biology. Studies in Biology. Edward Arnold (Pub.) Ltd.96: 8-38.

International Institute of Tropical Agriculture (IITA)., 1995. Yam research at IITA: 1971-1993. IITA Ibadan, Nigeria, 38pp.

International Institute for Tropi-cal Agriculture (IITA)., 2009. Yam (Dioscorea species). Available at: http://www.iita.org/yam. [Accessed: 15. March 2014].

International Institute for Tropi-cal Agriculture (IITA)., 2013. Healthy yam seed production. IITA Publications. Retrieved from IITA Website http://www.iita.org/publications

Inyang, E.U., 2005. An evaluation of tillage and storage systems applied by traditional root crop farmers in Cameroon. *Agriculture and Envroment.Journal.*, 7(2): 15-22.

Kutugi, A.D., 2002. Comparative analysis between indigenous and modern tillage practices in the production of *Dioscorearotundata*and *Dioscoreacayenensis*in the middle belt of Nigeria. *Journal of Agriculture Environ*., 2(1): 53-66.

Maikasuwa, M. A. and Ala, A. L. 2013. Determination of profitability and resource-use efficiency of yam production by women in Bosso local government area of Niger State, Nigeria. *European Scientifi c Journal*, 9(16): 196-205.

Mulebeke,R..Kironchi.G,.andTenywa, M. M., 2010. Enhancing water use efficiency of cassava and sorghum based cropping systems in drylands. Second RUFUROM biennial meeting, 20-24 September, 2010, Entebbe, Uganda http://news.mak.ac.ug/documents/RUFORUM/Mulebeke.pdf

Nahanga Verter and Věra Bečvářová (2015). Analysis of yam production in Nigeria. *Acta Universitatis Agriculturae Et Silviculturae Mendelianae Brunensis*., 63(2): 659-665.

Odjugo, P.A.O., 2008.The effect of tillage systems and mulching on soil microclimate, growth and yield of yellow yam (*Doiscoreacayenensis*) in Midwestern Nigeria. *African Journal of Biochemistry*. 7(24): 4500-4507.

Ofori, E.Oteng-Darko, P, Berchie, N. J., Nimako, F. O., Yeboah, S. and Owusu, D. E ., 2014. Monitoring of soil moisture regime and water use efficiency under maize cowpea. *International Journal of Current Microbiology Applied Science*. 3(10): 837-848.

Okoh, C.A., 2004. The effect of mulching on soil physicochemical properties and the yield of White Yam.*Tropical Journal of Root Tuber Crops*. 4(2): 24-31.

Olasantan,F.O, 2007. Effect of population density and sowing date of pumpkin on soil hydrothermal regime, weed control and crop growth in a yam – pumpkin intercrop. *Experimental Agriculture* 43: 365-380.

Olasantan, F.O., 1999. Effect of mulching on soil temperature and moisture regime and emergence, growth and yield of white yam in western Nigeria. *Soil and tillage research* 50: 215-221.

Shiru, M.S., S. Shahid, N. Alias, and E.S. Chung. 2018. Trend analysis of droughts during crop growing seasons of Nigeria. *Sustainability* 10(871): 1-13. https://doi.org/10.3390/ su10030871.

Susha, L. S.U., Singh, D. N. and Maryam, S. B., 2014. A critical review of soil moisture measurement. *Measurement* 54: 92–105.

Tiamiyu, S.A., J.N. Eze, T.M. Yusuf, A.T. Maji, and S.O. Bakare. 2015. Rainfall variability and its effect on yield of Rice in Nigeria. *International Letters of Natural Sciences* 49: 63-68.

Um, M., Y. Kim, D. Park, and J. Kim. 2017. Effects of different reference periods on drought index estimations from 1901 to 2014. *Hydrology and Earth System Sciences* 21: 4989-5007.

Yanmin, Y.,De Li, L.,Muhuddin, A., Garry, O.,Ian, M.,Yonghui, Y., 2015. Water use Efficiency and crop water balance of rain-fed wheat in a semi-arid environment: sensitivity of future changes to projected climate changes and soil type. *Theoretical and Applied Climatology l*DOI 10.1007/s00704-015-1376-3.

Zaknayiba, D. B. and Tanko, L. 2013. Costs and returns analysis of yam production among small scale farmers in Karu local government area, Nasarawa State, Nigeria. PAT, 9(1): 73-8.

Italian Journal of Agrometeorology
Rivista Italiana di Agrometeorologia

Firenze University Press
www.fupress.com/ijam

Citation: E. Topçu (2021) Testing of Drought Exceedance Probability Index (DEPI) for Turkey using PERSIANN data for 2000-2021 period. *Italian Journal of Agrometeorology* (2): 15-28. doi: 10.36253/ijam-1308

Received: May 06, 2021

Accepted: August 17, 2021

Published: December 27, 2021

Data Availability Statement: All relevant data are within the paper and its Supporting Information files.

Competing Interests: The Author(s) declare(s) no conflict of interest.

ORCID:
ET: 0000-0003-0728-7035

Testing of Drought Exceedance Probability Index (DEPI) for Turkey using PERSIANN data for 2000-2021 period

Emre Topçu

Kafkas University, Civil Engineering Department, 36100, Kars, Turkey
E-mail: emretopcu01@gmail.com

Abstract. Drought is a climatic event that threatens the environment and human life with an ambiguity of location and time. Recently, droughts can be analyzed for different periods with the help of different mathematical methods and developing technology. This study aims to perform a drought analysis in 126 designated study points of Turkey. The analyzed data includes monthly total precipitation values between March 2000 and February 2021, obtained from PERSIANN system (Precipitation Estimation from Remotely Sensed Information using Artificial Neural Networks). Monthly precipitation totals of these designated points were used as input parameters in the Drought Exceedance Probability Index (DEPI) which is a new drought analysis method. The analysis was conducted separately for the whole of Turkey from January to December. Moreover, the findings were compared with the Standardized Precipitation Index (SPI), a globally accepted and commonly used drought index, to measure the drought detection performance of DEPI. SPI was calculated for periods of 6, 12 and 24 months. Pearson correlation coefficients between drought values of SPI-6, SPI-12 and SPI-24 and DEPI results were calculated. The second part of the study includes possible trend of drought determined by the Mann-Kendall trend analysis method. Both DEPI and SPI results and trend analysis results were mapped and visualized with the help of ArcGIS package program. The highest correlation is between DEPI and SPI-12 with 0.75, while the lowest correlation is between DEPI and SPI-24 with a value of 0.62. SPI monthly drought maps indicated the wettest months were January and February, while the driest months were March and July. Besides the DEPI monthly drought maps, the wettest months were October and November, while the driest months were May and June. The Mann-Kendall trend maps showed a significant increase in drought for summer.

Keywords: drought, hydrology, climate, Turkey, drought exceedance probability index.

INTRODUCTION

Drought is a normal, recurring natural disaster that can occasionally affect the struggle of human survival. Therefore, understanding drought characteristics might assist in developing better mitigation plans to a large extent (Mallenahalli, 2020). While different drought definitions have been developed in the literature, there is a widely popular quadruple classification. These are meteorological, agricultural, hydrological drought and socio-economic drought (Wilhite and Glantz, 1985). Among the drought types, it can be stated that meteorological drought is over-studied in the literature and accepted as a forerunner of all other drought events.

Meteorological drought deals entirely with weather conditions and is defined as a reduction in normal precipitation over the minimum recorded 30-year precipitation series. Agricultural drought is considered to be the absence of sufficient soil moisture that causes wilting and plant death in agricultural areas. Even with adequate rainfall and water resources, agricultural drought might occur due to excessive use of water and insensible agricultural practices. Hydrological drought might also occur when the local population who benefit from water is high or rural activities and irrigation activities are undue, although the amount of precipitation and water in the reservoirs are sufficient (Topçu and Seçkin, 2016). Socio economic drought refers to droughts that adversely affect some social or economic function in life.

Drought impacts are evaluated by using drought indices in terms of severity, persistence, and spread. Some of these measures are; De Martonne Method (De Martonne, 1942), Palmer Drought Severity Index (Palmer, 1965), Decile Index (Gibbs and Maher, 1967), Aydeniz Method (Aydeniz, 1973), Erinç Method (Erinç, 1984), Standardized Precipitation Index (McKee et al., 1993), Aggregated Drought Index (Keyantash and Dracup, 2004), Reconnaissance Drought Index (Tsakiris and Vangelis, 2005), Streamflow Drought Index (Nalbantis, 2008), Actual Precipitation Index (API) (Şen and Almazroui, 2021). In addition to these indices, new drought monitoring indices continue to be developed.One of the newest index among these is the Drought Exceedance Probability Index (DEPI) developed by (Limones et al., 2022). DEPI is a modification of the ISSP (Indice Standardisé de Sécheresse Pluviométrique) developed by (Pita, 2000). Similar to other indices i.e. Standardized Precipitation Index (SPI) of (McKee et al., 1993) or the SPEI (Vicente-Serrano et al., 2010), DEPI is based on the calculation of cumulative monthly precipitation anomalies. On the other hand, each month's DEPI score shows the empirical probability of exceedance of the drought level experienced in that month (Limones et al., 2020).

The study aims to conduct periodic drought analysis of the period from January to December with the help of DEPI developed by (Limones et al., 2022) to monitor drought using monthly precipitation totals of 126 study points designated and located in Turkey. Precipitation data were obtained from the Precipitation Estimation from Remotely Sensed Information using Artificial Neural Networks (PERSIANN) system, based on the location of the meteorological stations of the Turkish State Meteorological Service. The DEPI, an alternative drought index, was compared to SPI, a classical method in drought analysis, to determine its reliability. Mann-Kendall trend analysis was also utilized to obtain information about the course of the drought. DEPI, SPI and trend values were mapped with the help of ArcGIS package program (ESRI, 2012) so that the results could be seen as spatial rather than tabulated. This paper is organized as follows. The first section gives a brief introduction of study area, and then the research methodology is reviewed. In the next section, the results of the application of the selected method in Turkey are presented and conclusions are drawn in the final section.

MATERIALS AND METHODS

Turkey is located at the intersection of Asia and Europe in the Mediterranean Basin. As it is surrounded on three sides by the sea and its geographical features are unique, a wide variety of climate types can be observed. Although drought events are very common, rainy periods are also seen.The elevation, the distance to the sea and the direction of the mountains are effective in the formation of diverse climatic conditions. For this reason, June, July and August are poor months in the amount of precipitation throughout Turkey, except for the northeast of the Eastern region and Northeast regions. In particular, April is rainy across the country. Turkey has Mediterranean climate in the south and west coastal areas, the Black Sea climate to the north, and a continental climate in the inland Anatolian region and the Eastern part. Mediterranean climate is common in the Mediterranean, Aegean seas and southern Marmara. However, the characteristics of the Mediterranean climate in Marmara are more severe. It is hot and dry in summers, warm and rainy in winters. It is suitable for the cultivation of citrus fruits. Since it is common in southern latitudes, frost and snowfall are rare in the coastal belt. The Black Sea climate is typical in the Black Sea coasts and northern Marmara. It is rainy in all seasons. Summers are cool, and winters are warm on the coasts, cold and snowy at high altitudes. Precipitation is distributed throughout the year, and there is no dry season. The vegetation is steppe in the continental climate. Summers are hot and dry, and winters are cold and snowy (Atalay, 2011; Öztürk et al., 2017).

The distributions of the 126 study points selected for the study are demonstrated on the physical map of Turkey and shown in Figure 1.

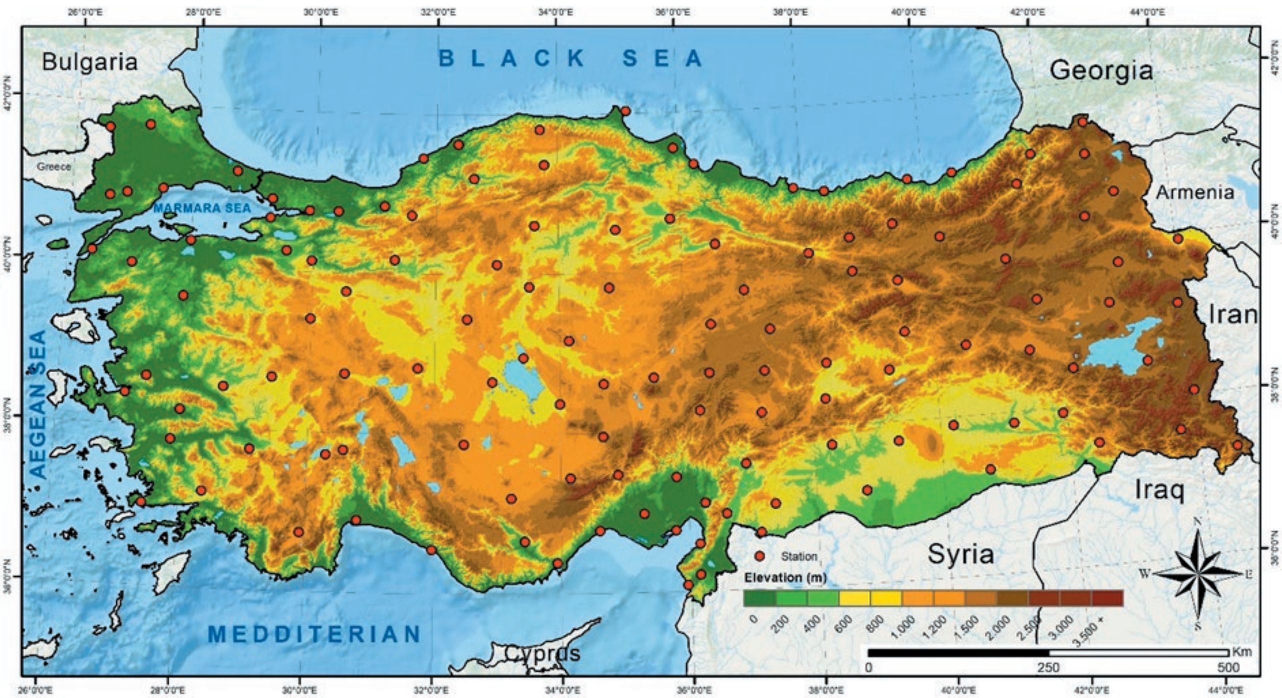

Fig. 1. Designated study points depicted on the physical map of Turkey.

The existing operational PERSIANN (Precipitation Estimation from Remotely Sensed Information Using Artificial Neural Networks) system uses neural network function classification / approximation procedures to calculate an estimate of the precipitation rate per 0.25° x 0.25° (about 625 km^2) pixel of the infrared brightness temperature image provided by geostationary (fixed-position) satellites. The PERSIANN system was based on fixed infrared images and then expanded to include the use of both infrared and daytime visible images. In this study, the PERSIANN algorithm was utilized to create global precipitation based on geostationary long-wave infrared images. The precipitation product consists of 50°S to 50°N globally. Model parameters are updated regularly using precipitation forecasts from low-orbit satellites (CHRS Data Portal, 2021).

The monthly precipitation values representing Turkey was obtained through the spatial average of 126 point precipitation data. Based on the areas of the designated points, the areal precipitation average was found. Accordingly, monthly precipitation values are depicted in Figure 2 from January to December for the 2000-2021 period.

When these graphs are examined, it can be monitored in which year and in which month the amount of precipitation decreases or increases. Figure 2 illustrates that the highest monthly precipitation average was measured in January 2007. The lowest average precipitation is in August. It was calculated for the January and February period for 2001-2021, and for the March and December period for 2000-2020. Because the PERSIANN system has made measurements between these periods until now, the determined periods are based on the existing data.

Detailed information about this system can be accessed from (Hsu et al., 1997; Hsu et al., 1999, 2000, 2002; Sorooshian et al., 2000, 2002; Sorooshian et al., 2014; Nguyen et al., 2019).Monthly precipitation point totals for March 2000 and February 2021 were obtained from the PERSIANN system.

DEPI (Limones et al., 2022) and SPI (McKee et al., 1993) were used in this study. The SPI method is not elaborated in this study since there are several studies about SPI worldwide. SPI is a meteorological drought analysis method that uses only the precipitation parameter. The SPI is obtained by dividing the difference from average precipitation over the specified period by the standard deviation. If the SPI value obtained is “0” and above, it represents wet conditions, and if it is below “0”, it indicates drought conditions. Calculations for 3, 6, 9, 12, 24-month periods can be performed to examine the effect of drought on water resources in different periods. 3, 6, and 9 months-long samples examine the effect of precipitation deficiency on soil moisture in the short and medium term, while 12 months or longer time intervals reveal the impact of drought on water resources such

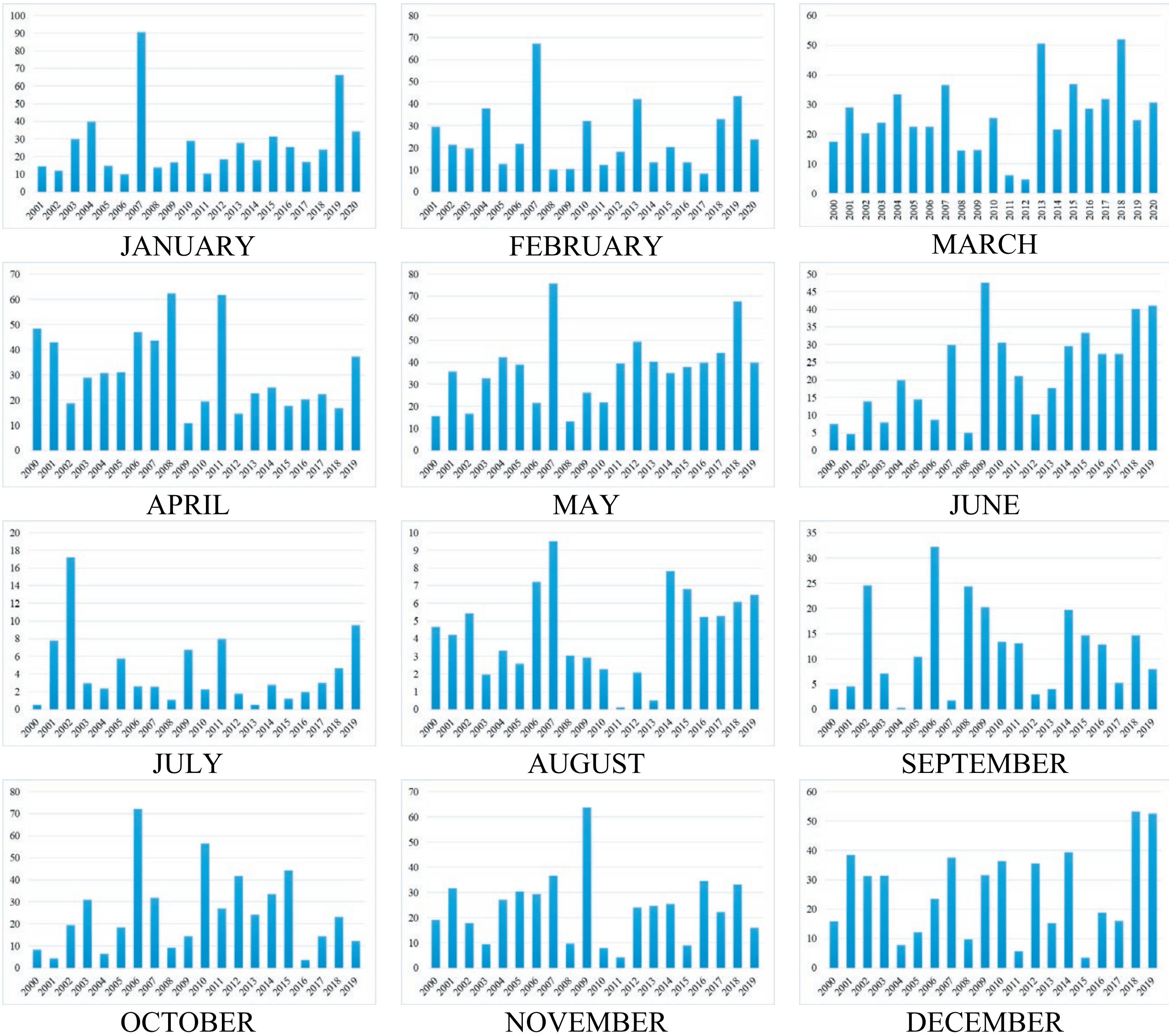

Fig. 2. Turkey's monthly precipitation values for period of 2000-2021 (mm).

as reservoirs. The 6, 12, and 24-month long SPI values examining drought in the short, medium and long term were analyzed in this study. SPI calculation steps are presented in detail in (McKee et al., 1993) and Topçu and Seçkin's (2016) studies. Drought categories with SPI values are available in Table 1.

DEPI calculation is carried out in the following consecutive stages: In the first step, the precipitation anomalies (*AP*) of each month of the series are calculated from the following expression:

$$AP_i = P_i - P_{MEDi} \qquad (1)$$

where P_i = Precipitation of the month i;

P_{MEDi} = Median precipitation of the month i for the whole study period.

An example of the calculation of these monthly anomalies is presented in Figure 3 and Figure 4.

As it is considered more appropriate than the average for highly variable meteorological regimes, the index utilized the median to identify surpluses and deficits (Pita, 2000). Second, cumulative precipitation anomalies are identified from the first month of the series. After a negative anomaly is found, a dry sequence begins, and then the accumulation is restarted in that particular month. Following this restart, month-to-month addition of anomalies proceeds. After ensuing accumulations, as

Table 1. SPI drought classifications according to SPI values (Mckee et al., 1993).

SPI values	Drought severity level
>0.00	Wet conditions
-0.99 to 0.00	Mild drought
−1.00 to -1.49	Moderate drought
−1.50 to -1.99	Severe drought
<-2.00	Extreme drought

soon as the cumulative anomalies become positive again, the dry run ends. In this wet run, anomalies carried on adding until a new negative precipitation anomaly is found. As expected, at that point a new dry sequence starts, which is estimated by using the same method. The methodology consists of continuous addition of surpluses that allows for precise anomaly prioritization and stops in the condition of negative anomaly. Thus, the evaluation of this second step match with the expression:

$$APAc_1 = AP_1,$$
$$APAc_1 = \sum_{j=r}^{i} AP_1 \quad i > 1 \qquad (2)$$

where $APAc_1$ = precipitation cumulative anomaly of the month i; r = the value marking the start of the dry run and follows the expression:

$r = max\ \{k{:}1 \leq k \leq i,\ AP_k < 0,\ APAc_{k\text{-}1} \geq 0\}$, k: parameter from 1 to i to determine which month the drought started.

It is critical to mention that if $AP_1 < 0$ *and* $APAc_{k\text{-}1} \geq 0$, then $r = i$ and, as a result $APAc_1 = AP_1$, specifying the beginning of a new dry series. In sum, in the third step, it is required to sort the series of cumulative precipitation anomalies identified in the previous stage from lowest to highest, i.e. from the months with the largest negative cumulative anomalies, or deficits, to the months with the largest positive ones, or surpluses. Following the steps outlined above is required to obtain the empirical probabilities of exceedance matching with each month of the series. After the sorting process has been performed, the formulation of DEPI requires calculating the probability of exceeding the detected event each month by utilizing the plotting positions method developed by (Weibull, 1939):

$$Pexced_{APAci} = DEPI_i = M_{APAci} \ / \ (n + 1) \qquad (3)$$

where; $Pexced_{APAci}$ =empirical probability of exceedance of the month i, namely, the DEPI of the month i; M_{APAci}

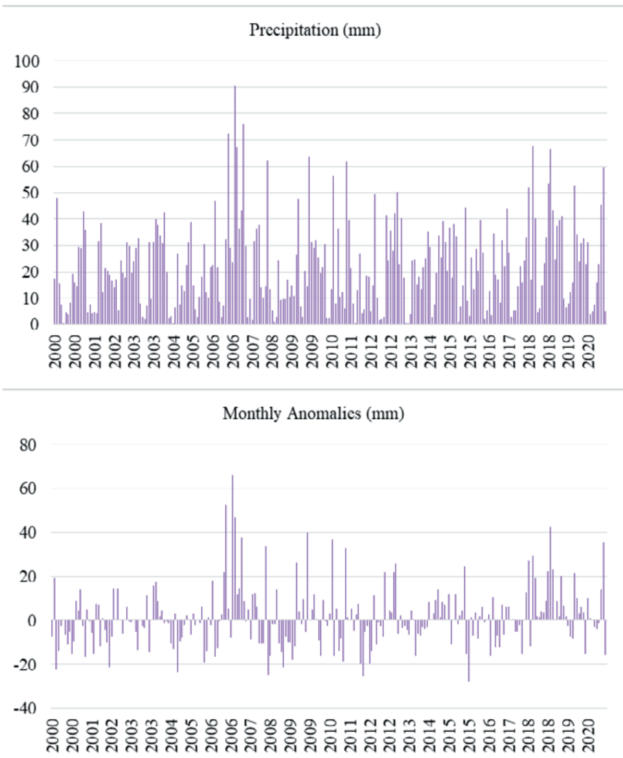

Fig. 3. Process of implementing the Drought Exceedance Probability Index (DEPI) in the precipitation series of Turkey, 2000-2021.

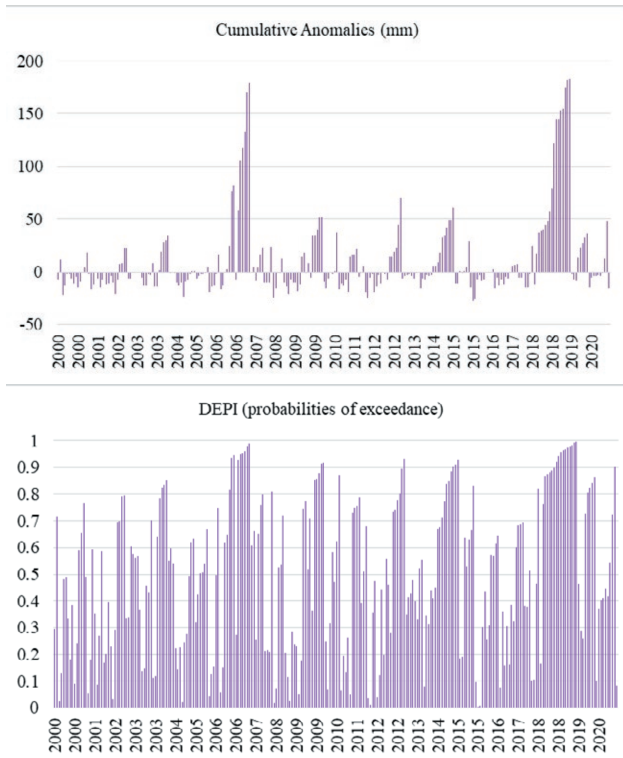

Fig. 4. Process of implementing the Drought Exceedance Probability Index (DEPI) in the precipitation series of Turkey, 2000-2021 (Continue).

Table 2. DEPI drought classifications according to DEPI values (Limones et al., 2022).

DEPI values (probabilities of exceedance)	Drought severity level	% months of a series within the interval	Return period (years)
DEPI≥0.5	Wet conditions	50	2
0.5>DEPI≥0.16	Mild drought	34	6
0.16>DEPI≥0.07	Moderate drought	9	15
0.07>DEPI≥0.02	Severe drought	5	20
DEPI<0.02	Extreme drought	2	50

= position of the precipitation cumulative anomaly of the month in the sorted series, from lowest to highest cumulative anomaly or largest observed deficit, n = total number of months in the series. Thus, the DEPI for a given month is exactly the probability of exceedance ascribed to its cumulative rainfall anomaly, determined as described above. The probability values not only contains an estimate of the hazard but also with DEPI values below 0.5 indicates significant accumulation of anomalies (not likely to be exceeded). So droughts are becoming more severe as they approach 0. The significance of the index and its further advances over other similar ones, is that it restarts with measurement of cumulative anomalies whenever a new dry month (AP_1 < 0) arises within a surplus period (with $APAc_{i-1} \geq 0$). This guarantees the proper identification of dry runs of different lengths from a single calculation of the index. DEPI drought classification values are seen in Table 2.

In this study, trend analysis was carried out to determine whether drought is decreasing or increasing over the years with the calculated index values. Drought index values were analyzed with Mann-Kendall trend analysis. Mann-Kendall test, null hypothesis H0 against xi observations randomly sorted over time, the alternative hypothesis that has an increasing or decreasing monotonic course of observations was applied to test H1. The data are treated as sequential time series. Each data value is compared with the consequent value. In the present paper, 5% level of significance is used to check increasing or decreasing trend. Since the Mann-Kendall method is a frequently used trend analysis, there are plenty of annotated sources in the literature. MAKESENS (Salmi et al., 2002) excel macro was also used.

RESULTS AND DISCUSSION

Before mapping, monthly DEPI values were graphed for data-available periods. Figure 5 highlights the annual change of DEPI values by months.

A DEPI value of 0.5, which indicates the boundary between dry and wet conditions, is indicated by a red line on the graphs. It can be asserted that the closer the DEPI values to 0, the more severe drought is experienced. The years when DEPI exceeded 0.5 were observed as wet years. According to the results, while the lowest DEPI value was observed in 2009 for January, the highest DEPI value was measured in 2019. There was a dry period between 2011 and 2014. DEPI values for February were similar to January. However, the DEPI values dropped sharply to drought values after 2020. The lowest DEPI value was measured in 2009 and 2012, while the highest was observed in 2007 and 2019 for March. A dry period was observed between the years 2008-2013 for April. While the lowest DEPI was measure in 2009, DEPI values started to decrease as of 2019 for May. The lowest DEPI values were measured in 2002, 2006, 2009 and 2012 for June. A dry period was observed between 2000 and 2004. The month of July draws a similar trend to June. The wet period was between 2017 and 2020. The lowest DEPI was measured in August in 2012, a dry period was observed between 2000 and 2006 in September, October, November and December. The DEPI values started to decrease to dry values after 2019 in December. Drought values for 6, 12 and 24 months were calculated with SPI. The Pearson correlation method was used to determine whether the findings were compatible with DEPI. It was examined whether DEPI increased (decreases) while SPI values increase (decrease) with this method in a sequence. The correlation between SPI and DEPI was visually mapped for Turkey through the Pearson correlation coefficient values SPI6-DEPI, SPI12-DEPI and SPI24-DEPI. Pearson correlation coefficient maps for SPI6-DEPI, SPI12-DEPI and SPI24-DEPI on Turkey are available in Figure 6, Figure 7 and Figure 8, respectively.

The Pearson correlation coefficient values ranged between 0.50 and 0.87. The average correlation coefficient values were 0.73, 0.75 and 0.62 for SPI6-DEPI, SPI12-DEPI and SPI24-DEPI. Figure 6 demonstrates that the lowest correlation value was observed in the inner parts of Eastern Anatolia, while the highest correlation was in the west of Southeastern Anatolia. Besides, Figure 7 indicates that the lowest correlation was found for the east of the Eastern Anatolia Region and the highest in the west of the Marmara Region and the Aegean Region. Moreover, Figure 8 illustrates that the lowest parallelism was observed for the Southeast Anatolia Region and the inner parts of the Central Anatolia Region, while the highest was for the Aegean coasts and Central Mediterranean Region. These results revealed that the highest correlation was between SPI12 and DEPI.

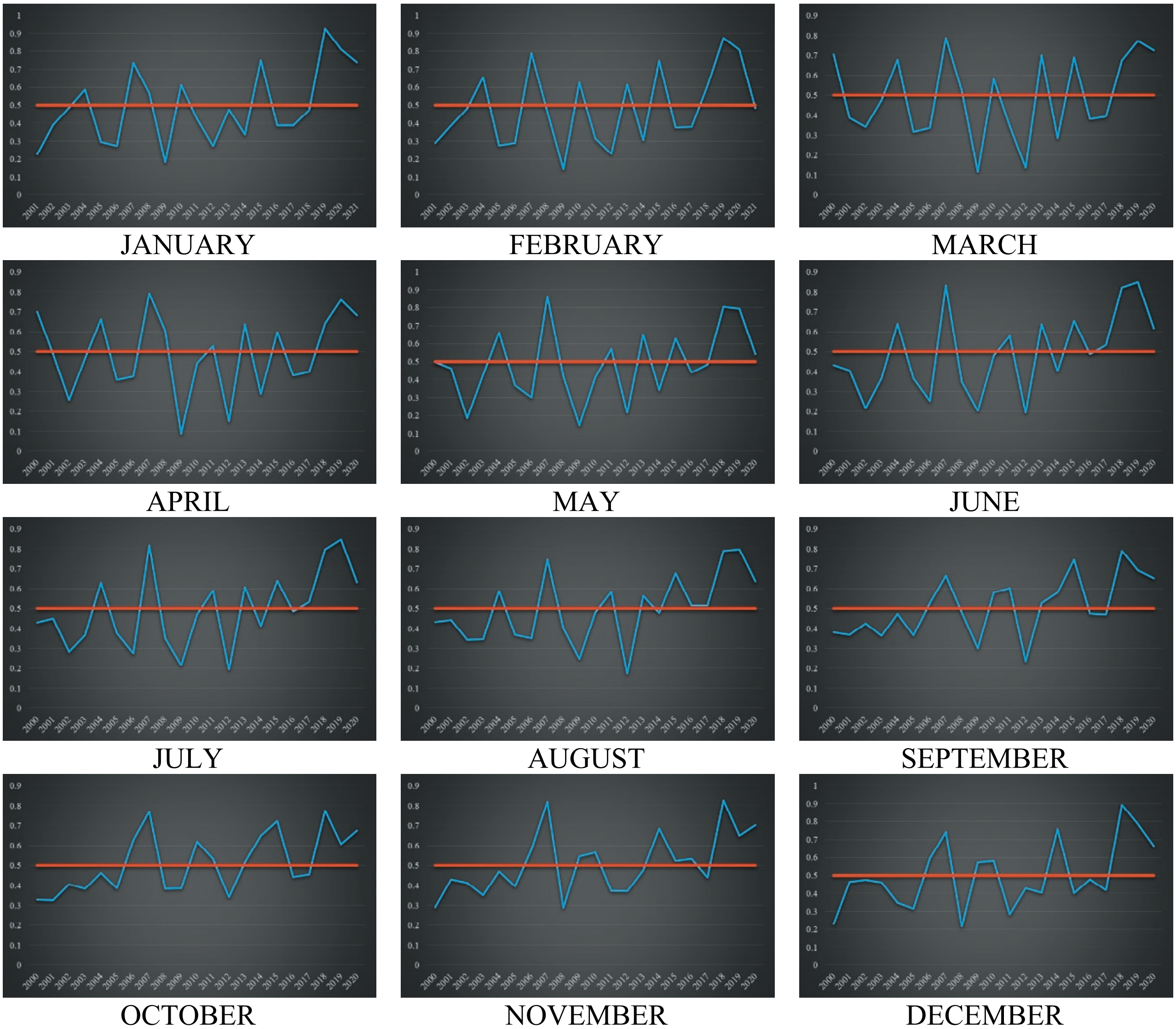

Fig. 5. Yearly change of monthly DEPI values in Turkey.

After the DEPI and SPI values were obtained, the mapping was performed using the Inverse Distance Weighted (IDW) interpolation method. A specific color scale has been determined so that the drought classification based on DEPI and SPI values can be distinguished on maps. The color scales corresponding to DEPI and SPI values is located at the end of Figure 9. It is mapped for 2001-2021 period for January and February, and for March and December 2000-2020 period, where PERSIANN precipitation data can be obtained.

Thus, the SPI12 drought values, which have the highest correlation with DEPI, were mapped. Different SPI and DEPI calculation methods have led to a difference in the drought assessment in Turkey, especially for some months. For reader-friendlier maps, the same colors were used in the SPI and DEPI drought classifications. Monthly SPI12 and DEPI maps were collaged together to reveal this difference in the best way.

These maps may indicate that the whole of Turkey is in the wet and mild drought category. The drought and wetness vary spatially by month. Another reason for the monthly drought analysis in this study is that the changes in the months cause seasonal changes. This is of vital importance especially for issues that require water resources planning such as dams and hydroelectric power plants.

The SPI12 map for January in Figure 9 indicates that wet conditions prevail throughout the country, except for

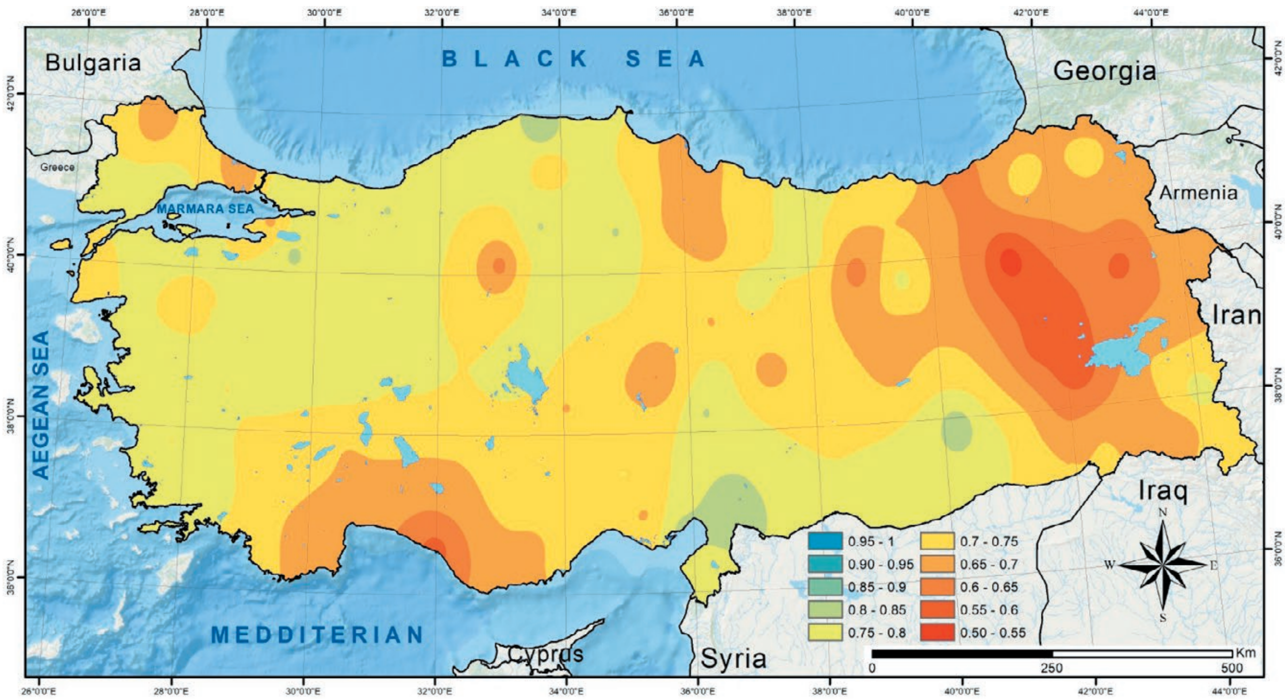

Fig. 6. Correlation coefficient map of SPI6-DEPI for Turkey.

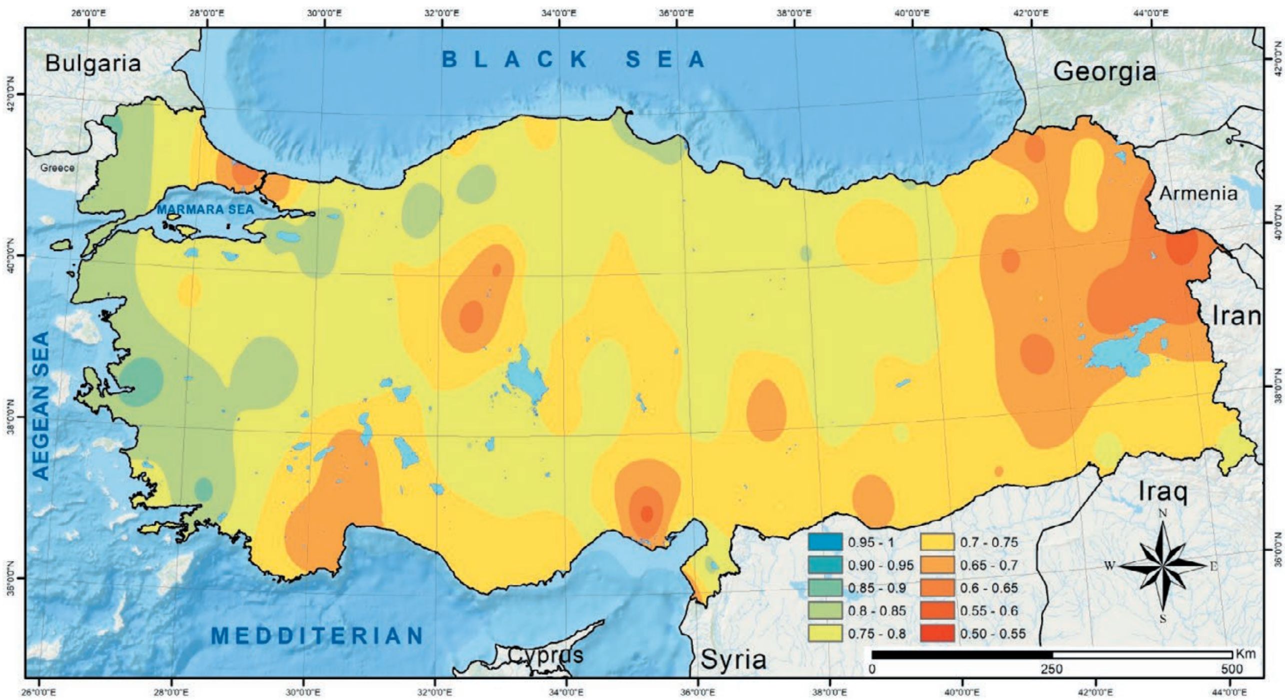

Fig. 7. Correlation coefficient map of SPI12-DEPI for Turkey.

the Southeastern Anatolia Region. However, the January DEPI map shows mild drought conditions are common except for the inner parts of the Inner Aegean, Southeastern Anatolia and Eastern Anatolia. The February maps exhibit similar conditions with January. The western parts of the country are wet in SPI12 for March,

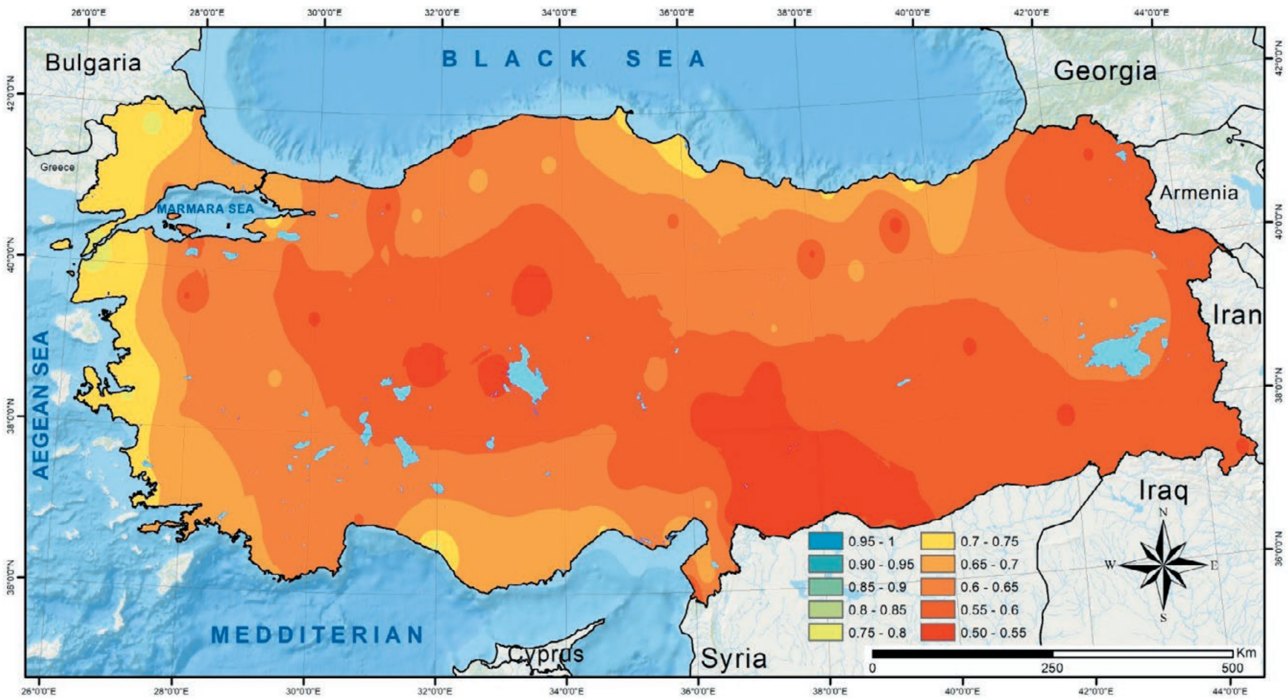

Fig. 8. Correlation coefficient map of SPI24-DEPI for Turkey.

while the other parts are mildly dry. The DEPI map indicates mild drought in the country except for the western Mediterranean and eastern Anatolia regions. Besides, the SPI12 map for April illustrates wet conditions except for the eastern Mediterranean and southeast Anatolia, while the DEPI map shows mild drought except for the south and interior parts. Almost half of the country is wet in SPI12, while some parts are wet in DEPI for May. The eastern Mediterranean, southeast Anatolia and the west of eastern Anatolia are wet in SPI12 for May, as it is wet in DEPI although similar to the SPI12 map, the inner parts of the west of the country are also mildly dry. September was similar to August in SPI12 as a mild drought was observed in the country's east by DEPI. October was similar to September in SPI12, while a mild drought was dominant in the interior parts of the eastern Black Sea region in DEPI. November SPI12 was similar to September. However, wet conditions are observed in DEPI except for the inner and western regions. December was similar to November in regards to DEPI, but the mild drought area was larger.

The drought detection success of DEPI is at a level that can be considered adequate after the comparison with SPI12. Correlation rates also support this. While SPI12 described most of the country through wet conditions, mild drought was presented in DEPI. Wet and mild drought conditions were measured by the precipitation amount calculated by the PERSIANN system and the methods used in Turkey. The results are entirely dependent on the reliability of the PERSIANN system. The mild drought occurs in cases where there is little or no precipitation, while wet conditions are classified as cases where precipitation is higher than the average. However, the lack of precipitation in a region does not mean that there is a drought, or very high precipitation does not mean that there is no drought. Because it is necessary to examine the long-term (min. 30 years) statistical precipitation series of that region. In the summer months, a large number of "0" values are encountered in the monthly precipitation total series. It should also be taken into account that only 20 years of precipitation data is used. Sudden and heavy rains as a result of the change of seasons can cause different results in the drought calculation.

Another analysis conducted in this study is the Mann-Kendall trend analysis. These analysis results are also visually mapped in Figure 10.

Only the trend maps of the DEPI values were provided since the correlation (reciprocal increase and decrease) between SPI12 and DEPI at an adequate level, and the Mann-Kendall trend analysis looks at the increase and decrease in drought values. The color scale and significance levels corresponding to these colors and whether the trend is decreasing or

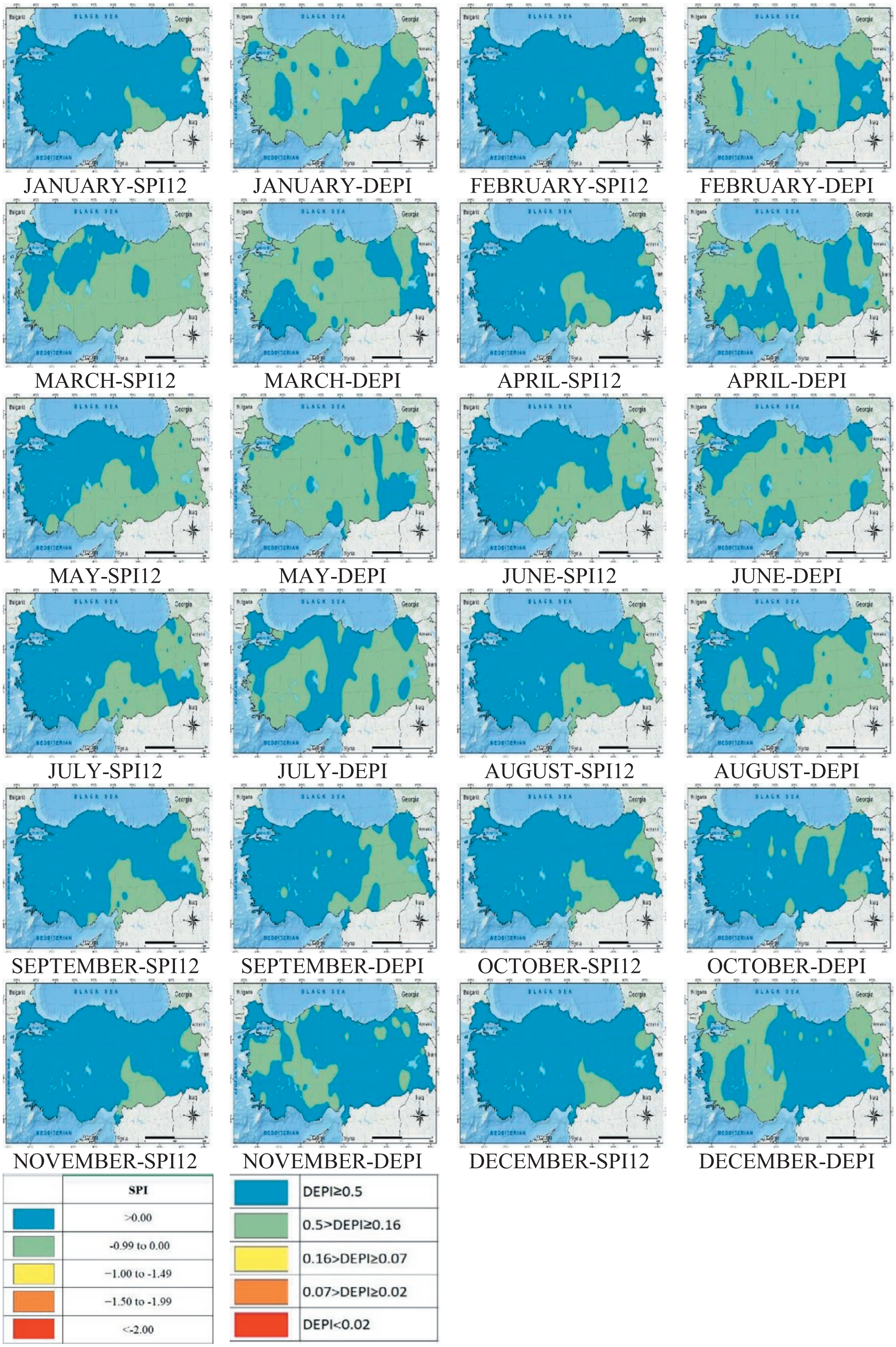

Fig. 9. Comparison of Turkey's monthly SPI-12 and DEPI maps.

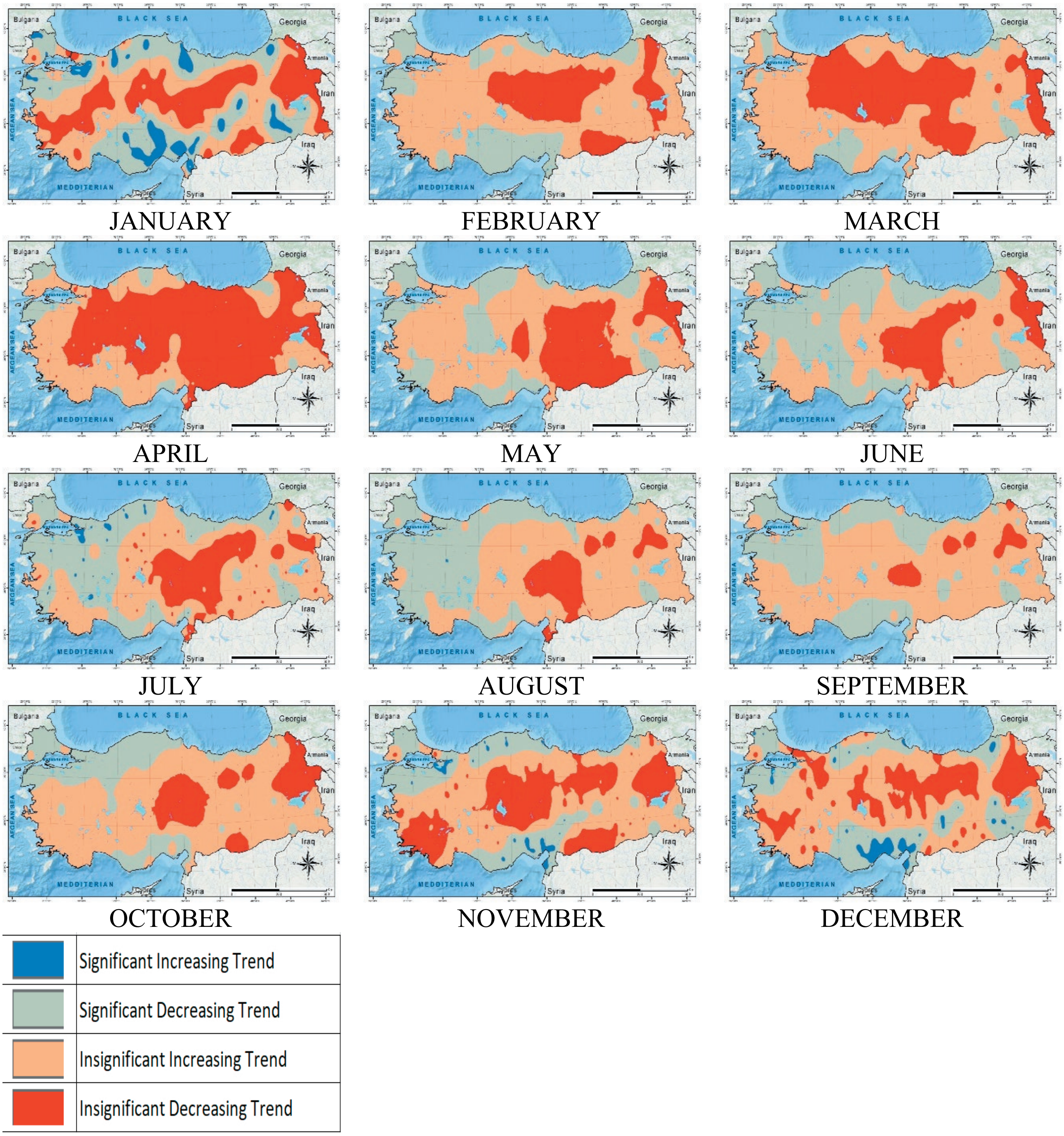

Fig. 10.Monthly trend analysis maps of Turkey's DEPI values.

increasing are given at the end of Figure 10. Mapping was performed through 4 different trends: significant increasing trend, significant decreasing trend, insignificant increasing trend and insignificant decreasing trend. As the DEPI values change between "0" and "1", the increasing trend represents the decrease in drought conditions, and the decreasing trend represents the increase.

As the trend analysis maps in Figure 10 shows a significant decreasing trend was observed in the northern and southern regions, while a significant increasing trend is observed for certain areas in January. Besides, an insignificant decreasing trend was observed in the inner parts during February. Similar conditions to February was observed in March, while the insignificant trend spread to more areas. An insignificant decreasing trend was measured throughout the country, excluding the Aegean and Mediterranean regions, in April. Another insignificant decreasing trend was detected in the east of the country in May. However, a significant decreasing trend was observed, especially in the western parts of the country, in June, July and August. Another significant decreasing trend was detected in the Central Mediterranean, Marmara, Central and Western Black Sea sections in September. A significant decreasing trend is observed, especially in the northwest of the country, in October. A significant increasing trend was observed in a limited area within the Eastern Mediterranean in November and December. Except for the regions above in the country, an insignificant decreasing trend was measured.

Drought analysis are made based on the values of long annual climatic parameters (precipitation, temperature, humidity, etc.) for the past period. The longer the climatic parameter series are, the more accurate results can be obtained in terms of the drought of a region. Today, automatic or manual meteorological observation stations cannot be installed everywhere because of lack of financial resources or unsuitable land. However, satellite remote sensing methods such as PERSIANN fill this gap. High-resolution measurements in a wide range of areas are reassuring. Satellite-sourced data were also used in our study i.e. Turkey drought assessment study. Moreover, since they recently started collecting data (about 20 years), the obtained data series quite short. It is recommended to have a minimum of 30 years of data in meteorological drought assessment indexes, such as SPI, which use monthly precipitation as data. Otherwise, it is stated that the reliability of the results might decrease.

CONCLUSIONS

Drought is a climatic catastrophe that can be seen all over the world and in any type of climate, causing deep wounds on the ecosystem. Today, with the help of developing technology, satellite data, and complex mathematical algorithms, the area and duration of the drought can be easily determined.

This drought analysis study was carried out in Turkey, one of the countries most affected by drought and global climate change, which has increased its impact in recent years. The quantity of hot days has been increasing in Turkey. An average temperature of 14.7 °C is measured in Turkey for 2019, as this is 1.2 °C higher than the normal 1981-2010 (13.5 °C) temperature. Moreover, 2018 was the second while2019 was the fourth hottest year since 1971 (MGM, 2019).

Instead of precipitation data obtained from meteorological stations observing at ground level, it was preferred to use satellite-sourced precipitation data. Because it is thought that the use of satellite data might become widespread in the future. With the help of spatial mapping, the use of which has increased frequently in recent years, the country's month-specific drought situation and drought trends have been visualized. The correlation coefficient values between SPI12 and DEPI, available in the drought maps, suggest that DEPI gives similar results with SPI, which is a classical and common method, especially for August, September, October and November. However, using only precipitation data is the only limitation of this study. Because the more the other parameters of the hydrological cycle are examined, the more definite climatic drought can be reached.

The findings indicate that there was a significant decrease in drought for certain parts of the country in January, an insignificant increase in drought has been detected throughout the country, especially in the interior, in April. A significant increase in drought was determined in the summer months. One of the consequences of climate change is seasonal shifts. A further step in this study was the examination of seasonal shifts that occur after monthly changes. Although not statistically significant, especially in the spring months, there is a shift to the summer climate and sudden and heavy rainy periods in the summer. Sudden and severe precipitation can of course deceive drought calculation methods. It can be added that rainy seasons are shortened and dry seasons are prolonged.

Agriculture is the sector that most needs water. The cultivation areas, which show a sporadic nature in Turkey, occupy broad areas in certain places and vice versa. The summers are generally hot and dry in Turkey as water is a problem in agriculture. Turkey is a developed country in terms of agriculture and animal husbandry. The water demand is increasing daily due to its ever-increasing population and growing cities. The best management of the existing water resources in the country is mandatory in all aspects in industrial, agricultural and social terms. Therefore, drought studies have become bestowed with much more scientific value. There are few drought analysis studies in the country with satellite-sourced data. Thus, the findings of this study will broaden the current literature. For this reason, it is thought that this drought analysis study will shed light on the water resources projects planned for the future of the country and will contribute to the literature because of its method and periodic monthly based analysis.

REFERENCES

Atalay I., 2011. Türkiye İklim Atlası, İnkılâp Kitabevi, İstanbul.

Aydeniz A., 1973. Tarımda verimliliğin sağlanmasında önemli etken olan su ve sulama durumumuz,Our water and irrigation status, which are important factors in ensuring productivity in agriculture Verimlilik Dergisi, 3/1: 177-199 [in Turkish].

CHRS Data Portal, Available at http://chrs.web.uci.edu/SP_activities00.php [Accessed: 01.03.2021].

De Martonne E., 1942. Nouvelle carte mondiale de l'indice d'aridité. Annales de Géographie 51: 242–250.

Environmental Systems Research Institute (ESRI). 2012. ArcView GIS version 10.1, A computer software to visualize, explores, query and analyze data spatially, USA.

Erinç S., 1984. Klimatoloji ve Metotları, Climatology and Methods, İ.T.Ü. Deniz Bilimleri ve Coğrafya Enstitüsü, İstanbul, [in Turkish].

Gibbs J.W., Maher V.J., 1967. Rainfall Deciles as Drought Indicators, Bureau of Meteorology. Australia, 48, 33s.

Hsu K., Gao X., Sorooshian S., Gupta H.V., 1997. Precipitation estimation from remotely sensed information using artificial neural networks, Journal of Applied Meteorology, vol 36, no 9, 1176-1190.

Hsu K., Gupta H.V., Gao X., Sorooshian S., 1999. Estimation of physical variables from multiple channel remotely sensed imagery using a neural network: Application to rainfall estimation, Water Resources Research, 35(5), 1605-1618.

Hsu K., Gupta H.V., Gao X., Sorooshian S., 2000. Rainfall estimation from satellite imagery, chapter 11 of artificial neural networks in hydrology, edited by Govindaraju, R. S., Rao, A. R., published by Kluwer Academic Publishers, The Netherlands, pp 209-234.

Hsu K., Gupta H.V., Gao X., Sorooshian S., Imam B., 2002. SOLO-An artificial neural network suitable for hydrologic modelling and analysis, Water Resources Research, vol 38, no 12, 1302.

Keyantash A.J., Dracup A.J., 2004. An aggregate drought index: Assessing drought severity based on fluctuations in the hydrologic cycle and surface water storage, Water Resources Research, Vol 40, W09304. doi:10.1029/2003WR002610

Limones N., Pita-López M.F., Camarillo M.J., 2022. A new index to assess meteorological drought: the 1 Drought Exceedance Probability Index (DEPI)", Atmósfera, Vol 35 (1), enero (early online release). https://doi.org/10.20937/ATM.52870

Limones N., Marzo-Artigas J., Wijnen M., Serrat-Capdevilla A., 2020. Evaluating drought risk in data-scarce contexts. The case of southern Angola, Journal of Water and Climate Change, Vol 11, Issue S1. doi: 10.2166/wcc.2020.101

Mallenahalli N.K., 2020. Comparison of parametric and nonparametric standardized precipitation index for detecting meteorological drought over the Indian region, Theoretical and Applied Climatology, 142:219–236. https://doi.org/10.1007/s00704-020-03296-z

McKee T.B., Doesken N.J., Kleist J., 1993. The Relationship of Drought Frequency and Duration to Time Scales, in Proceedings of the 8th Conference on Applied Climatology, 17.

Meteoroloji Genel Müdürlüğü (MGM). 2019. 2019 Climate Assessment, Ministry of Agriculture and Forestry, General Directorate of Meteorology, January 2020, Ankara.

Nalbantis I., 2008. Evaluation of a Hydrological Drought Index, European Water Publications, 23/24:67-77.

Nguyen P., Shearer E.J., Tran H., Ombadi M., Hayatbini N., Palacios T., Huynh P., Updegraff G., Hsu K., Kuligowski B., Logan W.S., Sorooshian S., 2019. The CHRS data portal, an easily accessible public repository for PERSIANN global satellite precipitation data, Nature Scientific Data, Vol 6, Article 180296.

Öztürk Z.M., Çetinkaya G., Aydın S., 2017. Climate Types of Turkey According to Köppen-Geiger Climate Classification, Journal of Geography, 35:17-27.

Palmer W.C., 1965. Meteorological Drought, U.S.weather Bureau, Research Paper No.45.

Pita M.F., 2000. Un nouvel indice de sécheresse pour les domains méditerranéens. Application au bassin du Gaudalquivir sudouest de l'Espagne, A new drought index for Mediterranean domains. Application to the Guadalquivir riverbasin in southwestern Spain, Publ. Assoc. Int. Climatol. 13, 225–234.

Salmi T., Maata A., Antilla P., Ruoho-Airola T., Amnell T., 2002. Detecting trends of annual values of atmospheric pollutants by the Mann–Kendall test and Sen's slope estimates – the Excel template application Makesens, Finnish Meteorological Institute, Helsinki, Finland, 35 pp.

Şen, Z., Almazroui M., 2021. Actual Precipitation Index (API) for Drought Classification, Earth Systems and Environment, 5:59–70. https://doi.org/10.1007/s41748-021-00201-0

Sorooshian S., Gao X., Hsu K., Maddox R.A., Hong Y., Imam B., and Gupta H.V., 2002. Diurnal variability of tropical rainfall retrieved from combined GOES and TRMM Satellite Information, Journal of Climate vol 15, 983-1001.

Sorooshian S., Hsu K., Gao X., Gupta H.V., Imam B., Braithwaite D., 2000. Evaluation of PERSIANN system satellite-based estimates of tropical rainfall", Bulletin of the American Meteorology Society, vol 81, no 9, 2035-2046.

Sorooshian S., Nguyen P., Sellars S., Braithwaite D., Aghakouchak A., and Hsu K., 2014. Satellite-based remote sensing estimation of precipitation for early warning systems, Extreme Natural Hazards, Disaster Risks and Societal Implications, Cambridge University Press, 99-111.

Topçu E., Seçkin N., 2016. Drought Analysis of the Seyhan Basin by Using Standardized Precipitation Index (SPI) and L-Moments, Journal of Agricultural Sciences, 22:196-215. DOI: 10.1501/Tarimbil_0000001381

Tsakiris G., Vangelis H., 2005. Establishing a Drought Index Incorporating Evapotranpiration, European Water Publications, 9/10:3-11.

Vicente-Serrano SM., Santiago Beguería S., López-Moreno J., 2010. A multi-scalar drought index sensitive to global warming: the standardized precipitation evapotranspiration index – SPEI. J. Clim. 23, 1696–1718.

Weibull W., 1939. A statistical theory of strength of materials. Ing. Vetensk. Akad. Handl., 151: 1-45.

Wilhite D.A., Glantz M.H., 1985. Understanding: the drought phenomenon: the role of definitions, Water Int, 10(3):111-120. https://doi.org/10.1080/02508068508686328

Italian Journal of
Agrometeorology
Rivista Italiana di Agrometeorologia

Firenze University Press
www.fupress.com/ijam

OPEN ACCESS

Citation: B. Douh, A. Mguidiche, M. Jar Allah al-Marri, M. Moussa, H. Rjeb (2021) Assessment of deficit irrigation impact on agronomic parameters and water use efficiency of six chickpea (*Cicer Arietinum* L.) cultivars under Mediterranean semi-arid climate. *Italian Journal of Agrometeorology* (2): 29-42. doi: 10.36253/ijam-1261

Received: March 25, 2021

Accepted: October 10, 2021

Published: December 27, 2021

Data Availability Statement: All relevant data are within the paper and its Supporting Information files.

Competing Interests: The Author(s) declare(s) no conflict of interest.

Assessment of deficit irrigation impact on agronomic parameters and water use efficiency of six chickpea (*Cicer Arietinum* L.) cultivars under Mediterranean semi-arid climate

Boutheina Douh[1,*], Amel Mguidiche[2,*], Massoud Jar Allah al-Marri[3], Mohamed Moussa[4], Hichem Rjeb[5]

[1] *Department of Engineering of Horticultural Systems and Natural Environments, Higher Institute of Agronomy of chott Meriem, University of Sousse, BP 47, 4042 Sousse, Tunisia,* boutheina_douh@yahoo.fr
[2] *The Olive tree Institute, Ibn Khaldoun 14, Sousse 4061, Tunisia; University of Sfax, Tunisia,* amelmguidiche@yahoo.fr
[3] *Food Security Department, Ministry of Municipality and Environment, Qatar,* mjm-marri@mme.gov.qa
[4] *Laboratory of Eremology and Desertification Control, Institute for Arid Regions of Medenin, Tunisia,* mohamed.Moussa@ira.rnrt.tn
[5] *Department of Horticulture and Landscape, Higher Institute of Agronomy of chott Meriem, University of Sousse, BP 47, 4042 Sousse, Tunisia,* hrejeb62@yahoo.fr
*Corresponding authors: boutheina_douh@yahoo.fr; amelmguidiche@yahoo.fr; the first and the second author contributed equally to this research

Abstract. Six kabuli chickpea genotypes (*Cicer Arietinum* L.) were evaluated under three water levelss at the open field during February -June 2018. This study was conducted to evaluate the chickpea water stress, on soil water dynamic, agromorphological traits, and water use efficiency to estimate variability levels between varieties and to identify the varieties of chickpea adaptable on semi-arid bioclimatic stage. For this purpose, a trial was conducted at the Higher Agronomic Institute of Chott Mariem (Tunisia). There is no effect of the treatment on the height, biological yield, and branching number. The seeds weigh, PCG, seed yield, harvest index, and water use efficiency relative to seed have the highest value in T1 (100% of ETc) when water use efficiency relative to biological yield, number of pods and of seeds recorded the highest values in T3 (50% of ETc). Univariate analysis showed highly significant differences between genotypes for many traits. Principal Component Analysis was performed for all traits and allowed to define two axes. The first one explains 49.30% of the variability of the total trait and was formed by genotypes 'Beja', 'Nayer' and' 'Rebha'. Genotypes forming this axe are closely related to each other according to their common morphological characters like height (r=0.88), biological yield (r=0.93), bringing the number (r=0.53), seed yield (r=0.81), WUE relative to seed (r=0.75), harvest index (r=0.65) and WUE relative to biological yield (r=0.94). The second clustered genotypes 'Bochra' and 'Nour'. This second axe (27.99%) is represented by pods number (r=0.87), seed number (r=0.87) and PCG (r=0.78).

Keywords: Soil Water Content, evapotranspiration, chickpea, harvest index, Seed yield, Mediterranean region.

INTRODUCTION

The sustainability of agricultural production depends on conservation and appropriate use and management of water resources. Water scarcity exacerbated by climate change is expected to define food production in the coming decades. Recently, water crisis has become one of the most significant problems in the world especially in the Mediterranean region where irrigation is required for improving productivity (Douh et Boujelben, 2011; Rabi et al., 2012). The amount of water available for agriculture in the Mediterranean is decreasing due to pressure from the growing population and an increased frequency of drought. The pressure of using water in agriculture sector is increasing, to create ways to improve water use efficiency and taking a full advantage of available water (Stewar, 2001).

Fabaceae are quality foods given their richness in proteins which can correct the deficit in animal proteins. Besides, they are rich in essential minerals and lysine, so they are complementary to the nutritional profiles of cereals (Bacha et Ounane, 2003). In Tunisia, chickpea (*Cicer arietinum* L.), particularly Kabuli genotypes, is the second pulse crop after fababean. It is grown, in spring rainfed conditions (Wery, 1990), in humid and sub-humid regions, mainly at Bizerte, Mateur, Beja, Jendouba, and Nabeul areas (Ben Mbarek and al., 2011). It is cultivated on an average annual area of 19 650 ha, which represents 1.1% of the areas sown to field crops. Annual production is of the order of 13 520 tonnes with an average yield of 670 kg ha^{-1}. To meet the needs of the concept, the Tunisian government uses imports on the order of 19 000 t year^{-1}, which represents 141% of national production. The chickpea suffers from many difficulties, apart from the environmental conditions and the lack of mastery of cultivation techniques which are not insignificant causes of the weakness of production; it seems that the major problem remains that of an abiotic factor such as the deficiency in phosphorus, salinity, and drought. The latter is a major factor, which in the event of low availability, constrains the production of legume crops. Two types of droughts affect the chickpea crop in Tunisia, a spring caused by the breakdown of rainfall and a terminal one occurs at the end of the crop's growth cycle due to a lack of rainfall and drying out of water reserves in soil (Wery et al., 1994).

Most of the chickpea crop in the world is produced on residual moisture but supplemental irrigation can enhance production. Especially irrigation during the pre-flowering period and at early pod fill resulted in increased yield at several locations in India (Saxena, 1980). Many studies have been conducted to assess the yield potential of chickpea under different irrigation levels (Ali (2017), Kadam et al. (2014)). Ali (2017) proved that the variety had a significant effect on yield attributes and seed yield. Besides, the highest water use efficiency of 263.01 kg ha^{-1} cm^{-1} was also found in the treatment which received no irrigation. From the results of his study, it is revealed that under the prevailing climatic and soil condition, the chickpea cultivars do not need any irrigation at Magura, rather it reduces yield. Ilhe et al. (2009), conducted field experiment at Ahmednagar, India, to evaluate water production function for chickpea under sprinkler irrigation. They concluded that growing of chickpea resulted in the more seed yield 25.90 q ha^{-1} and maximum benefit in terms of cost ratio 2.57 as compared to the surface irrigation method.

The main objectives of this study were assessing the best chickpea genotypes which adapt to the central of Tunisia climatic conditions by identifying agronomic attributes whose selection would lead to improvement in chickpea seed yield. Added to that this research help producer to manage their inputs to maximize efficiency of the available water resources. Certainly, the evaluation of varieties from the national chickpea improvement program is of particular interest to ensure food security and help smallholders cope with climate change.

MATERIAL AND METHODS

1. Experimental sites

The test was carried out in spring cultivation on a plot of the experimental domain of the Higher Agronomic Institute of Chott Mariem located in the Center East of Tunisia which is part of the semi-arid bioclimatic stage below a latitude of 35°91' North and a longitude of 10°55' East, Altitude 19 m above sea level. The climate is semi-arid superior to temperate winter and hot summer. Climatic data during the study period was provided by a meteorological station located 100 m from the experimental site. The monitoring of climatic data was used for irrigation management. Thus, the minimum and maximum temperatures have the respective average values of 10 and 23°C. The relative humidity and the wind speed are 70% and 2.3 m s^{-1}, respectively. This area is characterized by an average annual rainfall and evaporation of 270 mm/year and 1243 mm/year, respectively, and a drought that extends for five months out of twelve (May – September). It is defined by reduced and scarce precipitation, evaporation, and high maximum temperatures.

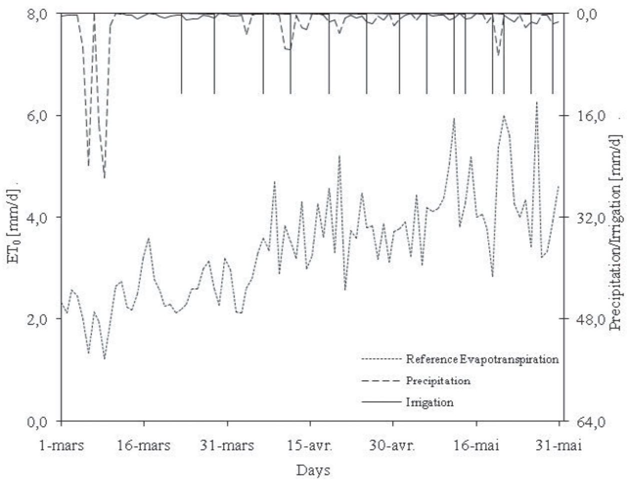

Figure 1. Daily values of precipitation, Full irrigation and reference evapotranspiration during the study period**.**

Figure 1 shows the daily values of reference evapotranspiration (ET0), which increased with climatic conditions from about 2 mm/day in early March to a maximum of about 6 mm/day at the end of May. Daily rainfall values and Full irrigation levels are also presented.

In this research, we chose six varieties of chickpea of the Kabuli type registered in Tunisia as support to determine the behaviour of its varieties to water stress and its adaptation to the climate. The six varieties are Beja, Rabha, Nayer, Nour, Amdoun and Bouchra. The spring chickpea thrives, mainly, on the water supply in the soil. The latter is gradually exhausted with the development of culture. From the end of the vegetative development phase until maturity, the crop has undergone water stress which affects many parameters by morphological, physiological, and metabolic changes that occur in all the organs of the plant and result in a reduction yield (Cochard et al., 2002).

2. Experimental design

The trial was carried out on a plot of the experimental domain of the Higher Agronomic Institute Chott Mariem. Sowing was carried out in February with a density of 12.5 plants/m^2 with a spacing of 0.2 m between rows and 0.4 m on the row. Each elementary plot was made up of nine lines five meters in length. The experimental setup adopted was in randomized blocks with three replications. The test plots were divided into blocks spaced 1.5 m apart. The previous crop was a worked fallow. Sowing took place on February 26 and harvest took place on June 18.

3. Soil characterization

The method used is the particle size analysis method by sedimentation (the ROBINSON pipette). The pipette apparatus conforms to NEN5357 and ISO/DIS 11,277. The method is based on the difference in sedimentation rates between light particles and larger ones.

3.1. Electrical conductivity

By determining the electrical conductivity (EC) of the soil, we can deduce the salinity of the soil extract. The laboratory preparation with the soil saturation phase after air-drying is considered. The principle of this method is to take a sample of soil (200 g) with distilled water until saturation is reached and to extract the filtrate by vacuum filtration. The EC of this extract is thus measured by a conductometer.

$$S = 0.64\ EC \qquad (1)$$

With: – S: Salinity of the measured sample (g/l).
EC: Electrical conductivity (mS/cm).

Three replications are considered for each depth 20, 40, and 60 cm.

3.2. Hydrodynamic properties of the soil

Soil Water content (SWC)

The measurements of the water content by weight are made before and after each irrigation by layer [0–20 cm], [20–40 cm], and [40–60 cm]. The samples are excreted from the soil by the auger and brought to the laboratory for weighing in a fresh state and placed in an oven for 24 hours to then determine the dry mass of each sample. The water content by weight in each sample corresponds to the ratio of its mass of water to its mass in the fresh state. This water content is multiplied by the bulk density to determine the volume of water content.

Water content at field capacity (θ_{fc})

The water content at field capacity represents the maximum amount of water that the soil can hold. It is determined in the laboratory with a pressure cooker. The determination of the water content at the field capacity was made with a pressure cooker.

Water content at permanent wilting point (θ_{pwp})

The moisture content at the permanent wilting point is the moisture in the soil from which the plant can no longer draw water, and wilts then die if this moisture level continues. The determination of the wilting point was made with a pressure cooker (15atm).

4. Irrigation and crop water requirement

Three irrigation levels were applied to the crop to study the behavior of the six varieties to water stress. The irrigation system used is the drip irrigation system with integrated drippers delivering a flow rate of 4l h^{-1}. The spacing between the drippers is 40 cm while that between the ramps is 20 cm.

Field data from the Regional Research center on Horticulture and Organic Agriculture of Chott Meriem weather station were used to estimate reference evapotranspiration and to calculate crop water requirements using CROPWAT 8.0 model. The reference evapotranspiration was used to simulate optimal irrigation schedule. Irrigation water supplies are made based on the crop's potential evapotranspiration (ETc). The crop coefficient (Kc) and the duration of the physiological phases of chickpea adopted are those used by the FAO 56. In addition, the reported information on climate, soil and crop constituted the input data. At the field studies, various irrigation treatments were applied to chickpea crops, full irrigation T1 corresponds to 100% of ETC and deficit irrigation T2 and T3 respectively 75 and 50% of ETC (Table 1).

CROPWAT Model input parameters are:

- Climate: temperature, rainfall, wind speed, relative air humidity, solar radiation
- Crop: Kc, Maximum rooting depth, area covered by plant,
- Soil: Initial soil moisture, Daily Soil Moisture, Deficit soil condition

5. Agronomic parameters related to vegetative development

5.1. Plant height

The height growth of continuously driven plants was measured using a graduated ruler at each vegetative stage on six plants of each variety and each treatment.

Table 1. Cumulative precipitation, Irrigation levels and total water consumption for the different treatments during the growing season of Chickpea.

	Cumulative precipitation (mm)	Irrigation level (mm)	Total water consumption (mm)
T1	68	175	243
T2	68	114	182
T3	68	54	122

5.2. Root dry matter rate (RDMR)

The root mass of the sacrificed plants, carefully rinsed with distilled water and wrung out with filter paper, was weighed, using a laboratory precision balance, in the fresh state and the dry state after drying in an oven at 80° C for 48 hours. The RDMR (%) is calculated by the formula:

$$RDMR = \frac{Dw}{Fw} * 100 \quad (2)$$

With:
Dw: the weight of the dry matter of the roots of the sacrificed plants (g).
Fw: the fresh weight of the roots of the sacrificed plants (g).

5.3. Root fineness (RF)

In response to nutrient-limiting conditions, plants may increase root fineness or specific root length. Root fitness is defined as the root length per gram root weight. It is calculated by the following formula:

$$RF = Rl/Dw \quad (3)$$

With:
Rl: the length of the root system of the sacrificed plants (cm);
Dw: the weight of the dry matter of the roots of the sacrificed plants (g).

These measurements were made at the end of the growing season with 15 plants per treatment and per variety.

5.4. Above-ground biomass (AB)

It is the product of the mass of the aerial part per plant, weighed at harvest, by the density of the seedling.

5.5. Leaf area index (LAI)

At the end of each stage, chickpea plants, at the rate of three plants per variety and treatment, are removed. Leaf area is defined as the area of green leaves in a plant canopy. This operation is carried out by a rectangular grid of length 1.2 m and width 0.8 m, composed of 96 elementary sections of dimensions 10 cm by 10 cm (figure 2). It consists of fixing the grid on two lines of each processing; we always try not to change the location of

Figure 2. Determination of the soil cover rate per plant.

the grid in each reading. These are the sections of which at least half are covered by the sacrificed plant. In the laboratory, the leaves, made up of leaflets and rachis, were amputated. The leaf area was measured in cm^2, using 'Image J' software. The leaf area index corresponds to the ratio of the leaf area to the area occupied per plant in cm^2 according to the formula:

$$LAI = LA/Ss \quad (4)$$

LA: Leaf Area of the sacrificed plant (cm);
Ss: Surface occupied by the plant (cm).

5.6. Agronomic parameters related to production

The following parameters were measured on ten plants selected at random for each variety and each treatment:

- pods/plant: the number of pods per plant at harvest, the pods of each plant were removed and counted; pod weight (g/plant): this is the product of the weight of pods harvested per plant and the density of the sowing.
- The number of seeds per plant were counted and divided with total number of pods recorded from each plant to obtain number of seeds/pod.
- SY: the seed yield was recorded from each plot and expressed as kg ha^{-1}: the weight of the seeds collected per plant, from each plot after the color of the plant and pod turned yellow, is extrapolated to the hectare;
- PCG: the weight of 100 grains was recorded from each plot and expressed in gram (g);
- HI: Harvest index defined as the ratio of the weight of the seeds (SY) harvested to that of the biological yield (BY) per plant. It is calculated according to the formula of Yoshida (1981) as follows:

$$HI = \frac{SY}{BY} \quad (5)$$

SY: Seed Yield (kg ha^{-1});
BY: Biological Yield (kg ha^{-1}).

5.7. Water use efficiency (WUE)

It defines the quantity of production obtained by a unit of water used. It is calculated considering organic and seed yields. From this, we can distinguish the efficiency of use of dry matter and seed water. This notion takes into account the need to maximize production per unit of available water in the context of increasing food demand and limited water resources (Molden et al., 2010). Siddique et al., (2001), clarified that the WUE could be determined according to the dry matter yield according to the formula:

$$WUE_{bio} = DW / ETc \quad (6)$$

WUE_{bio}: Biological Water Use Efficiency (g mm^{-1})
DW: Dry Weight (g)
ETc: Crop evapotranspiration (mm)

According to Bamouh (1998), WUE_{DW} is probably the most suitable for arid and semi-arid zones since in these regions the yield of straw is important or even more than that of seeds. The WUE can also be determined according to the biological yield (organic WUE) (Oweis et al., 2004) or according to the seed yield (the WUE s) according to the formula:

$$WUE_s = \frac{SY}{ETc} \quad (7)$$

WUE_s: Seed Water Use Efficiency (kg ha^{-1} mm^{-1})
SY: Seed Yield (kg ha^{-1})
ETc: Crop evapotranspiration (mm)

6. Statistical analysis

The data was subject to obtained underwent analysis of variance (ANOVA) with the procedure (GLM), for General Linear Model was conducted using SPSS software (version 23). The means fitted to the model (LSMEANS) were calculated for each treatment through the Student-Newman-Keuls test (SNK) at the 5% threshold for the comparison of the means.

The present study was aimed to evaluate the agronomic parameters of chickpea for identify and rank important traits and genotype based on Principal Component Analysis (PCA) for evolving better hybrid in chickpea adapted to semi-arid climatic conditions. The result of PCA explained the genetic diversity among the chickpea genotypes.

Ascending Hierarchical Classification (AHC) is an algorithm that groups similar objects into groups called clusters. The endpoint is a set of clusters, where each cluster is distinct from each other cluster, and the objects within each cluster are broadly similar to each other.

PCA and AHC were performed with XLSTAT software.

RESULTS

1. Physical and hydrodynamic characteristics of the soil

The soils of Chott Mariem have been described in three horizons [0–20 cm], [20–40 cm], and [40–60 cm] since there was a change in color of the layers at different depths. As the soil texture is relatively balanced and homogeneous, almost the same parameters as water content at permanent wilting point (θ_{pwp}) and field capacity (θ_{fc}), saturated hydraulic conductivity (K_s) were recorded for all three horizons. The results are presented in Table 2.

According to the United States Department of Agriculture soil classification (USDA, 1951), all three layers of Chott Mariem soil belong to the same sandy-clay textural class. Thus, the soil is homogeneous, leading to the same hydrodynamic behavior. Up to 60 cm deep, the presence of abundant roots from previous crops and biological activity acting on soil life and fertility for the benefit of the crop is reported.

2. Soil water content Evolution at different depths

The variation of the SWC at different depths (20, 40 and 60 cm) and for different treatments T1, T2 and T3 respectively 100, 75 and 50% of ETc are illustrated in figure 3 (a, b and c). The three curves present the same appearance. The fluctuations are due to the inflow of water. The volume water content in the soil for T1 and T2, has a significant variation, at 60 cm depth ranging from 6 to 32%, while, at the depth of 20 and 40 cm, it varies between 10 to 35% with a slight difference less than 5%. The values of the SWC T3 are almost constant with a slight difference of less than 7%, which is relatively more stable than T1 and T2. Indeed, the present study has shown that the water content of the soil increases after water supply (either by irrigation or by rain). However, it decreases over time as the crop's water needs increase. This decrease in water content indicates that the chickpea was more stressed during the ripening phase than at other phases. This phase coincided with the end of May until mid-June during which rain was scarce and even absent. All water supplies are by irrigation during this period 88.12 mm. The results show that the soil moisture is more stable and more uniform for the T3 treatment than the T1 and T2 treatments with a slight difference. The analysis of the variance of SWC allowed us to conclude that there is a significant difference between the treatments at the threshold of $\alpha = 5\%$. This is because the SNK test classified the water content into two groups. The first group consists of the T1 treatment, and the second class contains the T3 and T2 treatments. A comparison of the mean reveals two homogeneous groups that interfere with each other. The highest SWC is reached with the full irrigation at the soil surface 0–20 cm, while the lowest value is recorded at 60 cm depth with 50% of water requirements.

Table 2. Physical and hydrodynamic soil characteristics of Chott Meriem.

Soil layer (cm)	Clay (%)	Silt (%)	Sand (%)	θ_{fc} (%)	θ_{pwp} (%)	K_s (cm h^{-1})	pH [-]	EC (mS/cm)
00–20	11.57	3.63	81.8	25.25	9.84	1.36	7.5	0.83
20–40	12.71	2.95	81.3	25.15	9.74	1.42	7.5	0.77
40–60	12.49	2.31	82.2	24.9	9.49	1.38	7.5	0.76

3. Agronomorphologic parameters

Figure 4 shows the variation in the height of chickpea varieties depending on the water levels. The length of the stem is proportional to the irrigation levels and varies from 34 to 50.33 cm. The comparison of the means showed that three homogeneous groups interfere with each other, and which represent the three irrigation levels, except for Amdoun and Bouchra which did not show any significant difference between T2 and T3. For the deficit irrigation T3, Nayer and Amdoun varieties are characterized by the longest stems and have respectively 45.83 and 45.17 cm while Rabha, Beja and Nour are characterized by the shorter stems respectively 34, 34.5 and 36 cm. The other varieties have stems of intermediate lengths. As a result, it is possible to use the stem length trait as a criterion for identifying the variety most sensitive to water stress. In our case, we can say that the Amdoun and Nayer varieties are the most resistant to water stress while the Rabha, Beja, and Nour varieties are the most sensitive to water stress.

Figure 5 shows the leaf area index according to the irrigation levels. The comparison of the means showed

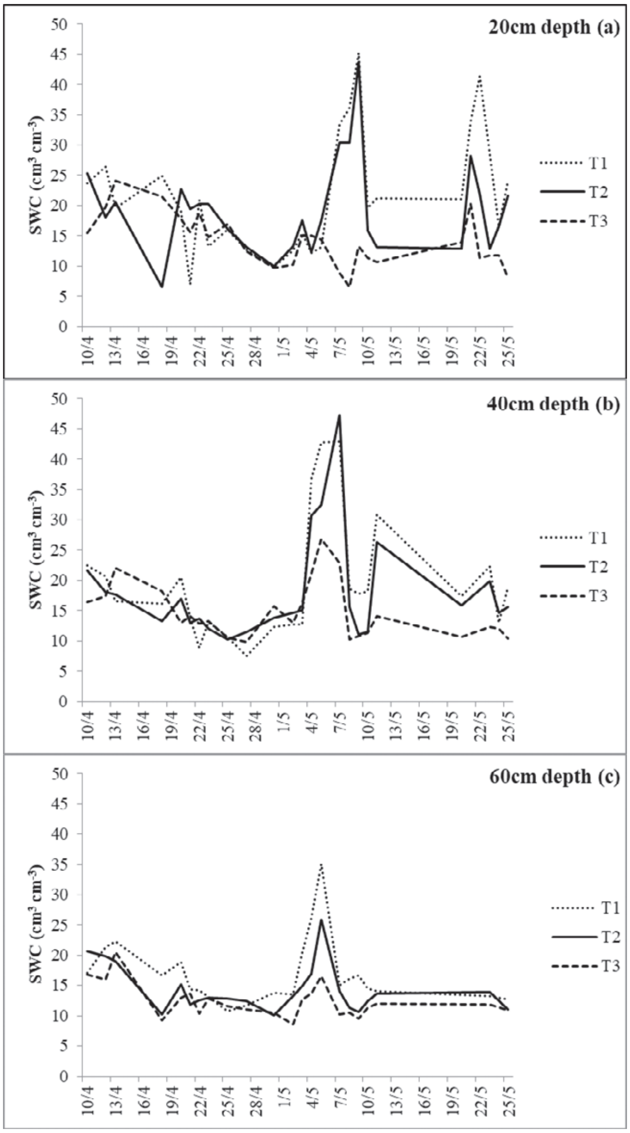

Figure 3. SWC for different treatments T1, T2 and T3, at different depths 20, 40 and 60 cm respectively (a), (b) and (c).

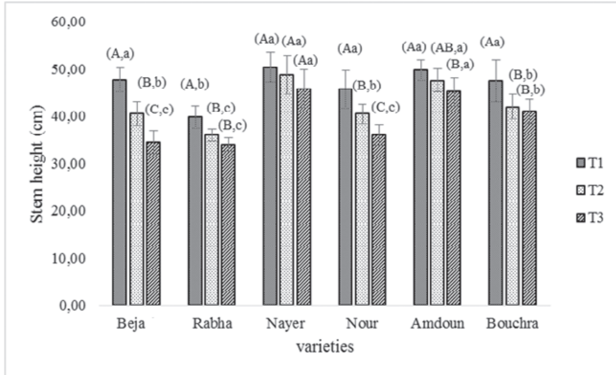

A B and C: present the height classification groups according to the irrigation level.
a, b and c: presents the height classification groups according to the variety.
Means followed by the same letters have no significant difference based on the LSD test at 5% error probability.

Fig. 4. Mean values of the stem height as a function of the interaction's varieties × Irrigation level.

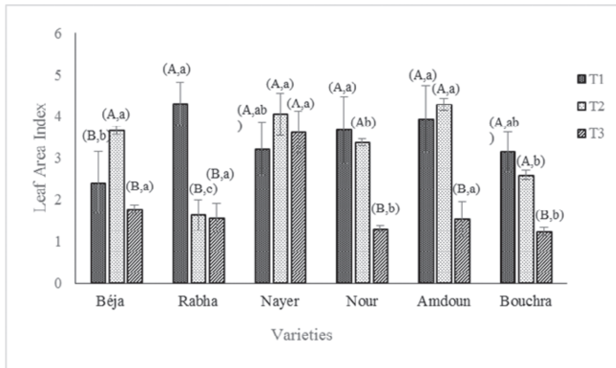

A B and C: present the height classification groups according to the irrigation level.
a, b and c: presents the height classification groups according to the variety.
Means followed by the same letters have no significant difference based on the LSD test at 5% error probability.

Fig. 5. Mean values of LAI as a function of the interaction's varieties × Irrigation level.

that two homogeneous groups represent the three irrigation levels (A and B). The comparison of the means showed that the highest leaf area index is 3.39 and recorded with the full irrigation (T1 treatment); while the lowest index is 1.83 and recorded at processing level T3. The leaf area index of chickpea varieties ranges from 2.32 to 3.63. The comparison of the means showed that there is a single homogeneous group that represents the six varieties. Similar values indicate that there is no varietal variability for this parameter. At the interaction level (Varieties × Irrigation levels), the leaf area index varies from 1.23 to 4.32. It is highest with T1 in Rabha and the lowest with the 50% level of ETc in Bouchra. The comparison of the leaf area index of the chickpea varieties under the different irrigation levels showed two homogeneous groups (A and B). The first group, characterized by high LAI, consists of Rabha, Nayer, Nour, Amdoun and plugged with the irrigation level 100% of ETc; Beja, Nayer, Nour, Amdoun and Bouchra with the irrigation level 75% of ETc and Nayer with the lowest level of ETc 50%. The second group, characterized by low LAI, is made up of Beja with the 100% level of ETc, Rabha with

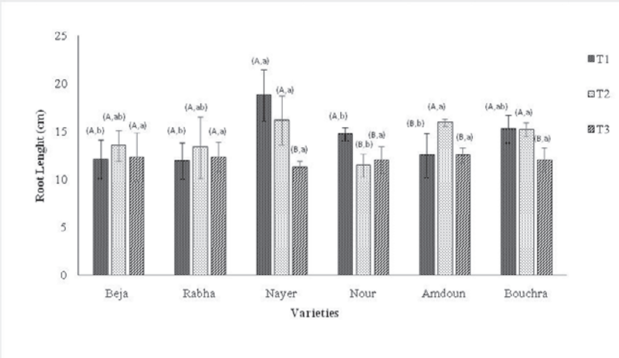

A B and C: present the height classification groups according to the irrigation level.
a, b and c: presents the height classification groups according to the variety.
Means followed by the same letters have no significant difference based on the LSD test at 5% error probability.

Fig. 6. Mean values of the root system length as a function of the interaction's varieties × Irrigation level.

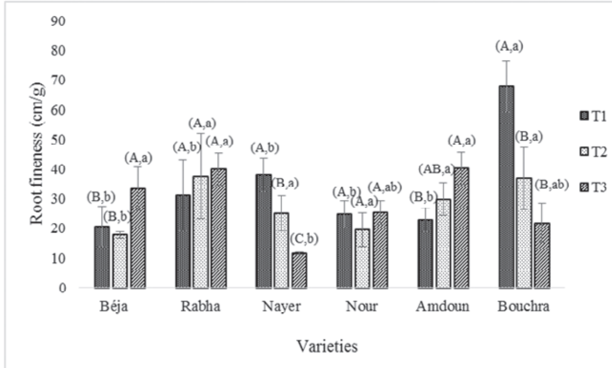

A B and C: present the height classification groups according to the irrigation level.
a, b and c: presents the height classification groups according to the variety.
Means followed by the same letters have no significant difference based on the LSD test at 5% error probability.

Fig. 7. Mean values of root fineness as a function of the interaction's varieties × Irrigation level.

the 75% level of ETc and Beja, Rabha, Nour, Amdoun and Bouchra with the level. 50% of ETc. We can see that the Nayer variety develops even in conditions of water deficit.

Figure 6 shows the variation in the length of the root system as a function of interactions (varieties × irrigation levels). The interaction (varieties × irrigation levels) has no significant effect on the length of the root system. But comparing the means has shown that two homogeneous groups interfere with each other. The longest root system is produced by the Nayer variety with the 100% rate of ETc (18 cm); while the shortest root system is produced by the Nour variety with the 50% level of ETc.

Figure 7 presents a comparison of the variations in root fineness values as a function of interactions (Varieties × Irrigation levels). The fineness of the root or specific length of the roots is proportional to the irrigation levels. The comparison of means showed that there is only one homogeneous group. With all three irrigation levels, the RF values are considered similar. But a slight increase is noted with the lower level (50% of ETc). RF plays an important role in the drought resistance of plants. The comparison of the average RF values showed that it is proportional to the variety and reveals three homogeneous groups that interfere with each other. For the full irrigation, the highest value of RF is produced by the Bouchra variety with 67.8 cm g^{-1}, the lowest value is produced by Beja 20.5 cm g^{-1}. While for the deficit irrigation 50% of the crop evapotranspiration the highest value of RF is produced by Amdoun, Rebha and Beja wich recorded an average of 40.1 cm $g^{-1}$and the lowest are for Nayer 11.4 cm g^{-1}.

The variation in the dry matter content in the roots is shown in Figure 8. The RDMR values vary between 14.6 and 32.2% for T1, 28.0 and 42.7% for T2 and 24.6 and 33.6% for T3. Indeed, the more the plant is subjected to water stress, the more the plant devel-

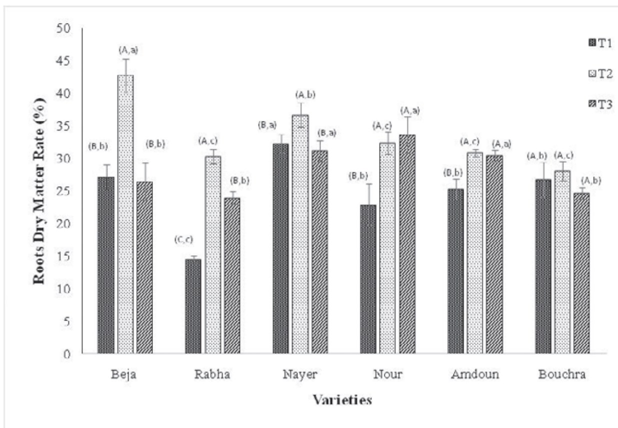

A B and C: present the height classification groups according to the irrigation level.
a, b and c: presents the height classification groups according to the variety.
Means followed by the same letters have no significant difference based on the LSD test at 5% error probability.

Fig. 8. Mean values of dry matter rate in the roots as a function of the interaction's varieties × Irrigation level.

ops its root system to extract water from the soil. The RDMR varies are depending on the variety of chickpea. The comparison of means revealed two homogeneous groups that interfere with each other. For T1, the root system of the Nayer variety is the richest (32.2%), while Rabha is the poorest in the dry matter (14.6%). Statistical analysis using the SNK test allowed us to detect a highly significant difference between the different irrigation treatments for each variety except for the Bouchra where the RDMR is not affected by the irrigation levels.

4. Agronomic parameters related to production

The number of seeds per plant varies with the irrigation tratment. The comparison of the mean revealed two homogeneous groups. The first one consists of T1 and T2 (100% and 75% of ETc) while the lowest level (50%) is presented by the second group. Under the different irrigation levels, the weight of 100 seeds varies from 14.479 ± 4.75 to 36.259 ± 10.22 g. The comparison of averages revealed three groups that interfere with each other. The highest PCG was recorded for full irrigation. These results indicate that the 50% irrigation level of ETc caused intense water stress which greatly reduced pod filling and resulted in the formation of empty pods and stunted seeds. Under the effect Irrigation level, the highest seed yield values were recorded for the full irrigation, and it varies from 220.229 ± 51.13 kg ha^{-1} (T1) to 490.667 ± 16.61 kg ha^{-1} (T3). The water use efficiency relative to biological yield is inversely proportional to the irrigation level. The comparison of means revealed three homogeneous groups. The first group contains the highest values of 0.125 ± 0.029 g/mm found with the lowest level (50% of the ETc), the second group contains the intermediate values (0.090 ± 0.01 g/mm) recorded by the irrigation level 75% of the ETc while the last group includes the values of 0.067 ± 0.02g/mm recorded by the full irrigation.

Table 3 showed that, statistically, there is no effect of the treatment on the plant height, biological yield, and branching number. The PCG (weight of 100 seeds (g/100 seeds)), seed yield per hectare (SY), harvest index, and water use efficiency relative to seed have the highest value in T1 (100% of ETc) when water use efficiency relative to biological yield, number of pods and seeds recorded the highest values in T3 (50% of ETc).

The more the plant is subject to water stress, the higher the number of pods per plant and the higher the number of seeds, while seed weights are low and consequently seed yield and harvest index are negatively affected by water stress.

Principal Component Analysis and individual variations

Data were considered in each component with Eigen value > 1 which determined at least 10% of the variation. The higher Eigen values were considered as best representative of system attributes in principal components. Eigen values of five component axes and percentage of variation accounting for them obtained from the principal component analysis are presented in Table 4. The results of the PCA showed that the variables represented 77.29% of the total inertia on the first two axes, which constitutes a strong plan in the discrimination of the variables.

Table 3. Mean quality Agronomic parameters related to production.

Variable	T1	T2	T3
Plant height (cm)	36.767 ± 2.32 (a)	38.567 ± 2.93(a)	36.233 ± 3.45(a)
Biological yield (g)	21.794 ± 5.30(a)	22.199 ± 3.19(a)	20.413 ± 4.67(a)
Branching number	5.283 ± 0.71(a)	4.633 ± 0.64(a)	5.017 ± 0.51(a)
Pods/plant	20.333 ± 5.28 (ab)	19.767 ± 3.09(b)	23.800 ± 3.48(a)
Number of seeds	12.183 ± 2.86(b)	12.467 ± 0.83(b)	14.533 ± 2.16(a)
Seeds weight (g)	3.925 ± 0.13(a)	3.317 ± 0.32(b)	1.762 ± 0.41(c)
PCG (g/100 seeds)	36.259 ± 10.22(a)	27.777 ± 2.39(a)	14.479 ± 4.75(b)
SY (kg/ha)	490.667 ± 16.61(a)	414.667 ± 40.34(b)	220.229±51.13(c)
Harvest Index	0.199 ± 0.05(a)	0.164 ± 0.05 (ab)	0.096 ± 0.03(b)
WUEs (kg/ha/mm)	1,499 ± 0.05(a)	1,689 ± 0.16(a)	1,346 ± 0.31(b)
WUE bio (g/mm)	0.067 ± 0.02(c)	0.090 ± 0.01(b)	0.125 ± 0.029(a)

a,b and c: present the height classification groups according to the irrigation level.
Means followed by the same letters have no significant difference based on the LSD test at 5% error probability.

Table 4. Eigen value, contribution of variability and Eigen vectors for the principal component axes in chickpea.

	F1	F2	F3	F4	F5
Eigenvalue	5.423	3.079	2.260	0.197	0.042
Variability (%)	49.300	27.987	20.542	1.791	0.379
Cumulative %	49.300	77.288	97.830	99.621	100.000

The higher Eigen values were considered as best representative of system attributes in principal components. Only three components showed more than 1 Eigen value and exhibited about 97.83% cumulative variability, therefore these two PCs were given due important for the further explanation. Analysis of the parameters studied shows that the two axes have respectively 49.30 and 27.99% of the total inertia (Figure 9). Axis 1 (49.30%) is represented by the measurements of height (r = 0.88), biological yield (r = 0.93), bringing the number (r = 0.53), seed yield (r = 0.81), WUE relative to seed (r = 0.75), harvest index (r = 0.65) and WUE relative to biological yield (r = 0.94). For varieties, axis 1 influenced Beja (r = 0.40), Nayer (r = 0.79) and Rebha (r = 0.75). This axis is positively correlated with most of the parameters studied and especially with production. However, Axis 2 (27.99%) is represented by pod number (r = 0.87), seed number (r = 0.87) and PCG (r = 0.78). For varieties, axis 2 influenced Bochra (r = 0.60) and Nour (r = 0.78). This axis represents vegetative development.

Ascending Hierarchical Classification (AHC)

Based on the various measurements carried out, the ascending hierarchical classification made it possible to distinguish three classes (figure 10).

– ***Classes 1*** Nayer and Beja: They are made up of highly developed individuals, with strong vegetative development and production, having the highest average values for height (40.23 cm), PCG (30.83), SY (387.42), WUEs (1.59), WUE bio (0.11). These two varieties can be adapted to any region and are more tolerant of water stress.

– ***Classes 2*** Bochra and Nour: They are composed of plants with an average potential, but which have a slight superiority for the parameters Number of seeds per plant (14.43) and Number of Pods (23.33).

– ***Class 3*** Amdoun and Rebha: this class is made up of fragile individuals, poorly developed relative to plants of other classes with low productive power. These varieties are very sensitive to water stress and can only be grown in areas that have a humid climate.

DISCUSSION

From the literature, it is revealed that the response of irrigation to chickpea seed yield depends on the initial soil moisture reserve, atmospheric water demand, and the cultivar. The main objective of the present study was to evaluate the yield potential of new cultivars of chickpea under different soil moisture regimes (Ali, 2017).

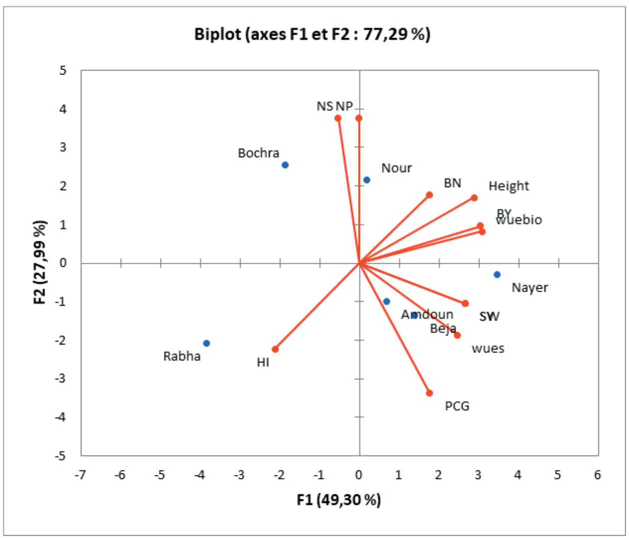

Fig. 9. Biplot graphical display for WUE of the tested Chickpea genotypes for different levels irrigation.

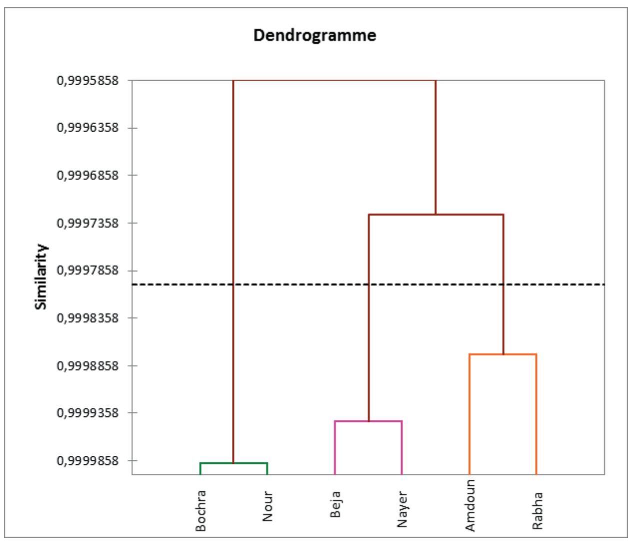

Fig. 10. Ascending Hierarchical Classification of the six studied genotypes of chickpea.

Mguidiche et al. (2018) study the effect of deficit irrigation on Wheat Yield and Water Use Efficiency in the North of Tunisia and proved that due to the severe climatic conditions and increased crop water requirements root extraction increased, SWC decreases to 14% in all soil profiles at the end of the growing season. Krouma et al. (2015), prove that drought-induced loss in crop yield probably exceeds losses from all other causes, since both the severity and duration of the stress are critical. Added to that Water potential measured in leaves shows a clear decrease of this potential when plants are subjected to drought.

Levit (1980) observed that too much water could adversely affect the growth of aboveground biomass in chickpea, while a water deficit inhibits the growth of stems and leaves. Osmotic regulation can enable the maintenance of cell turgor for survival or assist plant growth under severe drought conditions in pearl millet (Berninger et al., 2000). Aspinal (1986), indicated that the water deficit results in a reduction in the height and diameter of the stem, a shortening of the internodes, and a decrease in the leaf area. The results found are confirmed with those of Slim et al. (2006), who was able to classify chickpea varieties into two groups, notably, tall ones such as Amdoun and short ones such as Beja and Bochra. Ben Naceur et al. (2014), noted that stem height and leaf area of durum wheat were negatively affected by water deficit. Aspinal (1986), indicated that the water deficit results in a reduction in the height and diameter of the stem, a shortening of the internodes, and a decrease in the leaf area. According to Ben Mbarek et al. (2011), the leaf area index of chickpea ranges from 0.5 to 3.5. Daaloul et al. (2007), have shown that root flexibility is reflected in the improvement of the growth of its root system under conditions of water deficit by the allocation of dry matter. This proves the results of the variation in dry matter content in the roots as a function of the irrigation level. LAI results are confirmed with Singh et al. (1995), who reported that at 128 days after sowing, the leaf area index is estimated at 1.1 in the early irrigated treatments and 2.8 in the fully irrigated treatment. Likewise, Sheldrake and Saxena (1979) found a difference between the leaf area indices of a variety of chickpea grown in different areas and attributed this difference to climatic conditions and more specifically to rainfall.

These results indicate that the root fineness is dependent on the variety (genetic dependence) which is confirmed by Daaloul et al. (2007) who indicated the predominance of genetic control over root fineness. Albouchi et al., (2003), indicated that, under conditions of water stress, the growth of the aerial parts of stressed plants is more affected than that of the roots. Under such conditions, the response of a plant results in a preferential supply of biomass to the roots. Pacucci et al., (2006) indicated that additional irrigation of chickpeas, applied at the flowering and pod filling stages, increased the number of seeds by 14 to 27%. Gan et al., (2004) noticed that chickpea of the kabuli type produces a high number of empty pods. Early in pod formation, water stress increases the abortion rate and reduces chickpea pod production. The filling of chickpea pods strongly depends on climatic conditions and varies from 9 to 57% (Pundir et al., 1992). Lawlor and Cornic (2002) indicate that determination of water status and relations in plants demonstrated that drought decreased water potential, relative water content and osmotic adjustment. The utilization of leaf root water content as an indicator of the plant water status is usually.

According to Tiznado et al. (2012), the weight of 100 field-grown Kabuli-type chickpea seeds is highly variable and ranges from 28 to 70g. With the different levels of irrigation, the weights of 100 seeds are different. It is highest with the 100% ETc irrigation level and lowest with the 50% ETc level. Moinuddin and Khanna-Chopra, (2004) noted that the weight of 100 seeds is significantly affected by water stress.

Belhassen et al. (1995) found that the processes involved in developing the seed yield of a crop are influenced by two types of factors: genetic factors, intrinsic to the plant, and environmental factors. The environmental, abiotic stresses that affect a crop can cause considerable yield losses. Ben Mbarek (1990) pointed out that gene expression of potential yield depends on climatic conditions. Singh et al. (1995) noticed that delayed sowing of a chickpea (Cicer arietinum L.) crop, carried out in dry or irrigated conditions, allows its potential yield to be determined. With delayed sowing, water stress-tolerant genotypes produce 40–50% of their potential yields (Sabaghpour et al., 2006) ; while susceptible genotypes only produce 10%. Thus, the low seed yields obtained may be due to the effects of high temperature during the cycle. Also, Kamel (1990) stated that thermal and water stress, quite frequent at the end of the crop cycle, limit the yield from 42 to 75%. Gan et al., (2010) reported that the water use efficiency of Kabuli-type chickpeas is 5.3 kg ha^{-1} mm^{-1} or 20% less than the average WUE 6.6 kg ha^{-1} mm^{-1}. However, exposing a chickpea crop to a terminal drought shortens its crop cycle and reduces its water use efficiency (Brown et al., 1989).

Condon et al. (2004), indicate that water use efficiency is an important strategy for drought tolerance in crop plants, including chickpea. Pang et al. (2017), showed that a significant amount of genetic variability has been recorded on stressed conditions.

Bingru and Hongwen (2000) have stated that water use efficiency is an important factor in determining resistance to water stress.

CONCLUSION

To increase the production of chickpeas and mitigate the national limited water resources, it would be necessary to resort to a second alternative, which consists of extending the cultivation of this species to areas of semi-arid Tunisia. It is in this context that the present work is based on six varieties of chickpeas most cultivated in Tunisia. From the results found, it is clear that the efficiency of seed water use and biological yield varies with the irrigation level, as well as with the variety. It is important to tell farmers the most adaptable varieties for each bioclimatic region and each irrigation level. Indeed, in the region of Chott Mariem which belongs to the lower semi-arid bioclimatic stage, with an amount of 100% ETc the WUE in seeds is almost the same for all six varieties with a slight difference for Nour, Beja, and Nayer. The difference begins to be remarkable with the irrigation amount of 75% of ETc, of which it has been observed that the varieties Amdoun, Nayer and Beja perform well with a WUE which varies from 1.6; 1.58 and 1.53 kg ha^{-1} mm^{-1} respectively for the three varieties, which recorded a WUE of seeds with extreme values compared to Rabha, Nour, and Bochra varying respectively from 1.5, 1.48 and 1, 46 53 kg ha^{-1} mm^{-1} with an irrigation level of 50% of the ETc. Varieties that have shown tolerance to water stress should be grown on a large scale, in spring cultivation, in different Tunisian bioclimatic stages. Other aspects of this type of crop merit investigation, including the Rhizobium-genotype relationship tolerant to water stress and under conditions of low nitrogen content and the presence of sufficient rhizobia in the soil.

ACKNOWLEDGMENTS

This project was supported by the research unit, ‘UR 13 AGR06 Horticulture, Landscape, Environment’. Also, we wish to present our special thanks to the Regional Center for Field Crop Research in Beja (CRRGCB), IRESA Tunisia for kindly supplying seeds of chickpea.

REFERENCES

Albouchi A, Béjaoui Z. et El Aouani M.H. (2003). Influence d’un stress hydrique modéré ou sévère sur la croissance de jeunes plants de Casuarina (Casuarina glauca Sieb.). *Sécheresse* Vol.14; 3, 37-142.

Ali M.H. (2017). Response of Chickpea Varieties to Different Irrigation Regimes, *Asian Journal of Advances in Agricultural Research* 2(4): 1-7.

Aspinal D. (1986). Metabolic effects of water and salinity stress in relation to the expression of the leaf surface. *Aust. J. Plant Physiol.* 13: 59–73.

Bacha F. et Ounane S. M. (2003). Etude de l’effet du stress hydrique sur les Activités des enzymes nitrate réductase et nitrogénase de la culture du pois chiche (Cicer arietinum L.). *Institut National de la Recherche agronomique d’Algérie* 13: 1111-1992.

Bamouh A. (1998), Gestion de la contrainte pluviométrique pour l’amélioration de la production végétale et de l’efficience d’utilisation de l’eau. Bulletin de liaison du Programme National de Transfert de Technologie en Agriculture (PNTTA); Instituts, Rabat, Maroc; 10 p.

Belhassen E., This D. et Monneveux P. (1995). L’adaptation génétique face aux contraintes de sécheresse. *Cahiers Agriculture* 4: 251-261.

Ben Mbarek K., Douh B. and Boujelben A. (2011). Effects of Irrigation on the Flowering and Maturity of Chickpea Genotypes, Chapter in book irrigation-systems-and-practices-in-challenging-environments, Intech edition, pp 1-18.

Ben Naceur M., Khamassi K., Chaabane R., Khoufi S. et Kharrat M. (2014). Evaluation Agro-morphologique de Quelques Génotypes Locaux de Pois Chiche d’Hiver (*Cicer arietinum* L.) en Tunisie. *New Sciences*. Vol 5(2), 19p.

Berninger C. Li, F. , Koskela J. , Sonninen E. (2000). Drought responses of *Eucalyptus microtheca* F. Muell. Provenances depend on seasonality of rainfall in their place of origin. *Aust. J. Plant Physiol*. 27: 21-238.

Bingru H. and Hongwen G. (2000). Root physiological characteristics associated with drought resistance in tall fescue cultivars. *Crop Sci.* 40: 196-2003.

Brown S.C., Gregory P.J., Cooper P.J.M., et Keating J.D. (1989). Root and shoot growthand water use of chickpea (Cicer arietinum L.) grown in dryland conditions effects of sowing date and genotype. *J. Agric. Sci.* 113: 41–50.

Cochard H., Coll L., Roux X.L. et Amyglio T. (2002). Unraveling the Effects of Plant Hydraulics on Stomata1 Closure during Water Stress in Walnut. *Plant Physiology* 128: 282-290.

Condon, A. G., Richards, R. A., Rebetzke, G. J., Farquhar, G. D. (2004). Breeding for high water-use efficiency. *J. Exp. Bot*. 55: 2447-2460.

Daaloul A., Bchini H., et Sayar R. (2007). Variabilité génétique de quelques paramètres du système racinaire du blé dur (*Triticum durum* Desf.) sous deux régimes hydriques. *Bioversity International* - FAO. 129: 25-31.

Douh, B. and Boujelben, A. 2011. Improving water use efciency for a sustainable productivity of agricultural systems with using subsurface drip irrigation for maize (*Zea mays* L.). J. *Agric. Sci. Technol.* B 1: 881-888.

Ilhe SS, Patil HM, Macharekar RJ. (2009). Water production function for chickpea under sprinkler method of irrigation. *International Journal of Agricultural Sciences* 5(1): 221-225.

Gan Y. T., Warkentin D.T., Bing D.J.,.Stevenson F.C., McDonald C.L. (2010). Chickpea water use efficiency in relation to cropping system, cultivar, soil nitrogen and Rhizobial inoculation in semiarid environments, *Agricultural Water Management* 97(9): 1375-1381

Gan, Y., Wang J., Angadi S.V. et Mc Donald C.L. (2004). Response of chickpea to short periods of high temperature and water stress at different developmental stages. New directions for a diverse planet: Proceedings of the 4th International Crop Science Congress. Brisbane, Australia, 26 Sep.-1 Oct.

Kadam CS, Thanki JD, Gudadhe NN. (2014). Response of chickpea to irrigation methods, fertilisers and biofertiliser under south Gujarat condition. *Indian J. Fert*. 10(4): 20-24.

Kamel M. (1990). Winter chickpea: Status and prospects. *Option Méditerranéenne Séries, Séminaires* 9: 145-150.

Krouma Abdelmajid, Fujimura T., Abdelly C., 2015. Growth, photosynthetic activity and water relations in three Tunisian chickpea genotypes (*cicer arietinum l.*) subjected to a progressive water deficit stress, *Agricultural Science Research Journal* 5(12): 206-214.

Mguidiche Belhaj A., Douh B., Gazouani H., Harbaoui K., Sahbi F. (2018) Wheat Yield and Water Use Efficiency in the North of Tunisia Under Supplemental Irrigation. *In: Kallel A., Ksibi M., Ben Dhia H., Khélifi N. (eds) Recent Advances in Environmental Science from the Euro-Mediterranean and Surrounding Regions. EMCEI 2017.* Advances in Science, Technology & Innovation (IEREK Interdisciplinary Series for Sustainable Development). Springer, Cham.

Moinuddin A. S. and Khanna-Chopra R. (2004). Osmotic adjustment in chickpea in relation to seed yield and yield parameters, *Crop Science* 44(2): 449-455.

Molden D., Theib O., Pasquale S., Prem B., Munir A H. et Jacob K. (2010). Improving agricultural water productivity: between optimism and caution. *Agric. Water Manage*. 97: 528-535.

Rabi A., Martín I. and Rodriguez-Clemente R., 2012. Conceptual Frame on Technological Perspective for Water Resources Management in the Mediterranean Region. In: Choukr-Allah R., Ragab R., RodriguezClemente R. (eds) Integrated Water Resources Management in the Mediterranean Region. Springer Netherlands, pp 57-65.

Lawlor DW, Cornic G (2002). Photosynthetic carbon assimilation and associated metabolism in relation to water deficits in higher plants. *Plant Cell Environ*. 25: 275-294.

Oweis T., Hachum A. et Pala M. (2004). Water use efficiency of winter-sown chickpea under supplemental irrigation in à Mediterranean environment. *Agricultural Water Management* 66: 163-179.

Pacucci G., Troccoli C. et Leoni B. (2006). Supplementary Irrigation on Yield of Chickpea Genotypes in a Mediterranen Climate. Agricultural Engineering International: *The CIGR Ejournal. Manuscript LW* 04 005. Vol. VIII. May 2006.

Pundir R.P.S., Reddy K.N. et Mengesha (1992). Pod volume and pod filling as useful traits of chickpea. *International Chickpea Newsletter* 17: 18-20.

Sabaghpour, S. H., Mahmodi, A. A., Saeed, A., Kamel, M., Malhotra, R. S. (2006). Study on chickpea drought tolerance lines under dryland condition of Iran. *Indian J. Crop Sci*. 1: 70-73.

Saxena MC. (1980). Recent advances in chickpea agronomy. In: Proc. Int. Workshop on Chickpea Improvement, 28 Feb–2 Mar 1979, Hyderabad, India, 89–105.

Sheldrake R. and Saxena N.P., 1979. Comparisons of Earlier- and Later-formed Pods of Chickpeas (Cicer arietinum L.), *Annals of Botany* 43(4): 467-473.

Siddique K.H.M., Regan K.L., Tennant D., et Thomson B.D. (2001). Water use and water use efficiency of cool season grain legumes in low rainfall Mediterranean-type environments. *European Journal of Agronomy* 15(4): 267-280.

Singh K.B., Malhotra R.S., Saxena M.C., et Bejiga G. (1995). Analysis of a decade of winter/spring chickpea. In: Germplasm program legumes; Annual report; International Center for Agricultural Research in the Dry Areas (ICARDA); P.O. Box 5466. Aleppo, Syria, 210 p.

Slim N., Sifi B. et Triki S. (2006). Criblage de variétés de pois chiche (Cicer arietinum L.) pour la résistance au stress hydrique. In: Gestion des Ressources et Applications Biotechnologiques en Aridoculture et Cultures Sahariennes : Perspectives pour la valorisation des potentialités du Sahara. Séminaire International; Djerba, du 25 au 28 Décembre 2006.

Stewar W.M., 2001, Balanced Fertilization Increases Water Use Efficiency, regional newsletter, the Potash and Phosphate Institute (PPI) and the Potash and Phosphate Institute of Canada (PPIC).

Tiznado J. Garzón, Ochoa-Lugo M., Heiras-Palazuelos M., Domínguez-Arispuro D., Rodríguez E., Gutiérrez-Dorado R., Milán-Carrillo J. and Reyes-Moreno C., (2012). Acceptability Properties and Antioxidant Pontential of Desi Chickpea (Cicer arietinum L.) Cultivars, *Food and Nutrition Sciences* 3(9): 1281-1289.

USDA (1951). Soil Survey Manual. U.S.Department of Agriculture, Edition Washington D.C. 503 pp.

Wery, J. (1990). Adaptation to frost and drought stress in chickpea and implications in plant breeding. In: Saxena M.C; Cubero J.I. and Wery (Eds), Present status and future prospects of chickpea crop production and improvement in the Mediterranean countries, Options Méditerranéennes, Série Séminaires n° 9, CIHEAM, Paris. pp 77-85.

Italian Journal of Agrometeorology
Rivista Italiana di Agrometeorologia

Firenze University Press
www.fupress.com/ijam

OPEN ACCESS

Citation: H. Farrokhi, A. Asgharzadeh, M. Kazemi Samadi (2021) Yield and qualitative and biochemical characteristics of saffron (*Crocus sativus* L.) cultivated in different soil, water, and climate conditions. *Italian Journal of Agrometeorology* (2): 43-55. doi: 10.36253/ijam-1216

Received: February 07, 2021

Accepted: October 12, 2021

Published: December 27, 2021

Data Availability Statement: All relevant data are within the paper and its Supporting Information files.

Competing Interests: The Author(s) declare(s) no conflict of interest.

ORCID:
XX: 0000-0000-0000-0000
XX: 0000-0000-0000-0000

Yield and qualitative and biochemical characteristics of saffron (*Crocus sativus* L.) cultivated in different soil, water, and climate conditions

Habibioallah Farrokhi[1], Ahmad Asgharzadeh[2,*], Malihe Kazemi Samadi[3]

[1] *P.hD student of Medicinal Plant, Shirvan Branch, Islamic Azad University, Shirvan, Iran*
[2] *Department of Horticulture, Shirvan Branch, Islamic Azad University, Shirvan, Iran*
[3] *Department of Chemistry, Faculty of Science, Bojnourd Branch, Islamic Azad University, Bojnourd, Iran*
*Corresponding author. E-mail: habibfarkhiy1@yahoo.com; asgharzadehahmad95@yahoo.com; kazemi@yahoo.com

Abstract. Saffron is highly valued for its unique aroma, taste, color, and medicinal properties. Iran is one of the most important saffron-producing countries. The present study aimed to investigate the effect of climatic and environmental characteristics of six sites (Shirvan, Faruj, Zavareh, Torbat-e Heydarieh, Ghayen, and Birjand) on the yield and qualitative, and biochemical characteristics of saffron. The studied sites were considered as treatments. The obtained data were analyzed based on a nested design, where the village within the site was considered an experimental error, and the farm within the village within each site was considered a sampling error. The Torbat-e Heydarieh treatment with altitudes of ~1323.3 m produced the maximum saffron flower yield (0.83 g m^2), stigma yield (0.098 g m^2), safranal content (15.8%), picrocrocin content (30.6%), and crocins content (69.3%). Evidently that the low maximum summer temperature in the area is one of the reasons for its superiority. The correlation analysis between traits shows that the maximum summer temperature had a significant negative correlation with saffron flower yield, stigma yield, and picrocrocin and crocin content. Results showed the highest total flavonoid and phenol content and DPPH activity related to Shirvan and Faruj. Although the results showed that selenium could increase the quantitative and qualitative yield of saffron, this requires further studies to confirm it. Based on the findings, it is concluded that I) qualitative and quantitative characteristics of saffron are strongly controlled by the environmental and climatic conditions and II) Razavi Khorasan province had a significant advantage in terms of flower and stigma yield and safranal, picrocrocin and crocin content of saffron and North Khorasan province in terms of biochemical characteristics.

Keywords: DPPH activity, maximum summer temperature, saffron flower yield, safranal content, selenium, stigma yield.

INTRODUCTION

Saffron (*Crocus sativus* L.) is one of the most expensive cash crops among medicinal plants in the world and thus it has been called "the red gold" (Cardone *et al*., 2020). From ancient times, saffron has been used as a dye for fabrics, a condiment to enrich food, and a drug to treat various human diseases (Cardone *et al*., 2019). Saffron is the most expensive spice globally, and it has a special place in Iran's industrial and export products (Kafi *et al*., 2018). In addition to the stigma and corm yield, the spice quality represents an important parameter that contributes to increase the saffron economic value. Quality is determined chemically by three main secondary metabolites: safranal ($C_{10}H_{14}O$, a major component of essential oil), picrocrocin ($C_{16}H_{26}O_7$, monoterpene glycoside, a precursor of safranal), and crocin ($C_{44}H_{64}O_{24}$, water-soluble crocetin esters), which are responsible for the odor, bitter taste, and color, respectively (Cardone *et al*., 2020).

Saffron is mainly cultivated in Iran (the source of more than 90% of world production), followed by India, Spain, Morocco, Greece, and Italy (Babaei *et al*., 2014; Shokrpour, 2019). Saffron global production is estimated at 418 t y^{-1} on 121,338 ha. It is known as beneficial for human health due to three main bioactive compounds: crocin, picrocrocin, and safranal (Cardone *et al*., 2020). Saffron cultivation dates back to more than 750 years in the southern and central regions of Khorasan, Iran (Kafi *et al*., 2018). Although Iran is the leading producer of this product in the world with an annual production of 200 tons of dry saffron from more than 60,000 ha of arable land, the maximum yield of saffron in Iran is about 7.5 kg ha^{-1}, and the average is 3.96 kg ha^{-1}, which shows a significant difference compared to countries such as Spain with 15 kg ha^{-1} and Pakistan with 9 kg ha^{-1} (Feli *et al*., 2018).

Recently, several researchers studied how different parameters such as temperature, humidity, light, substrate, mother corm dimension, planting density and application of nutritional elements, affect stigma and corm yield (Ghanbari *et al*., 2019; Cardone *et al*., 2020). Moreover, many factors are conducing to the growth, development, and yield of saffron, the most important of which are climatic and environmental conditions (Rahimi *et al*., 2017). Ecological and climatic conditions, e.g., temperature, soil, and water content, noticeably affect both the quantitative and qualitative traits of saffron (Amirnia *et al*., 2014). Maleki *et al*. (2017) reported that the flowering and yield of this plant are directly related to ecological conditions and field management. Temperature is the most critical environmental factor in controlling the growth and flowering in *Crocus* species. The optimum temperature for flower initiation and development of the corms is 23–27 °C (Rahimi *et al*., 2017). Besides, saffron cultivation in the world shows that the adaptability to soil types, temperatures, and day length encourages its production from the Mediterranean basin to the Middle East (Baghalian *et al*., 2010). This is why some scientists believe that although saffron reproduces only by vegetative propagation, it displays considerable morphological and biochemical variations between and within populations (Baghalian *et al*., 2010; Moradi *et al*., 2020). Saffron grows well in temperate and dry environments, while cold weather has a vital role in its vegetative growth. However, some reports suggest rainy autumns, mild winters, and warm summers as the optimal climatic conditions for this species (Ghorbani and Koocheki 2017; Hussain *et al*., 2019). In this regard, Lage and Cantrell (2009) reported that the analysis of the environment effect on saffron quality showed that just the altitude affects crocins. Using principal component analysis (PCA), Cardone *et al*. (2019) demonstrated that the cultivation site with higher temperature and without excessive rain during the flowering period generated the best stigma yield with high-quality traits. In this regard, Perpina *et al*. (2013) showed that the most suitable areas for biomass production in Valencia (Spain) were located in the vicinity of residential zones. Maleki *et al*. (2017) reported that the soil and climatic variables have a major role in the development of saffron cultivation.

Secondary metabolic profiles have been studied in different plants such as saffron (Parizad et al., 2019). Environmental conditions associated with the geographical origin, including altitude, temperature, rainfall, humidity, and soil properties, influence the plant development and growth and may have strong effects on the plant's secondary metabolite production (Jelínek et al., 2012; Parizad et al., 2019). Parizad et al. (2019) reported that more than 92% of Iran' saffron is cultivated in Razavi Khorasan and South Khorasan provinces. Hence, this work aimed to study the yield, quality, and secondary metabolites of saffron in six cities of North, Razavi, and South Khorasan provinces.

MATERIALS AND METHODS

Experimental conditions and plant materials

The experiments were conducted on saffron cultivated (three-year-old) under diverse environments, including six cities in North, Razavi, and South Khorasan provinces (Shirvan, Faruj, Zavareh, Torbat-e Heydarieh, Ghayen, and Birjand) during the growing seasons 2018-

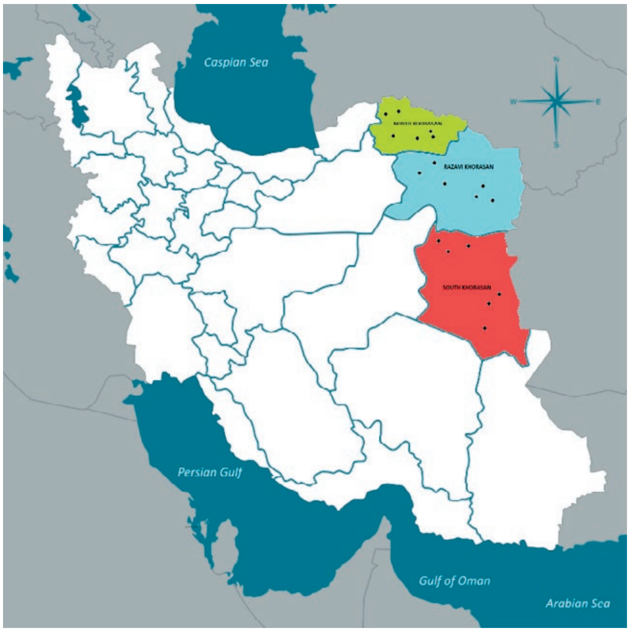

Fig. 1. Different sites location of North, Razavi, and South Khorasan provinces in the map of Iran.

2019. Six sites (with three villages in each site and three farms in each village) with different climates and altitudes were chosen for saffron cultivation (Fig. 1). In each site, geographical and climatic factors including relative humidity, maximum and minimum temperatures, annual frost days, average annual temperature, and rainfall were obtained from the nearest meteorology stations (Table 1).

Corms of 3.0–3.5 cm horizontal diameter and 14.0–19.0 g weight were sown in August at each site from Torbat-e Heydarieh origin. Corms were placed in raised beds, 80 cm wide and 30 cm high from soil level, with three rows of corms in each "bed" at 10 cm depth, 20 cm apart rows, and 5 or 6.7 cm within rows to the adopted density. The studied sites were considered treatments. The obtained data were analyzed based on a nested design. The village within the site was considered an experimental error, and the farm within the village within each site was considered a sampling error. In all areas, the soil was fallow in the previous year, and no fertilizer and no irrigation were applied. Weeds management was carried out by hand throughout the experiment.

Measurement of yield and qualitative characteristics

Whole flowers (in 1 m^2 for each farm) were manually picked daily early in the morning in the first hours after sunrise and before the flower had wholly opened. Immediately after flower picking, stigmas were separated by hand and dried in a forced-air oven (BM-55E, Fanazma-Gostar Company, Iran) at 30 °C for 24 h. The flower and stigma yield was calculated per unit area of 1 m^2.

To measure the content of crocins (color agent), picrocrocin (bitter taste agent), and safranal (odor agent), stigmas related to each farm were dried at 55 °C for 45 min, then weighed and powdered for chemical analysis. The chemical analysis was performed according to ISO-3632 method, from which exactly the Iranian National Standard No. 259-2 has been adapted (Maleki Farahani and Aghighi Shahverdi, 2015). For this purpose, UV/Visible spectrophotometer (Jenway-6305, France) measuring the number of crocins, safranal, and picrocrocin, were used at wavelengths of 440, 330, and 257 nm, respectively. To compare the mean of the treatments, equation [1] was used (Esfanjani *et al*., 2017).

$$E^{1\%}_{1cm} = 10000 \times OD/m\,(100-H) \qquad [1]$$

Whereas: $E^{1\%}_{1cm}$ is aqueous saffron extract; OD: specific absorption, m: the weight of sample load in grams per 100 ml; and H: moisture content of the dry stigmas, which is usually between 8 and 10%.

Biochemical analyzes

To measure the biochemical analyzes such as anthocyanin, total flavonoid, and total phenol content as well as DPPH radical scavenging activity, sampling of total flowers in three replications was performed by the following methods.

Measurement of anthocyanin content

The anthocyanin content was measured spectrophotometrically as described previously (Sakamoto and Suzuki, 2019), with modifications. Fresh samples (total flower) were promptly dried in an oven at 55 °C for six h. Dried samples were weighed and soaked in 1 ml methanol containing 1% HCl and were incubated at 95 °C for 15 min. The sample was then cooled to room temperature. After removing the solids, the absorbance of the supernatant was measured at 533 nm, and a standard calibration curve was prepared using cyanidin-3-glucoside (CY).

Measurement of total flavonoid content

The total flavonoid content of samples' extracts (total flower) in different sites was determined by Esmaeelian

Table 1. Details and environmental characteristics of the trials different sites of North, Razavi, and South Khorasan provinces of Iran.

Site number	Site name*	Province	Longitude (E)	Latitude (N)	Altitude (m.a.s.l)	Relative humidity (%)	Minimum winter temperature (°C)	Maximum summer temperature (°C)	Number of annual frost days	Average annual temperature (mm)	Average annual rainfall (mm)
S1	Shirvan	NK	57°99'111"	37°17'111"	1168.33	60	25.2	41.6	107	13.1	226.7
S2	Faruj	NK	58°17'222"	37°14'033"	1207.33	57	23.0	41.5	89	12.6	243.6
S3	Zavareh	RK	59°32'333"	35°16'689"	1370.33	45	24.0	41.0	89	14.5	245.0
S4	Torbat-e Heydarieh	RK	59°19'178"	35°39'089"	1323.33	45	24.6	40.6	88	14.3	246.2
S5	Ghayen	SK	58°95'856"	33°41'389"	1768.33	40	27.2	42.0	88	14.7	161.0
S6	Birjand	SK	59°34'467"	32°46'078"	1812.66	35	21.5	43.0	71	16.5	147.4

NK: North Khorasan; RK: Razavi Khorasan; SK: South Khorasan; m.a.s.l: meter above mean sea level.
* Shirvan villages: Vorg, Razmoghan, Feizabad; Faruj villages: Siahdasht, Seghonbad, Mafraangha; Zavareh villages: Karizbala, Dolatabad, Safiabad; Torbat-e Heydarieh villages: Abrod, Damesk, Molkabad; Ghayen villages: Tajan, Andrik, Penhaei; Birjand villages: Nofrest, Galian, Chaj

et al. (2020) method. A 0.5 ml aliquot of 20 g L^{-1} $AlCl_3$ ethanolic solution was added to 0.5 ml of extract solution. After one hour at room temperature, the absorbance at 240 nm was measured. The yellow color indicated the presence of flavonoids. Extract samples were evaluated at a final concentration of 0.1 mg ml^{-1}, Total flavonoids content was expressed as Quercetin (QE) (mg QE/g DW).

Measurement of total phenol content

The total phenol content was measured spectrophotometrically using the Folin–Ciocalteu method described previously (Baba *et al.*, 2015), with slight modifications. The samples (50 mg fresh weight of total flower) were homogenized with 500 µL of 90% methanol. The sample was then centrifuged at 10,000× *g* for 5 min. The supernatant (20 µL) was diluted with 680 µL of distilled water, and 50 µL of phenol reagent was mixed. After adding 300 µL of 5% sodium carbonate, the mixture was incubated at 25 °C for 30 min in the dark. The supernatant's absorbance was measured at 765 nm, and a standard curve was prepared using gallic acid (GA).

Measurement of DPPH radical scavenging activity

The 1,1-diphenyl-2-picrylhydrazyl (DPPH) radical scavenging activity was determined by using the method described by Sánchez-Vioque *et al.* (2012). The reaction mixture (total volume 3 ml), consisting of 0.5 ml of 0.5 M acetic acid buffer solution at pH 5.5, 1 ml of 0.2 mM DPPH in ethanol, and 150, 200, and 250 µmol ml^{-1} solution, was shaken vigorously with various samples (total flower). After incubation at room temperature for 30 min, the remaining DPPH was determined by absorbance at 517 nm, and the radical scavenging activity of each sample was expressed using the ratio of the absorption decrease of DPPH (%) to that of the control DPPH solution (100%) in the absence of the sample. The radical scavenging activity was calculated (%) =100(A-B)/A, where A and B are 517 nm absorption of the control and the corrected absorption of the sample reaction mixture.

Measurement of selenium, cadmium, arsenic, lead, and nickel content in saffron, water, and soil

The samples (soil and plant) were dried in the oven (60 to 65 °C). One-gram sample was added to 15 ml of a combination of three acids (nitric, perchloride, and sulfuric acids with 5:1:1 ratio, respectively). The mixtures were then digested at 80 °C until a clear solution was obtained, which was reduced to 50 mL using distilled water. The solutions were measured to determine the concentration of the heavy metals (Williams and Lambert, 1959). Also, the soils collected from the farms were transferred to the laboratory after drying and passing through 2 mm sieve. One-gram dry soil was mixed in a ratio of 1:3 with 6 M hydrochloric acid and concentrated nitric acid and heated for 24 h at 90 °C with nitric acid 2 M to a volume of 50 ml (Chen and Ma, 2001). Finally, the concentrations of heavy metals such as selenium, cadmium, arsenic, lead, and nickel in the saffron, water, and soils under study were determined using an atomic absorption spectrometer (Avanta-P model, GBC-Australia).

Statistical analysis

After checking the data distribution normality assumption through employing Kolmogorov-Smirnov and Shapiro-Wilk tests, data were analyzed using a Statistical Analysis System software (SAS Institute, Cary, NC, USA, Version 9.2) and Minitab version 19. Statistical analysis was performed using nested design and means were compared with a Least Significant Difference (LSD) test at $p\leq0.05$. The *p*-values of less than 0.05 were considered statistically significant. Data collected from different sites have been compared by correlation coefficients, PCA, and cluster analysis by Statistical Analysis System software and Minitab software.

RESULTS

Quantitative (flower and stigma yield) and qualitative (safranal, picrocrocin, and crocins content) traits

According to the variance analysis of the studied traits (Table 2), there were significant differences among cultivation sites concerning the saffron quantitative (flower and stigma yield) and qualitative (safranal and crocins content) characteristics ($p\leq0.05$). The S4 treatment (Torbat-e Heydarieh) with altitudes of ~1323.33 m.a.s.l produced the maximum saffron flower yield (0.83 g m^{-2}), stigma yield (0.098 g m^{-2}), safranal content (15.8%), picrocrocin content (30.6%), and crocins content (69.3%). Results showed the lowest saffron flower yield (0.63 g m^{-2}), safranal content (11.7%), and picrocrocin content (22.2%) were achieved in S5 (Ghayen). Also, Zavareh (S3) and Birjand (S6) showed the lowest stigma yield (0.081 g m^{-2}) and crocins content (39.9%), respectively (Table 3).

Biochemical traits

As shown in Table 2, the effect of treatment (sites) was significant on total flavonoid content ($p\leq0.01$), total phenol content ($p\leq0.01$), and DPPH activity in 150, 200, and 250 µmol ml^{-1} concentrations ($p\leq0.05$). Means comparison showed the highest total flavonoid content (14.01 and 14.14 mg QE g^{-1} DW) and total phenol content (125.5 and 126.5 mg GA g^{-1} DW) and DPPH activity related to S1 (Shirvan) and S2 (Faruj). Moreover, Zavareh (S3) site produced the maximum means of total flavonoid and phenol content (14.16 mg QE g^{-1} DW and 126.6 mg GA g^{-1} DW). While S5 (Ghayen site) had the lowest total flavonoid (13.4 mg QE g^{-1} DW) and phenol (117.3 mg GA g^{-1} DW) content and DPPH activity in 150, 200,and 250 µmol ml^{-1} concentrations (29.9, 39.8, 59.6%, respectively) (Table 3). The results indicated that saffron cultivated in S1 and S2 sites (North Khorasan province) has the highest phenol and flavonoids content as well as total antioxidant activity (DPPH) and S5 and S6 sites (South Khorasan province) has the lowest range of mean traits.

Heavy metals content in water, soil, and saffron

The analysis of saffron, soil, and water in saffron cultivation in the studied areas is different in terms of the amount of heavy elements namely, selenium, lead, nickel, cadmium, and arsenic. Data analysis results indicated that there was selenium in saffron, cadmium in soil, arsenic in saffron and soil, and nickel and lead in saffron, water, and soil. The analysis of variance of the data showed a significant difference in the saffron selenium in different sites (Table 4). As shown in Fig. 2, the highest saffron selenium was related to S4 (2.021 mg

Table 2. Variance analysis of yield, qualitative, and biochemical traits of saffron plant in the different sites of North, Razavi, and South Khorasan provinces of Iran.

S.O.V	df	Mean square (MS)										
		Saffron flower yield	Stigma yield	Safranal content	Picrocrocin content	Crocins content	Anthocyanin content	Total flavonoid content	Total phenol content	DPPH (µmol ml^{-1})		
										150	200	250
Treatment	5	0.0534*	0.00039*	22.07*	85.70ns	994.9*	0.052ns	0.916**	145.6**	268.2*	271.9*	472.3*
Experimental error*	12	0.0152	0.00011	8.19	36.49	357.6	0.060	0.168	19.83	68.77	76.72	133.4
Sampling error**	36	0.0022	0.00004	0.098	0.27	0.74	0.018	0.0033	0.34	0.21	0.28	0.33
CV (%)	-	6.21	7.91	2.28	2.11	1.52	4.38	0.41	0.47	1.24	1.15	0.86

ns: non-significant; * and **: significant at 5 and 1% probably level, respectively.
* Village within site was considered as an experimental error.
** Farm within the village within each site was considered as a sampling error.

Table 3. Mean comparison of yield, qualitative, and biochemical traits of saffron plant in the different sites of North, Razavi and South Khorasan provinces of Iran.

Sites	Saffron flower yield (g m^{-2})	Stigma yield (g m^{-2})	Safranal content (%)	Picrocrocin content (%)	Crocins content (%)	Anthocyanin content (mg CY g^{-1} DW)	Total flavonoid content (mg QE g^{-1} DW)	Total phenol content (mg GA g^{-1} DW)	DPPH activity (%) (μmol ml^{-1})		
									150	200	250
S1	0.80± 0.02 ab	0.091± 0.003 abc	14.5± 0.22 ab	25.4± 1.38 a	59.8± 5.7 ab	3.21± 0.05 a	14.01± 0.053 a	125.5± 0.42 a	41.3± 2.13 ab	51.0± 2.63 a	72.3± 2.65 a
S2	0.78± 0.01 ab	0.092± 0.002 ab	14.0± 0.16 ab	24.8± 0.50 a	54.9± 3.1 ab	3.11± 0.04 a	14.14± 0.066 a	126.5± 0.95 a	44.5± 1.94 a	53.2± 2.11 a	74.8± 2.80 a
S3	0.69± 0.02 bc	0.081± 0.002 c	12.02± 0.28 b	24.2± 0.30 a	63.9± 0.33 a	3.19± 0.05 a	14.16± 0.014 a	126.6± 0.17 a	38.8± 0.26 abc	47.1± 0.074 ab	72.4± 0.192 a
S4	0.83± 0.03 a	0.098± 0.002 a	15.8± 1.11 a	30.6± 1.93 a	69.3± 3.06 a	3.04± 0.06 a	13.5± 0.133 bc	119.7± 1.48 b	32.7± 1.22 cd	40.1± 1.06 b	58.3± 2.56 b
S5	0.63± 0.01 c	0.081± 0.002 bc	11.7± 0.21 b	22.2± 0.38 a	52.3± 0.43 ab	3.10± 0.07 a	13.4± 0.067 c	117.3± 0.36 b	29.9± 1.2 d	39.8± 0.62 b	59.6± 0.92 b
S6	0.79± 0.02 ab	0.090± 0.004 abc	14.2± 0.38 ab	22.2± 0.30 a	39.9± 3.34 b	3.03± 0.05 a	13.90± 0.01 ab	120.3± 0.21 b	35.4± 0.53 bcd	45.1± 0.22 ab	63.3± 0.30 ab
LSD	0.126	0.011	3.11	3.40	19.90	0.25	0.42	4.57	8.51	8.99	11.86

Data are expressed as the mean ± standard error (n = 3) based on three replicates at each site. Means with different letters in a column show differences at a significance level of 5% according to Duncan's multiple range test (DMRT).
Shirvan (S1); Faruj (S2); Zavareh (S3); Torbat-e Heydarieh (S4); Ghayen (S5); Birjand (S6).

Table 4. Mean comparison of the heavy metals content in water, soil, and saffron cultivated in the different sites of North, Razavi, and South Khorasan provinces of Iran.

S.O.V.	df	Mean square (MS)														
		Selenium (Se)			Lead (Pb)			Nickel (Ni)			Cadmium (Cd)			Arsenic (As)		
		Saffron	Water	Soil	Saffron	Water	Soil	Saffron	Water	Soil	Saffron	Water	Soil	Saffron	Water	Soil
Treatment	5	0.55**	-	-	139.1*	54.9ns	26.2**	3.78ns	2.85*	88229.4*	-	-	0.086*	91.9**	-	15.8**
Experimental error*	12	0.080	-	-	35.43	63.14	2.58	7.90	0.87	17847.3	-	-	0.021	16.38	-	1.98
Sampling error**	36	0.0151	-	-	0.014	0.41	0.115	0.013	0.010	3.72	-	-	0.00005	0.0008	-	0.042
CV (%)	-	7.33	-	-	3.10	20.80	3.51	3.67	45.29	1.85	-	-	18.21	1.63	-	3.68

ns: non-significant; * and **: significant at 5 and 1% probably level, respectively.
* Village within site was considered as an experimental error.
** Farm within the village within each site was considered as a sampling error.

kg^{-1}), and the lowest was S5 (1.435 mg kg^{-1}). The water and soil of sites lacked selenium.

The highest lead content in saffron (11.92 mg kg^{-1}), water (6.75 mg kg^{-1}), and soil (11.62 and 11.79 mg kg^{-1}) were related to S2, S1, and S1 and S5 sites, respectively. The lowest saffron lead in the S1 and S5 (1.903 and 1.824 mg kg^{-1}) was observed. S4 and S2 showed the lowest means of soil and water lead (7.983 and 0 mg kg^{-1}), respectively. Overall, the results showed that the highest lead content was in North Khorasan province, and the other two areas did not differ much in terms of the average of this trait (Fig. 3).

Nickel content in soil was much higher than water and plant samples in all studied sites. Also, soil nickel content in Khorasan Razavi province increased by 88.4% and 68.8% compared to North and South Khorasan, respectively. The highest soil and saffron nickel was achieved at S3 (235.2 mg kg^{-1}) and S6 (3.761 mg kg^{-1}), respectively. In contrast, S5 and S1 showed the lowest means of soil and saffron nickel content (19.15 and 2.088 mg kg^{-1}), respectively. Only the nickel was observed in the water sample of the S4 site (1.38 mg kg^{-1}) (Fig. 4).

The results showed that the cadmium was observed only in the soil of the S1 site by 0.241 mg kg^{-1}, and other sites and water and saffron lacked this element (Fig. 5).

As shown in Fig. 6, the highest soil arsenic content (6.985 mg kg^{-1}) was related to the S3 site, and the lowest

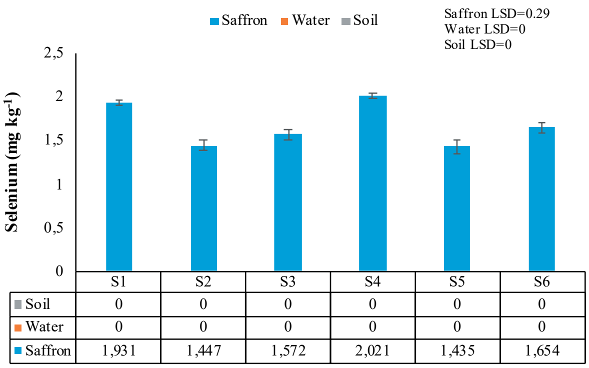

	S1	S2	S3	S4	S5	S6
Soil	0	0	0	0	0	0
Water	0	0	0	0	0	0
Saffron	1,931	1,447	1,572	2,021	1,435	1,654

Fig. 2. Selenium content in water, soil, and saffron cultivated in the different sites of North, Razavi, and South Khorasan provinces of Iran (Shirvan (S1); Faruj (S2); Zavareh (S3); Torbat-e Heydarieh (S4); Ghayen (S5); Birjand (S6)).

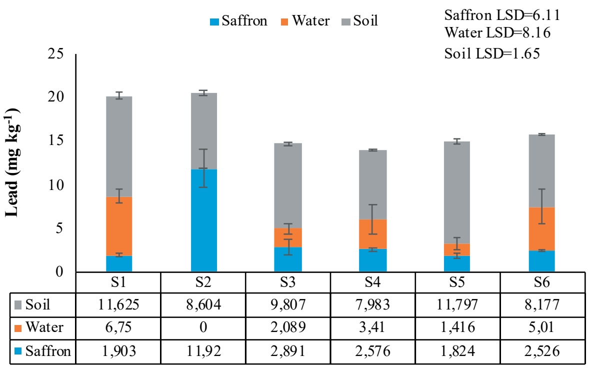

	S1	S2	S3	S4	S5	S6
Soil	11,625	8,604	9,807	7,983	11,797	8,177
Water	6,75	0	2,089	3,41	1,416	5,01
Saffron	1,903	11,92	2,891	2,576	1,824	2,526

Fig. 3. Lead content in water, soil, and saffron cultivated in the different sites of North, Razavi, and South Khorasan provinces of Iran (Shirvan (S1); Faruj (S2); Zavareh (S3); Torbat-e Heydarieh (S4); Ghayen (S5); Birjand (S6)).

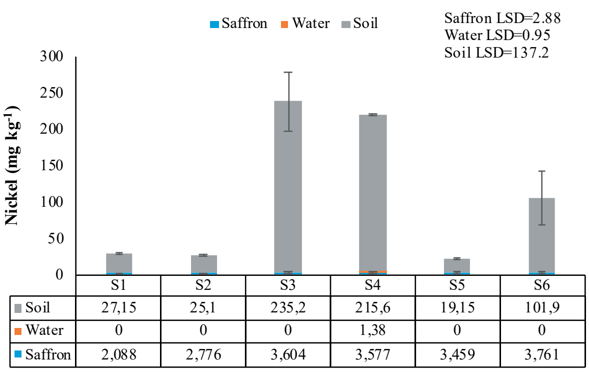

	S1	S2	S3	S4	S5	S6
Soil	27,15	25,1	235,2	215,6	19,15	101,9
Water	0	0	0	1,38	0	0
Saffron	2,088	2,776	3,604	3,577	3,459	3,761

Fig. 4. Nickel content in water, soil, and saffron cultivated in the different sites of North, Razavi, and South Khorasan provinces of Iran (Shirvan (S1); Faruj (S2); Zavareh (S3); Torbat-e Heydarieh (S4); Ghayen (S5); Birjand (S6)).

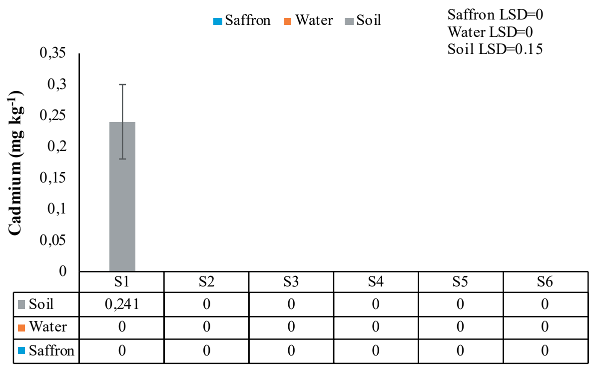

	S1	S2	S3	S4	S5	S6
Soil	0,241	0	0	0	0	0
Water	0	0	0	0	0	0
Saffron	0	0	0	0	0	0

Fig. 5. Cadmium content in water, soil, and saffron cultivated in the different sites of North, Razavi and, South Khorasan provinces of Iran (Shirvan (S1); Faruj (S2); Zavareh (S3); Torbat-e Heydarieh (S4); Ghayen (S5); Birjand (S6).

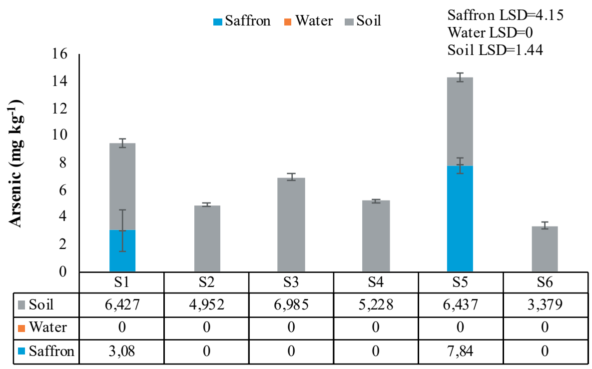

	S1	S2	S3	S4	S5	S6
Soil	6,427	4,952	6,985	5,228	6,437	3,379
Water	0	0	0	0	0	0
Saffron	3,08	0	0	0	7,84	0

Fig. 6. Arsenic content in water, soil, and saffron cultivated in the different sites of North, Razavi and South Khorasan provinces of Iran (Shirvan (S1); Faruj (S2); Zavareh (S3); Torbat-e Heydarieh (S4); Ghayen (S5); Birjand (S6).

(3.379 mg kg^{-1}) to S6. Water samples from the tested sites did not contain arsenic. Also, saffron samples grown at S1 and S5 sites had arsenic elements (3.08 and 7.84 mg kg^{-1}, respectively).

Simple correlation coefficient, PCA, and cluster analysis

Pearson's correlation coefficient matrix of all the measured variables with quantitative (flower and stigma yield) and qualitative (safranal, picrocrocin, and crocins content) traits is reported in Table 5. There were significantly negative and positive correlations among quantitative and qualitative properties as well as environmental and climatic characteristics. For example, the stigma yield was significantly and positively correlated with saffron flower yield, safranal and picrocrocin content, and

Table 5. Pearson correlation coefficient between environmental and climatic traits and biochemical attribute with flower and stigma yield and quality of saffron in different sites of North, Razavi, and South Khorasan provinces of Iran.

	Saffron flower yield	Stigma yield	Safranal content	Picrocrocin content	Crocins content
Saffron flower yield	1				
Stigma yield	0.60	1			
Safranal content	0.85	0.68	1		
Picrocrocin content	0.59	0.47	0.72	1	
Crocins content	0.24	0.16	0.27	0.78	1
Anthocyanin content	0.13	-0.01	0.09	0.04	0.04
Total flavonoid content	0.24	-0.01	0.21	0.07	-0.04
Total phenol content	0.24	0.03	0.22	0.19	0.14
DPPH-150	0.16	-0.02	0.16	0.01	-0.14
DPPH-200	0.09	-0.12	0.09	-0.09	-0.23
DPPH-250	0.05	-0.16	0.08	-0.01	-0.08
Se-saffron	0.40	0.28	0.44	0.50	0.32
Pb-saffron	0.20	0.20	0.08	-0.03	0.09
Ni-saffron	-0.13	-0.25	-0.19	0.04	0.24
As-saffron	-0.31	-0.18	-0.27	-0.04	0.16
Pb-water	0.15	0.18	0.09	-0.02	-0.07
Ni-water	0.00	0.21	-0.03	0.16	0.19
Pb-Soil	-0.36	-0.26	-0.36	-0.21	0.06
Ni-Soil	0.09	-0.05	0.06	0.29	0.42
Cd-Soil	0.28	0.23	0.18	0.14	0.21
As-Soil	-0.54	-0.49	-0.51	-0.09	0.28
Relative humidity	0.25	0.28	0.18	0.22	0.31
Minimum winter temperature	-0.38	-0.21	-0.27	0.05	0.29
Maximum summer temperature	-0.37	-0.55	-0.12	-0.55	-0.70
Number of annual frost days	0.04	0.02	0.04	0.22	0.43
Average annual temperature	-0.12	-0.15	-0.09	-0.25	-0.38
Average annual rainfall	0.25	0.20	0.19	0.48	0.60
Altitude	-0.30	-0.23	-0.19	-0.34	-0.44
Latitude	0.27	0.22	0.20	0.31	0.41
Longitude	-0.10	-0.03	-0.16	-0.09	-0.09

-1	-0.9	-0.8	-0.7	-0.6	-0.5	-0.4	-0.3	-0.2	-0.1	0	0.1	0.2	0.3	0.4	0.5	0.6	0.7	0.8	0.9	1
High negative correlation										Non-correlation										High positive correlation

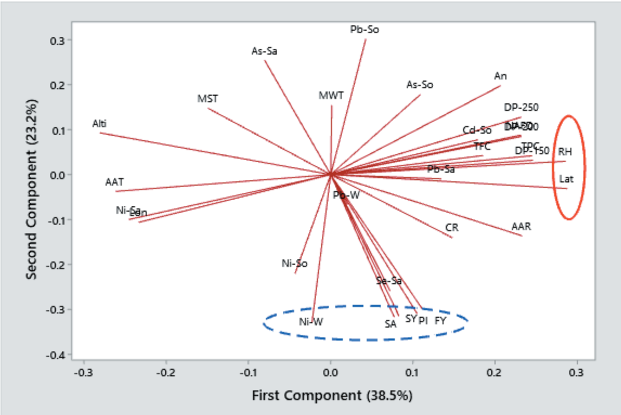

Fig. 7. Principal components analyses for yield, quality, and biochemical characteristics as well as environmental and climatic traits.

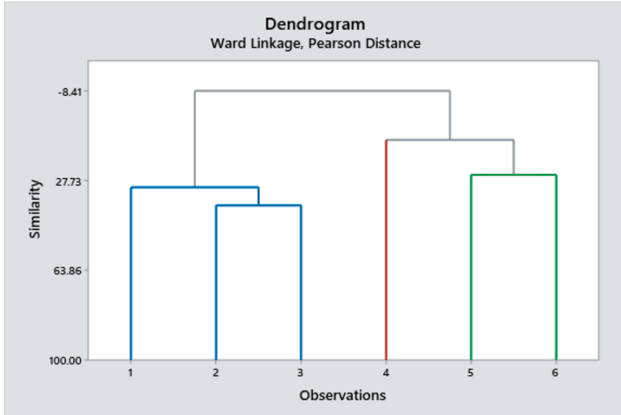

Fig. 8. Cluster analysis for yield, quality, and biochemical characteristics as well as environmental and climatic traits.

Se-saffron content. However, the saffron flower yield and stigma yield were negatively and significantly correlated with the Pb-soil, As-soil, and the maximum summer temperature. Interestingly, Se-saffron and latitude had a positive effect on increasing the flowers and stigmas yield as well as quality. While increasing the altitude and maximum summer temperature leads to a decrease in yield and quality in saffron. Moreover, saffron's biochemical traits had no significant negative or positive correlation with quantitative and qualitative yield. In general, the results of this section showed that increasing climatic parameters, average annual rainfall, average humidity, and latitude leads to increased quantitative and qualitative performance.

Table 6. Cluster analysis and grouping for yield, quality, and biochemical characteristics saffron.

Variable	Cluster 1	Cluster 2	Cluster 3	Grand centroid
Saffron flower yield	0.76	**<u>0.84</u>**	0.71	0.76
Stigma yield	0.09	**<u>0.10</u>**	0.09	0.09
Safranal content	13.55	15.84	13.04	13.76
Picrocrocin content	24.84	30.63	22.26	24.95
Crocins content	59.58	69.38	46.18	56.75
Anthocyanin content	3.18	3.05	3.07	3.12
Total flavonoid content	14.11	13.55	13.65	13.86
Total phenol content	126.21	119.77	118.83	122.68
DPPH-150	41.55	32.77	32.67	37.13
DPPH-200	50.48	40.18	42.52	46.11
DPPH-250	73.20	58.34	61.46	66.81
Se-saffron	1.65	2.02	1.54	1.68
Pb-saffron	5.57	2.58	2.17	3.94
Ni-saffron	2.82	3.58	3.61	3.21
Pb-water	1.03	0.00	3.92	1.82
Pb-Soil	2.95	3.41	3.21	3.11
Ni-Soil	0.00	1.38	0.00	0.23
Number of sites in each cluster	3	1	2	-

Regarding the relationship among quantity, quality, biochemical, environmental, and climatic characteristics, all studied characteristics were analyzed by using PCA. Combined, PC1 (38.5%) and PC2 (23.2%) accounted for 61.7% of the total variance of the data (Fig. 7). The first PC (PC1) is characterized by relative humidity and latitude. This is appropriate because the Pearson correlation showed a significant correlation between yield and quality traits with relative humidity and latitude (Table 5). The second PC (PC2) is characterized by flower and stigma yield and quality attributes such as picrocrocin and safranal content. According to the findings, the PC1 can be called climatic and environmental factor, and the PC2 can be called quantitative and qualitative yield.

The goal of cluster analysis is to build a tree diagram where the sites that were viewed as most similar by the attributes in the study are placed on branches that are close together. As shown in Table 6 and Fig. 8, six sites were classified into three clusters, the first cluster included 3 sites (S1, S2, and S3), the second had 1 site (S4), and the S5 and S6 as the third cluster. The first cluster in terms of biochemical characteristics such as anthocyanin, total flavonoid, and total phenol content, as well as DPPH activity and the second cluster in terms of quantitative and qualitative characteristics including flower and stigma yield and safranal, picrocrocin, and crocins content had the highest coefficients.

DISCUSSION

The purpose of this study was to compare the quantitative and qualitative performance of saffron in six sites of major saffron producing provinces in Iran. The results showed significant differences in saffron flower yield, stigma yield, crocin, and safranal content in the studied areas. Rahimi *et al*. (2017) reported that the significant difference among the cultivation areas in terms of quality and quantity traits confirms the findings of the present study. Saffron quantitative and qualitative characteristics depend on the concentration of its primary metabolites and environmental conditions. According to the mean comparison and cluster analysis, saffron grown in S4 (Torbat-e Heydarieh: Khorasan Razavi province) resulted in significantly higher yield and quality than those produced in the other sites. It seems that the low maximum summer temperature in the area is one of the reasons for its superiority. In this regard, the correlation analysis shows that the maximum summer temperature had a significant negative correlation with saffron flower yield, stigma yield, picrocrocin and crocin content. On the other hand, a specific climatic parameter in the S4 site is the low maximum summer temperature and the high average annual rainfall. Accordingly, the simple correlation analysis shows that the average annual rainfall had a significant positive correlation with saffron quantitative and qualitative characteristics. Kamyabi *et al*. (2014) and Maleki *et al*. (2017) reported that annual rainfall and temperature had the highest impact on saffron cultivation among environmental factors, which confirms the findings of the present study. Temperature is the most important environmental factor controlling *Crocus* species' growth and flow (Haghighi *et al*., 2020). Moreover, Gresta *et al*. (2009) reported that temperature certainly plays a role in flowering induction and flower appearance. Saffron has been successfully grown under different geographic locations in the world (Husaini, 2014). This crop can be cultivated in temperate, semi-arid, and arid areas with 1500–2800 m.a.s.l (Rahimi *et al*., 2017). Ghorbani and Koocheki (2017) reported that the favorable climatic conditions for saffron's high yields are warm summers, autumn rains, and mild winters.

Environmental conditions such as altitude may also affect saffron yield and quality (Cardone *et al*., 2019; Parizad *et al*., 2019). In the current study, a negative relationship was obtained between the altitude and the quantitative and qualitative characteristics of saffron (Table 5). It seems that increasing the altitude too much leads to a decrease in the quantity and quality of saffron. This study's findings showed that an altitude of more than 1350 m.a.s.l decrease quantity and quality of the yield. In general, the altitude of 1250 to 1350 m.a.s.l seems desirable in achieving maximum quantitative and qualitative yield. However, in contrast with Al Madini *et al*. (2019), who point out that saffron cultivation is possible at altitudes of 1500 to 2800 m.a.s.l, our results show that the optimal altitude for maximum quantitative and qualitative yield was about 1300 m.a.s.l. However, saffron can also be cultivated with good yields in very different environmental conditions (Caser *et al*., 2019); a combination of certain environmental factors can be important to reach the optimum qualitative and quantitative yield (Rahimi *et al*., 2017). Finally, correlation analysis showed transparent relationships within quantitative parameters, within qualitative parameters, and between quantitative and qualitative traits (Gresta *et al*., 2009).

Biochemical properties of saffron such as flavonoid and total phenol content as well as DPPH free radical scavenging at different concentrations of the extract (150, 200, and 250 µmol ml^{-1}) showed significant differences at these sites. However, a decreasing trend was observed in the mean of total phenol and flavonoid metabolites as well as antioxidant activity of DPPH from north to south of Khorasan. Along with this trend, the climatic parameters of relative humidity and the number of annual frost days from North to South Khorasan decreased. In the climatic data, the low average annual temperature and altitude in North Khorasan province and the highest number of annual frost days are the index parameters of these sites. These three climatic factors seem to be environmental stressors of the plant. In response to these conditions, the plant changes its physiological interactions to increase defense mechanisms such as total phenol, flavonoids, and activity of DPPH free radical scavenging (Xu *et al*., 2015; Hashim *et al*., 2020). Zargoosh *et al*. (2019) reported that the effect of site on the antioxidant potential (DPPH) and total phenol amount of *Scrophularia striata* L. was significant. Therefore, it can be stated that the complexity of the effect of ecological factors on the one hand, and the emergence of different chemical processes in the plant under such effects, on the other hand, has led to the synthesis of various compounds with antioxidant potential in a plant in different regions (Zargoosh *et al*., 2019). Although genetic processes guide the production of active ingredients in medicinal plants, environmental factors are strongly influenced (Figueiredo *et al*., 2008). Therefore, environmental factors such as temperature cause changes in the growth of medicinal plants, as well as the quantity and quality of their active components, such as essential oils, glycosides, steroids, and alkaloids. The determinants of plant production are climate, soil, and geographic location. These factors can have a significant impact on increasing or decreasing the quantity and quality of plant performance (Liu *et al*., 2015; Zargoosh *et al*., 2019). Researchers believe that many factors, such as water, air, soil, altitude (m.a.s.l), and differences between species, extraction methods, and antioxidant measurements, affect the number of secondary metabolites in plants, including phenol and flavonoids (Hashim *et al*., 2020; Mykhailenko *et al*., 2020). Overall, the antioxidant properties and habitat effects the number of secondary metabolites (Zargoosh *et al*., 2019).

The heavy metals content (selenium, lead, nickel, cadmium, and arsenic) in water, soil, and saffron cultivated in the different sites of North, Razavi, and South Khorasan provinces indicated that the results present a wide variation. Selenium, lead, nickel, and arsenic were observed in saffron samples in the studied sites. On the other hand, in these sites' soil, there was lead, nickel, cadmium, and arsenic. Overall, the S4, S6, and S5 sites had the lowest averages in terms of lead, arsenic, and nickel, respectively. In other words, the high amount of heavy metals in South Khorasan province compared to the other two provinces leads to the conclusion that saffron grown in this province due to the high heavy metals content is less marketable and harms the consumer. The correlation between traits showed that the most negative effect on flower and stigma yield was related to soil arsenic followed by soil lead.

Esmaeili *et al*., (2013) reported that the low contents of heavy metals (lead, nickel, cadmium, and arsenic) are also important for the plant's quality. The results showed that the concentration of heavy metals in plant samples other than lead for the S2 site was lower than the standard level in other cases. Uptake of various elements by plants through the root system from the soil depends on the particular plant, botanical structure of specific tissue, soil type, and element (Shahid *et al*., 2018). Besides, microelements can enter the plant from the external environmental compartments (Esmaeili *et al*., 2013; Liu *et al*., 2018).

A significant point was the presence of selenium in saffron samples. This element had a positive and significant correlation with the quantitative and qualitative yield of saffron. In this regard, various researchers have expressed the positive effects of selenium. For example, Shahverdi *et al*., (2018) reported that selenium is a useful element for plant growth and production, which plays an important role in growth and biochemical traits such as antioxidant activity. Some studies have shown that selenium is an essential element for humans and animals, which plays some beneficial roles in higher plants (Iqbal *et al*., 2015). Selenium application caused an increasing growth in mung bean and wheat under both stressed and non-stressed conditions (salinity, drought, and heat stresses) (Shahzadi *et al*., 2017; Shahverdi *et al*., 2018; Shahverdi *et al*., 2020).

CONCLUSION

The current study focused on the effect of different climatic parameters on quantitative, qualitative, and biochemical characteristics of saffron in the six strategic saffron production regions (North, Razavi, and South Khorasan provinces) in Iran. Based on the present study results, qualitative and quantitative characteristics such as flower and stigma yield, crocins, safranal, and picrocrocin content are strongly controlled by the soil properties and climatic conditions in Shirvan, Faruj, Zavareh, Torbat-e Heydarieh, Ghayen, and Birjand regions. The saffron flower and stigma yield were more in Torbat-e Heydarieh (S4) than in other sites, while biochemical attributes were higher in S1 and S2 (Shirvan and Faruj sites) than that of other sites. Low maximum summer temperature and high relative humidity were two features of the climate index in the S4 region. This study's attractive result was the positive and significant relationship between selenium and quantitative and qualitative yield of saffron. It seems that the presence of selenium in the growth medium of the saffron increases the yield. Because there was a positive and significant correlation between selenium and quantitative and qualitative yield of saffron, in the saffron samples related to S4, a higher average of the element was observed compared to other sites. Based on the findings, it is concluded that Razavi Khorasan province (Especially Torbat-e Heydariyeh site) had a significant advantage in terms of quantitative and qualitative yield of saffron and North Khorasan province (Shirvan and Faruj sites) in terms of biochemical characteristics.

REFERENCE

Al Madini, AM., Sassine, YN., El-Ganainy, SM., Hourani, W., and Sebaaly, ZE. 2019. Comparative study on phenology, yield and quality of iranian saffron cultivated in lebanon and iran. Fresenius Environmental Bulletin, 28: 9655-9660.

Amirnia, R., Bayat, M., and Tajbakhsh, M. 2014. Effects of nano fertilizer application and maternal corm weight on flowering at some saffron (*Crocus sativus* L.) ecotypes. Turkish Journal of Field Crops, 19:158-168.

Baba, SA., Malik, AH., Wani, ZA., Mohiuddin, T., Shah, Z., Abbas, N., and Ashraf, N. 2015. Phytochemical analysis and antioxidant activity of different tissue types of *Crocus sativus* and oxidative stress alleviating potential of saffron extract in plants, bacteria, and yeast. South African Journal of Botany, 99: 80-87.

Babaei, S., Talebi, M., Bahar, M. and Zeinali, H. 2014. Analysis of genetic diversity among saffron (*Crocus sativus*) accessions from different regions of Iran as revealed by SRAP markers. Scientia Horticulturae, 171: 27-31.

Baghalian, K., Sheshtamand, MS., and Jamshidi, A. 2010. Genetic variation and heritability of agro-morphological and phytochemical traits in Iranian saffron (*Crocus sativus* L.) populations. Industrial Crops and Products, 31: 401-406.

Cardone, L., Castronuovo, D., Perniola, M., Cicco, N., and Candido, V. 2019. Evaluation of corm origin and climatic conditions on saffron (*Crocus sativus* L.) yield and quality. Journal of the Science of Food and Agriculture, 99: 5858-5869.

Cardone, L., Castronuovo, D., Perniola, M., Cicco, N., and Candido, V. 2020. Saffron (*Crocus sativus* L.), the king of spices: An overview. Scientia Horticulturae, 272: 109560.

Caser, M., Victorino, ÍMM., Demasi, S., Berruti, A., Donno, D., Lumini, E., Bianciotto, V., and Scariot, V. 2019. Saffron cultivation in marginal alpine environments: how AMF inoculation modulates yield and bioactive compounds. Agronomy, 9:12.

Chen, M., and Ma, LQ. 2001. Comparison of three aqua regia digestion methods for twenty Florida soils. Soil science society of America Journal, 65: 491-499.

Esfanjani, AF., Jafari, SM., and Assadpour, E. 2017. Preparation of a multiple emulsion based on pectin-whey protein complex for encapsulation of saffron extract nanodroplets. Food Chemistry, 221: 1962-1969.

Esmaeelian, M., Jahani, M., Feizy, J., and Einafshar, S. 2020. Effects of ultrasound-assisted and direct solvent extraction methods on the antioxidant and antibacterial properties of saffron (*Crocus sativus* L.) corm extract. Food Analytical Methods,1: 1-14.

Esmaeili, N., Ebrahimzadeh, H., Abdi, K., Mirmasoumi, M., Lamei, N., and Shamami, MA. 2013. Determination of metal content in *Crocus sativus* L. corms in dormancy and waking stages. Iranian Journal of Pharmaceutical Research, 12: 31-38.

Feli, A., Maleki Farahani, S., and Besharati, H. 2018. The effect of urea fertilizer and different organic and biofertilizers on quantitative and qualitative yield and some soil properties in Saffron cultivation. Journal of Crops Improvement, 20: 345-356.

Figueiredo, AC., Barroso, JG., Pedro, LG., and Scheffer, JJ. 2008. Factors affecting secondary metabolite production in plants: volatile components and essential oils. Flavour and Fragrance Journal, 23: 213-226.

Ghanbari, J., Khajoei-Nejad, G., van Ruth, S.M., Aghighi, S., 2019. The possibility for improvement of flowering, corm properties, bioactive compounds, and antioxidant activity in saffron (Crocus sativus L.) by different nutritional regimes. Industerial and Crop Production, 135: 301-310.

Ghorbani, R., and Koocheki, A. 2017. Sustainable cultivation of saffron in Iran.' in, Sustainable agriculture reviews (Springer Publisher).

Gresta, F., Avola, G., Lombardo, G., Siracusa, L., and Ruberto, G. 2009. Analysis of flowering, stigmas yield and qualitative traits of saffron (*Crocus sativus* L.) as affected by environmental conditions. Scientia Horticulturae, 119: 320-324.

Haghighi, R., Tabatabaei, BES., Maibody, SAMM., Talebi, M., Molina, R., Nebauer, SG., and Renau-Morata, B. 2020. A flowering inhibitor of the temperature-dependent pathway in *Crocus sativus* L. Molecular Biology Reports, 47: 2171-2179.

Hashim, AM., Alharbi, BM., Abdulmajeed, AM., Elkelish, A., Hozzein, WN., and Hassan, HM. 2020. Oxidative stress responses of some endemic plants to high altitudes by intensifying antioxidants and secondary metabolites content. Plants, 9: 869-877.

Husaini, AM. 2014. Challenges of climate change: Omics-based biology of saffron plants and organic agricultural biotechnology for sustainable saffron production. GM Crops & Food, 5: 97-105.

Hussain, A., Illahi, BA., Iqbal, AM., Jehaangir, I., and Hussain, ST. 2019. Agronomic management of saffron (*Crocus sativus*)-A review. Indian Journal of Agronomy, 64: 147-164.

Iqbal, M., Hussain, I., Liaqat, H., Ashraf, MA., Rasheed, R., and Rehman, AU. 2015. Exogenously applied selenium reduces oxidative stress and induces heat tolerance in spring wheat. Plant Physiology and Biochemistry, 94: 95-103.

Jelínek, L., Dolečková, M., Karabin, M., Hudcova, T., Kotlikova, B., and Dostalek, P. 2012. Influence of growing area, plant age, and virus infection on the contents of hop secondary metabolites. Czech Journal of Food Sciences, 30: 541-547.

Kafi, M., Kamili, AN., Husaini, AM., Ozturk, M., and Altay, V. 2018. An expensive spice saffron (*Crocus sativus* L.): a case study from Kashmir, Iran, and Turkey. in, *Global perspectives on underutilized crops* (Springer), pp:109-149.

Kamyabi, S., Habibi Nokhandan, M., and Rouhi, A. 2014. Effect of climatic factors affecting saffron using analytic hierarchy process (AHP);(Case study Roshtkhar

Region, Iran)'. Saffron Agronomy and Technology, 2: 75-90.

Lage, M., and Cantrell, CL. 2009. Quantification of saffron (*Crocus sativus* L.) metabolites crocins, picrocrocin and safranal for quality determination of the spice grown under different environmental Moroccan conditions. Scientia Horticulturae, 121: 366-373.

Liu, J., Dhungana, B., and Cobb, GP. 2018. Environmental behavior, potential phytotoxicity, and accumulation of copper oxide nanoparticles and arsenic in rice plants. Environmental Toxicology and Chemistry, 37: 11-20.

Liu, W., Liu, J., Yin, D., and Zhao, X. 2015. Influence of ecological factors on the production of active substances in the anti-cancer plant *Sinopodophyllum hexandrum* (Royle) TS Ying. PLoS One, 10: e0122981.

Maleki, F., Kazemi, H., Siahmarguee, A., and Kamkar, B. 2017. Development of a land use suitability model for saffron (*Crocus sativus* L.) cultivation by multi-criteria evaluation and spatial analysis. Ecological Engineering, 106: 140-153.

Maleki Farahani, S., and Aghighi Shahverdi, M. 2015. Evaluation the effect of nono-iron fertilizer in compare to iron chelate fertilizer on qualitative and quantitative yield of saffron. Journal of Crops Improvement, 17: 155-168.

Moradi, A., Zarinkamar, F., De Domenico, S., Mita, G., Di Sansebastiano, GP., and Caretto, S. 2020. Salycilic acid induces exudation of crocin and phenolics in saffron suspension-cultured cells. Plants, 9: 949-954.

Mykhailenko, O., Gudžinskas, Z., Kovalyov, V., Desenko, V., Ivanauskas, L., Bezruk, I., and Georgiyants, V. 2020. Effect of ecological factors on the accumulation of phenolic compounds in Iris species from Latvia, Lithuania and Ukraine. Phytochemical analysis, 31(5): 545-563.

Parizad, S., Dizadji, A., Habibi, MK., Winter, S., Kalantari, S., Movi, S., Tendero, CL., Alonso, GL., and Moratalla-Lopez, N. 2019. The effects of geographical origin and virus infection on the saffron (*Crocus sativus* L.) quality. Food Chemistry, 295: 387-394.

Perpina, C., Martinez-Llario, J.C., and Navarro, A., 2013. Multi-criteria assessment in GIS environments for sitting biomass plants. Land Use Policy, 31: 326-335.

Rahimi, H., Shokrpour, M., Tabrizi Raeini, L., and Esfandiari, E. 2017. A study on the effects of environmental factors on vegetative characteristics and corm yield of saffron (*Crocus sativus*). Iranian Journal of Horticultural Science, 48: 45-52.

Sakamoto, M., and Suzuki, T. 2019. Methyl jasmonate and salinity increase anthocyanin accumulation in radish sprouts. Horticulturae, 5: 62-74.

Sánchez-Vioque, R., Rodríguez-Conde, M., Reina-Ureña, J., Escolano-Tercero, M., Herraiz-Peñalver, D., and Santana-Méridas, O. 2012. In vitro antioxidant and metal chelating properties of corm, tepal and leaf from saffron (*Crocus sativus* L.). Industrial Crops and Products, 39: 149-153.

Shahid, M., Niazi, NK., Khalid, S., Murtaza, B., Bibi, I., and Rashid, MI. 2018. A critical review of selenium biogeochemical behavior in soil-plant system with an inference to human health. Environmental Pollution, 234: 915-934.

Shahverdi, MA., Omidi, H., and Damalas, CA. 2020. Foliar fertilization with micronutrients improves *Stevia rebaudiana* tolerance to salinity stress by improving root characteristics. Brazilian Journal of Botany, 43: 55-65.

Shahverdi, MA., Omidi, H., and Tabatabaei, SJ. 2018. Plant growth and steviol glycosides as affected by foliar application of selenium, boron, and iron under NaCl stress in *Stevia rebaudiana* Bertoni. Industrial Crops and Products, 125: 408-415.

Shahzadi, I., Iqbal, M., Rasheed, R., Ashraf, MA., Perveen, S., and Hussain, M. 2017. Foliar application of selenium increases fertility and grain yield in bread wheat under contrasting water availability regimes. Acta Physiologiae Plantarum, 39: 173-184.

Shokrpour, M. 2019. Saffron (*Crocus sativus* L.) breeding: opportunities and challenges. Advances in Plant Breeding Strategies: Industrial and Food Crops, 1: 675-706.

Williams, WT., and Lambert, JM. 1959. Multivariate methods in plant ecology: I. Association-analysis in plant communities. The Journal of Ecology, 47(1): 83-101.

Xu, Z., Jiang, Y., and Zhou, G. 2015. Response and adaptation of photosynthesis, respiration, and antioxidant systems to elevated CO_2 with environmental stress in plants. Frontiers in Plant Science, 6: 701-711.

Zargoosh, Z., Ghavam, M., Bacchetta, G., and Tavili, A. 2019. Effects of ecological factors on the antioxidant potential and total phenol content of *Scrophularia striata* Boiss. Scientific Reports, 9: 1-15.

Italian Journal of Agrometeorology
Rivista Italiana di Agrometeorologia

Firenze University Press
www.fupress.com/ijam

Citation: I. Volpi, D. Guidotti, M. Mammini, S. Marchi (2021) Predicting symptoms of downy mildew, powdery mildew, and gray mold diseases of grapevine through machine learning. *Italian Journal of Agrometeorology* (2): 57-69. doi: 10.36253/ijam-1131

Received: November 10, 2020

Accepted: August 14, 2021

Published: December 27, 2021

Data Availability Statement: All relevant data are within the paper and its Supporting Information files.

Competing Interests: The Author(s) declare(s) no conflict of interest.

Predicting symptoms of downy mildew, powdery mildew, and gray mold diseases of grapevine through machine learning

Iride Volpi, Diego Guidotti, Michele Mammini, Susanna Marchi

AEDIT s.r.l., Pontedera, Pisa, Italy
E-mail: volpi@aedit.it; guidotti@aedit.it; mammini@aedit.it; marchi@aedit.it

Abstract. Downy mildew, powdery mildew, and gray mold are major diseases of grapevine with a strong negative impact on fruit yield and fruit quality. These diseases are controlled by the application of chemicals, which may cause undesirable effects on the environment and on human health. Thus, monitoring and forecasting crop disease is essential to support integrated pest management (IPM) measures. In this study, two tree-based machine learning (ML) algorithms, random forest and C5.0, were compared to test their capability to predict the appearance of symptoms of grapevine diseases, considering meteorological conditions, spatial indices, the number of crop protection treatments and the frequency of monitoring days in which symptoms were recorded in the previous year. Data collected in Tuscany region (Italy), on the presence of symptoms on grapevine, from 2006 to 2017 were divided with an 80/20 proportion in training and test set, data collected in 2018 and 2019 were tested as independent years for downy mildew and powdery mildew. The frequency of symptoms in the previous year and the cumulative precipitation from April to seven days before the monitoring day were the most important variables among those considered in the analysis for predicting the occurrence of disease symptoms. The best performance in predicting the presence of symptoms of the three diseases was obtained with the algorithm C5.0 by applying (i) a technique to deal with imbalanced dataset (i.e., symptoms were detected in the minority of observations) and (ii) an optimized cut-off for predictions. The balanced accuracy achieved in the test set was 0.8 for downy mildew, 0.7 for powdery mildew and 0.9 for gray mold. The application of the models for downy mildew and powdery mildew in the two independent years (2018 and 2019) achieved a lower balanced accuracy, around 0.7 for both the diseases. Machine learning models were able to select the best predictors and to unravel the complex relationships among geographic indices, bioclimatic indices, protection treatments and the frequency of symptoms in the previous year.

Keywords: agrometeorology, ERA5, grape, IPM models, monitoring networks.

1. INTRODUCTION

Downy mildew, powdery mildew, and gray mold are major diseases of grapevine (*Vitis vinifera* L.), affecting leaves and fruits and causing yield loss and quality decrease of must and wine. Downy mildew is caused by the Oomycete *Plasmopara viticola* (Berk. & Curt.) Berl. & de Toni, with sexual spores determining primary infections and asexual spores causing secondary infections (Gessler et al., 2011). This pathogen infects leaves, shoots, and bunches, damaging up to 75% of the crop in one season when no treatments are applied (Buonassisi et al., 2017), thus leading to great economic losses. Powdery mildew is caused by *Erisyphe necato*r Schwein., a polycyclic disease with two distinct phases: primary infections are caused by sexual spores (ascospores) and secondary infections are determined by asexual spores (conidia) (Gadoury and Pearson, 1988), on all green tissues of grapevines, mainly leaves and berries (Gadoury et al., 2001; Caffi et al., 2011). *Botrytis cinerea* Pers. is the causal agent of gray mold and in grapevine infects all green tissues, particularly ripening berries, with different infection pathways for conidia (inflorescences, young clusters and ripening berries) and mycelium (berry-to-berry) (Elmer et al., 2007).

Because these pathogens may cause severe symptoms on grapevines at the beginning of infection, control strategies have focused on early treatments, even in integrated pest management (IPM), as prevention to stop the pathogen outbreak before its establishment. Applying fungicide treatments during the growing season remains the most common practice to control these diseases, from early spring onward, with differences between years due to weather conditions and to the geographic location of the vineyard (Chen et al., 2020; Lu et al., 2020; Molitor et al., 2016). However, concerns about the negative impact of chemicals on environmental and human health have resulted in restrictions to regulate fungicide use, such as the EU directives (i.e., Directive 1107/2009/EU) (Valdés-Gómez et al., 2017). European Commission currently enforces national action plans for pesticide reduction, encouraging the use of monitoring networks (Directive 128/2009/EC), forecasting models, and dissemination tools to share this information among growers and technicians (Pertot et al., 2017). Therefore, a reliable monitoring and forecasting system is essential for deriving prediction indices in support of sustainable protection measures (e.g., Marchi et al., 2016).

To this aim, various weather-driven models, either mechanistic (Rossi et al., 2008; Caffi et al., 2011; Legler et al., 2011; Gonzales et al., 2015) or empirical (Orlandini et al., 1993; Rodríguez-Rajo et al., 2010; Hill et al., 2019), have been developed for predicting grapevine diseases and assisting farmers in decision-making for crop protection. Decision support systems (DSSs), based on predictive models that use weather data and infection information, may provide this service to farmers (Rossi et al., 2014; Pertot et al., 2017). In particular, DSSs may help determine the time window for fungicide application to optimize their effects and to reduce the number of interventions during the growing season. Nevertheless, currently available models are mainly focused on predicting the risk of the outbreak, rather than the pressure of the disease. This approach may cause unnecessary fungicide applications and the use of untargeted chemical compounds, in turn contravening control regulations based on the maximum number of treatments allowed for each season (mandatory in IPM).

Since these three diseases are strongly influenced by seasonal weather conditions, albeit with different pathways among vectors, varying annually and driven by composite interactions between the disease agent and the host plant (growth stage and grapevine cultivar), models that provide information on infection risk need to combine numerous weather variables, crop parameters, and disease traits. Increasing computing power is providing the means to capture and process abundant data, and to reveal associations among variables that describe the weather-pathogen-host interactions. In particular, machine learning (ML) techniques allow considering a large number of variables, integrating diverse data sources in close real time, in order to assess the interactions among disease agent, host plant, and climatic variability, before visible symptoms are present, with the aim of ensuring effective and sustainable fungicide management (Lee et al., 2019; Sperschneider, 2019).

The potential of statistical models and ML algorithms to predict the occurrence of grapevine diseases has been rarely assessed (Chen et al., 2020). Here, we investigated the ability of ML algorithms to clarify the occurrence of symptoms of these three important diseases of grapevine based on prevailing weather conditions both within and between locations and years, generating temporal- and spatial-explicit projections of the infections. These models were implemented using as inputs: bioclimatic and geographic indices, the frequency of monitored symptoms in the previous year, and the number of crop protection treatments during the growing season. The aim of the study was to calculate the overall probability of symptom appearance at field scale, using the ML approach and the area-wide IPM monitoring network of Regione Toscana, providing farmers with a tool able to address timely and accurate grapevine disease forecasting.

2. MATERIALS AND METHODS

2.1 Monitoring grapevine diseases

Data on disease symptoms were obtained from Agroambiente.info (http://www.agroambiente.info/), the agricultural and environmental portal of Phytosanitary Service of Regione Toscana (Italy). Agroambiente.info stores data deriving from an area-wide IPM monitoring network, which covers most of the wine production area of Tuscany. Sampling is carried out weekly by trained field technicians, from the leaf development stage (mid-end of April) to harvest (mid-end of September), in a variable number of vineyards through years (112-179). In each vineyard, date and presence of symptoms of downy mildew, powdery mildew and gray mold are recorded inspecting leaves and/or bunches. In addition, the date of treatments is reported, as well as the active substance (maximum two active substances for each treatment), among those allowed by "Integrated Production Regulation" of Regione Toscana. A simplified index of disease severity for each disease is documented during the monitoring activity, though it was not used for the ML exercise. Considering that different cultivars may show variable susceptibilities to the three diseases, the monitoring network focuses only on the cv Sangiovese, which is the most widespread and important for Tuscany denomination of controlled origin red wines. A numeric identification code ("farm ID") is assigned to each of the selected vineyards.

In this study, we considered data from 2006 to 2019, excluding 2011 since no data was available for that year in the regional database. In each dataset of the three diseases, the observations were classified as "inf" or "no", according to the presence or absence of disease symptoms, respectively. Observations were classified as "inf" when symptoms were present on leaves and/or on bunches.

2.2 Variables associated with grapevine diseases

Variables were calculated for each vineyard and each disease to be used as features for the ML models. The set of variables included: bioclimatic indices, geographical indices, indices indicating the number of phytosanitary treatments applied, an index referring to the frequency of the presence of infection in the previous year, and the day-of-year (doy) (Tab. 1).

The package 'raster' (Hijmans, 2019a) of the R environment (R Core Team, 2020), was used to extract for each vineyard from the raster files of the Tuscany region: (i) the Euclidean distance from the sea (dis_sea) in m and (ii) the elevation above sea level (m), obtained from the Digital Elevation Model (dem).

Meteorological data were downloaded from the open access ERA5-Land dataset, the latest generation of ECMWF atmospheric reanalysis, which provides hourly data from 1981 to 2-3 months before present in a fixed grid and with a native resolution of 9 km (Copernicus Climate Change Service, 2017).

ERA5-Land dataset was selected over others (e.g., ERA5, ERA-Interim) because of its higher spatial resolution and its improved correlation with in situ measurements, especially concerning the water cycle (Muñoz-Sabater et al., 2021). Using reanalysis meteorological data, as ERA5-Land dataset, for modelling has the main advantages of providing data with a better temporal and spatial coverage with respect to the data collected with real weather stations that do not have a uniform spatial and temporal coverage and may be subjected to breaks (Padulano et a., 2021). Indeed, concerning the density of the weather monitoring network of Tuscany Region, the distance from each vineyard to its nearest station ranged between 120 m to 27000 m with an average value of 6640 m.

Meteorological data from the ERA5-Land dataset used to calculate daily maximum, minimum and average air temperature (°C) and daily precipitation (mm) for the period from 2006 to 2019 were: "2-m temperature", defined as the hourly temperature of air at 2 m above the ground, sea or inland waters, and "total precipitation", defined as accumulated liquid and frozen water, including rain and snow, that falls to the Earth's surface. The distance between each ERA5 grid-box and each georeferenced monitoring site was calculated through the R package 'geosphere' (Hijmans, 2019 b), with the aim of associating each sampling site with an ERA5 grid-box.

Bioclimatic indices were calculated starting from daily data on air temperature and precipitation, considering three different periods: (i) from November to January for the indices describing the weather conditions during overwintering (average of minimum, maximum and mean daily temperature), (ii) from November to March for monthly mean air temperature and cumulative precipitation, (iii) from April to October (monitoring period) for the bioclimatic indices describing the weather conditions in the interval from 14 to 7 days before the monitoring day or during the 7 days before the monitoring day. We considered these two time steps to identify the environmental conditions of the period during which the pathogen penetration into the host tissues was most probable (avg_14_7, avg_max_14_7, avg_min_14_7, cum_rain_14_7) (Chen et al., 2020; Carisse et al., 2009; Barka et al., 2002).

The phytosanitary treatments were included in the ML models as counts of the applications carried out in each vineyard from the beginning of the vegetative season, considering three periods: (i) cumulative number of treatments carried out until 14 days before the monitor-

Table 1. Set of variables associated with the three grapevine diseases.

Indices	Period	Description	Unit	Disease
w_mean_avg	November - January	Average of mean daily temperatures	°C	downy mildew, powdery mildew, gray mold
w_min_avg	November - January	Average of minimum daily temperatures	°C	downy mildew, powdery mildew, gray mold
w_rain_cum	November - January	Cumulative precipitation	mm	downy mildew, powdery mildew, gray mold
tavg_11	November	Average of mean daily temperatures	°C	downy mildew, powdery mildew, gray mold
tavg_12	December	Average of mean daily temperatures	°C	downy mildew, powdery mildew, gray mold
tavg_1	January	Average of mean daily temperatures	°C	downy mildew, powdery mildew, gray mold
tavg_2	February	Average of mean daily temperatures	°C	downy mildew, powdery mildew, gray mold
tavg_3	March	Average of mean daily temperatures	°C	downy mildew, powdery mildew, gray mold
psum_11	November	Cumulative precipitation	mm	downy mildew, powdery mildew, gray mold
psum_12	December	Cumulative precipitation	mm	downy mildew, powdery mildew, gray mold
psum_1	January	Cumulative precipitation	mm	downy mildew, powdery mildew, gray mold
psum_2	February	Cumulative precipitation	mm	downy mildew, powdery mildew, gray mold
psum_3	March	Cumulative precipitation	mm	downy mildew, powdery mildew, gray mold
avg_14_7	April - October	Average of mean daily temperatures from 14 days to 7 days before the monitoring day	°C	downy mildew, powdery mildew, gray mold
avg_max_14_7	April - October	Average of max daily temperatures from 14 days to 7 days before the monitoring day	°C	downy mildew, powdery mildew, gray mold
avg_min_14_7	April - October	Average of min daily temperatures from 14 days to 7 days before the monitoring day	°C	downy mildew, powdery mildew, gray mold
cum_rain_14_7	April - October	Cumulative precipitation from 14 days to 7 days before the monitoring day	mm	downy mildew, powdery mildew, gray mold
cum_rain_7	April - October	Cumulative precipitation from April to 7 days before the monitoring day	mm	downy mildew, powdery mildew, gray mold
gdd_apr_7	April - October	Cumulative degree day (mean air temperature) from April to 7 days before the monitoring day, with a lower threshold of 10 °C	°C	downy mildew, gray mold
gdd_jan_7	January - October	Cumulative degree day (mean air temperature) from January to 7 days before the monitoring day, with a lower threshold of 10 °C	°C	downy mildew, gray mold
gdd_7	April - October	Cumulative degree day from April to 7 days before the monitoring day, with a lower threshold of 6 °C and an upper threshold of 30.5 °C [1, 2]	°C	powdery mildew
dem100	n.a.	Elevation a.s.l.	m	downy mildew, powdery mildew, gray mold
dis_sea	n.a.	Euclidean distance from sea	m	downy mildew, powdery mildew, gray mold
count_tr_0_7	n.a.	Number of treatments in the 7 days before the monitoring day	n°	downy mildew, powdery mildew, gray mold
count_tr_7_14	n.a.	Number of treatments from 14 days to 7 days before the monitoring day	n°	downy mildew, powdery mildew, gray mold
count_tr_14	n.a.	Cumulative number of treatments 14 days before the monitoring day	n°	downy mildew, powdery mildew, gray mold
perc_inf	n.a.	Percentage of the observation in which was reported the presence of symptoms in the previous year	%	downy mildew, powdery mildew, gray mold
doy	n.a.	Day of the year	n.a.	downy mildew, powdery mildew, gray mold

[1] Allen (1976).
[2] Carisse et al. (2009).

ing day (count_tr_14), (ii) number of treatments carried out from 14 to 7 days before the monitoring day (count_tr_7_14), and (iii) number of treatments carried out in the 7 days before the monitoring day (count_tr_0_7).

In addition, the models included as a variable the frequency of monitoring days in which symptoms were recorded in the previous year, to consider the potential presence of the pathogens overwintering in the vineyard. The latter variable was calculated as the percentage of observations in which the presence of symptoms was observed in each year and in each vineyard, and it was assigned to the following monitoring year (perc_inf).

2.3 Data analysis

The three datasets on the symptoms observed of downy mildew, powdery mildew and gray mold covered a period from 2006 to 2019, excluding 2011 since no data were available for that year. The datasets had a different number of observations: 18857 for downy mildew, 14848 for powdery mildew, and 4960 for gray mold.

The dataset of each disease was partitioned with the aim of training and testing the ML models. The two datasets, downy mildew and powdery mildew, were divided in one training set and two test sets. In particular, data collected in the period from 2006 to 2017 were partitioned with an 80/20 proportion in “training” and “test 1”, respectively. The partition was carried out using the R package ‘healthcareai’ (Thatcher et al., 2020), considering the group “farm ID x year”, which allowed ensuring that observations from each vineyard in each year were not contained in both training set and test set. A further test (“test 2”) included data collected in 2018 and 2019 to evaluate the performance of the model on two independent years. Since less data were available in comparison with the other two diseases, the dataset on gray mold infection (2006-2019) was partitioned only in training set and test set with an 80/20 proportion in “training” and “test 20%”, considering the group “farm ID x year”.

The class “inf” was present in a different percentage of the total observations for the three diseases: 37% in training set, 35% in “test 1”, and 58% in “test 2” for downy mildew; (ii) 16% in training set, 15% in “test 1”, and 28% in “test 2” for powdery mildew; (iii) 10% in training set and 8% in test set for gray mold.

Spearman’s correlation among the variables associated with each disease was calculated with the R package ‘Hmisc’ (Harrell, 2019), to remove redundant features, highlighting variables that were highly correlated. Thus, in the case that the Spearman’s correlation coefficient between two variables was higher than 0.9 (absolute value), we selected the one with the highest importance, using a filter approach based on the Receiver Operating Characteristic (ROC) curve analysis, a plot of true positive rate (TPR) versus false positive rate (FPR) at various threshold settings.

Machine learning models selected for comparison were: (i) Random forest (RF), based on several decision trees, which operates as an ensemble to produce an output with low bias and lower variance than each single tree; and (ii) C5.0 based on single binary decision tree or a collection of rules with a boosted procedure. Both algorithms were tree-based models, being able to handle complex non-linear relationships and outperforming other ML algorithms in earth science and ecology applications (Thessen, 2016).

The train function of the R package ‘caret’ (Kuhn, 2020) was used to train and tune the two models, RF and C5.0, by means of the ROC metric, using a 10-fold cross-validation clustered by the grouping factor “farm ID x year”. Thus, while running the train function of ‘caret’, through the 10-fold cross-validation the training set is partitioned in 10 equal size subsamples of which 9 subsamples are used to train the model and a single subsample is retained as the validation data for testing the performance of the model with the aim of tuning the model parameters.

The models were evaluated using a confusion matrix among observed and predicted classes (Tab. 2) and a set of performance metrics on the training set and test set (Tab. 3).

The best performing algorithm (evaluated on training set and test set), was further optimized: (i) applying subsampling techniques for class imbalance during the training with the R package ‘caret’, and (ii) selecting the cut-off, to be applied on the probability outputs of the models for classification, which optimized the informedness (*Specificity*+*Sensitivity*-1) of the trained model, using the R package ‘MLeval’ (John, 2020).

For the best performing algorithm, the importance of variables in the modelling mechanism was extracted using the function varImp() of the R package “caret”.

3. RESULTS

The correlation analysis allowed removing highly correlated variables associated with each disease. Variables removed were: avg_14_7, avg_max_14_7, gdd_apr_7, gdd_jan_7, tavg_12, w_min_avg for downy mildew; avg_14_7, avg_max_14_7, doy, w_min_avg for powdery mildew and avg_14_7, avg_max_14_7, doy, gdd_apr_7, tavg_12, w_mean_avg, w_min_avg, w_rain_cum for gray mold.

The results of the cross-validation on the training set highlighted ROC-AUC values higher than 0.8 for both RF and C5.0 (Tab. 4).

AUC-PR was higher than 0.6 for downy mildew and gray mold, while it was around 0.6 for powdery mildew. The sensitivity was around 0.7 for downy mildew, while it was around 0.4 for powdery mildew and gray mold.

Table 2. Confusion matrix based on the number of observed and predicted classes. For each disease the class "inf" indicated the presence of symptoms on leaves or on grapes.

Predicted symptoms	Observed symptoms	
	inf	no
inf	True Positive (TP)	False Positive (FP)
no	False Negative (FN)	True Negative (TN)

Table 3. List of metrics used to evaluate the performance of the classification algorithms.

Evaluation metric	Data	Description
AUC-ROC	Training	Area under the ROC (Receiver operating characteristic) curve
AUC-PR	Training	Area under the Precision-Recall curve
Sensitivity = Recall	Training/Test	$\frac{TP}{TP+FN}$
Specificity	Training/Test	$\frac{TN}{TN+FP}$
Positive Predictive Value (PPV) = Precision	Test	$\frac{TP}{TP+FP}$
Negative Predictive Value (NPV)	Test	$\frac{TN}{TN+FN}$
F1	Test	$\frac{2 \times Precision \times Recall}{Precision + Recall}$
Accuracy	Test	$\frac{TN+TP}{TN+TP+FN+FP}$
Balanced accuracy	Test	$\frac{Sensitivity + Specificity}{2}$

Table 4. Performance of the two machine learning algorithms (RF and C5.0), tuned through the 10-fold cross-validation, on the training sets of the three diseases.

	RF			C5.0		
	Downy mildew	Powdery mildew	Gray mold	Downy mildew	Powdery mildew	Gray mold
AUC-ROC	0.85	0.87	0.91	0.84	0.87	0.90
AUC-PR	0.77	0.60	0.69	0.75	0.59	0.66
Sensitivity	0.66	0.43	0.45	0.65	0.50	0.48
Specificity	0.84	0.96	0.99	0.85	0.94	0.98

Table 5. Results of RF and C5.0 in predicting the presence of symptoms of the three diseases on the test sets "test 1".

	RF			C5.0		
	Downy mildew	Powdery mildew	Gray mold	Downy mildew	Powdery mildew	Gray mold
TP	701	129	44	705	158	52
FP	256	75	9	245	92	9
TN	1573	2024	967	1584	2007	967
FN	285	243	44	281	214	36
Sensitivity	0.71	0.35	0.50	0.71	0.42	0.59
Specificity	0.86	0.94	0.99	0.87	0.96	0.99
PPV	0.73	0.63	0.83	0.74	0.63	0.85
NPV	0.85	0.89	0.96	0.85	0.90	0.96
F1	0.72	0.45	0.62	0.73	0.51	0.70
Accuracy	0.81	0.87	0.95	0.81	0.88	0.96
Balanced accuracy	0.78	0.66	0.74	0.79	0.69	0.79

The specificity was around 0.8 for downy mildew, while it was higher than 0.9 for the other two diseases. The two algorithms performed similarly on the training set, with slightly better results for RF.

For all the three diseases, the algorithm C5.0 performed better than RF on the test set ("test 1"), reporting in particular a higher sensitivity and a higher balanced accuracy (Tab. 5).

The C5.0 algorithm predicted the presence of symptoms of downy mildew with a balanced accuracy of 78%. The overall predicted "inf" were correct for 71% of the cases, whereas the percentage of correctly predicted "no" on the total prediction of no symptoms was 87%. The percentage of cases in which "inf" was correctly identified was 74%, while for "no" it was 85%. The presence of symptoms of powdery mildew was predicted by C5.0 with a balanced accuracy of 69%. The overall predicted "inf" were correct for 42% of the cases, whereas the percentage of correctly predicted "no" on the total prediction of no symptoms was 96%. The percentage of cases in which "inf" was correctly identified was 63%, while for "no" it was 90%. The presence of symptoms of gray mold was predicted by C5.0 with a balanced accuracy of 79%. The overall predicted "inf" were correct for 59% of the cases, whereas the percentage of correctly predicted "no" on the total prediction of no symptoms was 99%. The percentage of cases in which "inf" was correctly identified was 85%, while for "no" it was 96%.

The subsampling technique "down" was selected as the best according to the performance on the test set of the three diseases (Tab. S1). Applying the subsampling technique to the algorithm C5.0 increased the percentage of cases in which "inf" was correctly identified and the balanced accuracy for all the three diseases (Tab. 6). Moreover, the informedness of the C5.0 algorithm with down-sampling was the highest when applying a cut-off equal to: (i) 0.46 for the prediction of downy mildew and

Table 6. Results of C5.0 on the test sets "test 1" applying: (i) down-sampling during training (C5.0 'down'), and (ii) the optimized cut-off for classification on the probability outputs of C5.0 'down'.

	C5.0 'down'			C5.0 'down' & cut-off opt.		
	Downy mildew	Powdery mildew	Gray mold	Downy mildew	Powdery mildew	Gray mold
TP	758	236	77	791	254	84
FP	378	252	64	446	329	137
TN	1451	1847	912	1383	1770	839
FN	228	136	11	195	118	4
Sensitivity	0.77	0.63	0.87	0.80	0.68	0.95
Specificity	0.79	0.88	0.93	0.76	0.84	0.86
PPV	0.67	0.48	0.55	0.64	0.46	0.38
NPV	0.86	0.93	0.99	0.88	0.86	0.99
F1	0.71	0.55	0.67	0.71	0.56	0.54
Accuracy	0.78	0.84	0.93	0.77	0.69	0.87
Balanced accuracy	0.78	0.76	0.90	0.78	0.70	0.91

Table 7. Results of the application of the optimized cut-off for classification on the probability outputs of C5.0 'down' on both the overall "test 2" and on the two years considered separately (2018 and 2019).

	C5.0 'down' & cut-off opt.					
	Downy mildew			Powdery mildew		
	test 2	2018	2019	test 2	2018	2019
TP	1662	1126	536	304	168	136
FP	385	47	338	201	89	112
TN	1503	855	648	1409	824	585
FN	964	721	243	313	221	92
Sensitivity	0.63	0.61	0.69	0.49	0.43	0.60
Specificity	0.8	0.95	0.66	0.87	0.9	0.84
PPV	0.81	0.96	0.61	0.6	0.65	0.55
NPV	0.61	0.54	0.73	0.82	0.79	0.86
F1	0.71	0.75	0.65	0.54	0.52	0.57
Accuracy	0.7	0.72	0.67	0.77	0.76	0.78
Balanced accuracy	0.71	0.78	0.67	0.68	0.67	0.72

powdery mildew symptoms and (ii) 0.36 for the prediction of gray mold. The application of the optimized cut-off on the results of the C5.0 algorithm with down-sampling improved the sensitivity, being 0.80 for downy mildew, 0.68 for powdery mildew and 0.95 for gray mold.

Results on "test 2", highlighted a prediction accuracy around 0.7 for both the symptoms of downy mildew and powdery mildew, in both 2018 and 2019 (Tab. 7).

Table 8. Importance of variables in the modelling process of the algorithm C5.0 'down' for the three diseases. The importance is calculated as the percentage of splits associated with each predictor (metric = 'splits').

C5.0 'down'					
Downy mildew		Powdery mildew		Gray mold	
perc_inf	12.3	perc_inf	7.3	perc_inf	11.2
doy	11.1	dis_sea	7.2	cum_rain_7	7.9
cum_rain_7	7.6	cum_rain_7	6.6	gdd_jan_7	7.8
dem100	6.2	gdd_7	6.5	cum_rain_14_7	7.3
psum_3	5.9	dem100	6.5	psum_12	7.3
psum_2	5.9	count_tr_14	5.7	avg_min_14_7	6.6
dis_sea	5.0	avg_min_14_7	5.7	psum_2	6.6
psum_12	4.3	psum_2	5.4	tavg_11	6.2
count_tr_14	4.3	psum_12	5	dis_sea	5
tavg_2	3.9	psum_3	4.5	psum_3	4.6
psum_1	3.8	tavg_11	4.3	count_tr_0_7	4.4
w_rain_cum	3.8	tavg_3	4.1	psum_11	4.3
psum_11	3.7	psum_1	4	dem100	4.2
tavg_1	3.6	psum_11	3.9	psum_1	3.5
tavg_11	3.3	count_tr_0_7	3.8	tavg_1	3
count_tr_0_7	3.0	w_mean_avg	3.8	count_tr_7_14	3
avg_min_14_7	2.9	w_rain_cum	3.8	tavg_3	2.9
cum_rain_14_7	2.7	cum_rain_14_7	3.2	tavg_2	2.3
tavg_3	2.4	tavg_1	3.2	count_tr_14	2.3
count_tr_7_14	2.4	tavg_2	3.1		
w_mean_avg	1.9	count_tr_7_14	2.2		

The importance of the variables in the modelling process for the three diseases is reported in Tab. 8.

Around 50% of the splits were associated with the first six most important variables for downy mildew, namely: the percentage of observations of the year before in which symptoms were present, day of year, the cumulative precipitation from April to 7 days before the monitoring day, the elevation, and the precipitation of March and February.

For powdery mildew, the first eight most important variables covered around 50% of the splits, being: the percentage of the observation of the previous year in which symptoms appeared, the distance from sea, the cumulative precipitation from April until 7 days before the monitoring day, cumulative degree day (gdd) from April until 7 days before the monitoring day, the elevation, the count of the treatments carried out until 14 days before the monitoring day, the average minimum temperature between 14 and 7 days before the monitoring day, the precipitation of February.

For gray mold, the first six most important variables were associated to around 50% of the splits: the

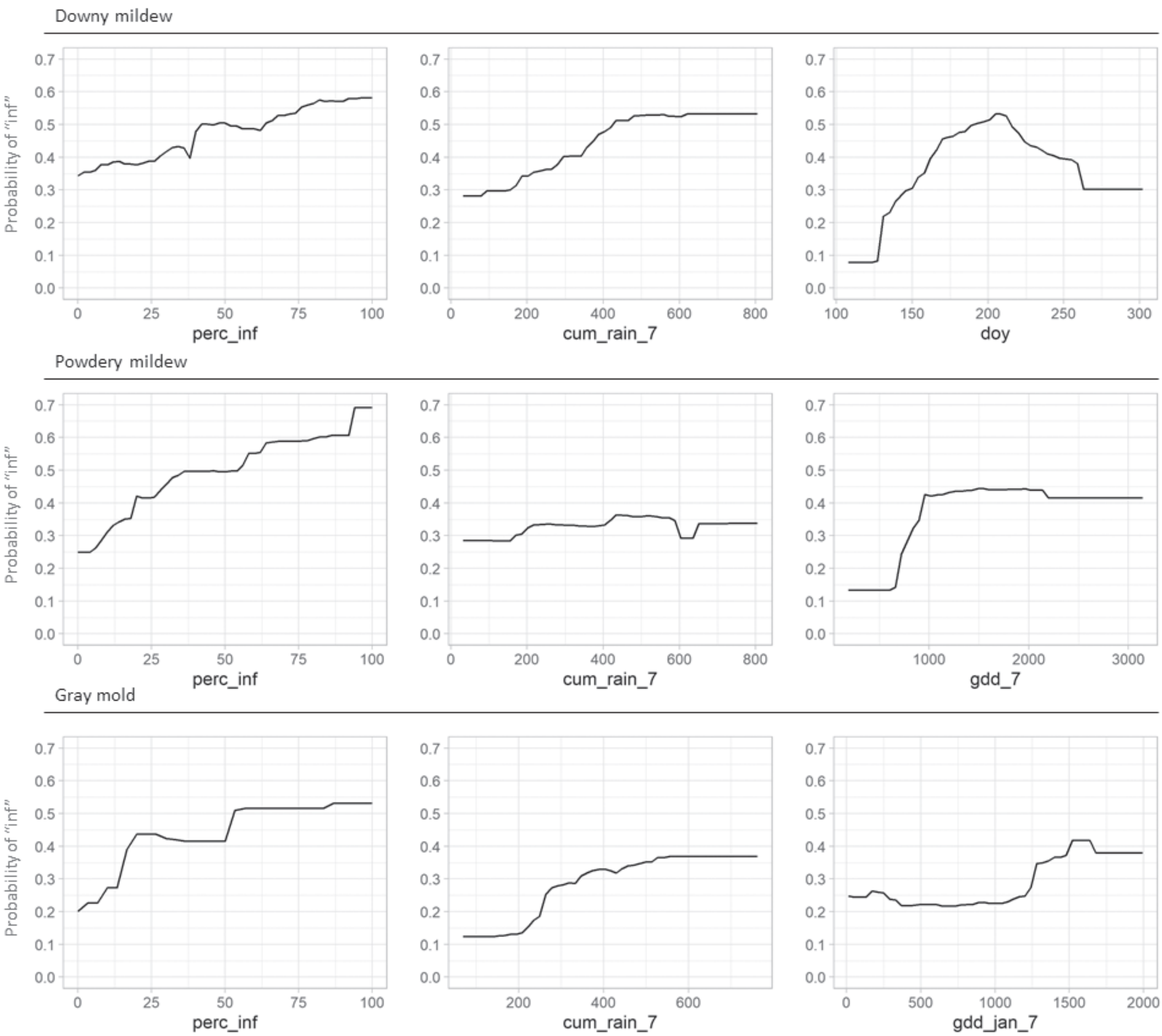

Fig. 1. Partial dependence plots for the marginal effect on the prediction of the class "inf" of the variables: (i) perc_inf, cum_rain_7 and doy for downy mildew; (ii) perc_inf, cum_rain_7 and gdd_7 for powdery mildew and (iii) perc_inf, cum_rain_7 and gdd_jan_7 for gray mold.

percentage of the observation of the previous year in which symptoms appeared, the cumulative precipitation from April until 7 days before the monitoring day and between 14 and 7 days before the monitoring day, the precipitation of December, the average minimum temperature between 14 and 7 days before the monitoring day.

Among the three models, common variables on the top of the list were: perc_inf and cum_rain_7. Similar variables, such as doy and gdd, were ranked within the top variables for all the three models. Partial dependence plots (pdp) (Fig. 1) represent the marginal effect of the latter variables on the probability of predicting the presence of symptoms for the three diseases. In particular, with increasing values of perc_inf and cum_rain_7, the probability of predicting "inf" increased for powdery mildew, until about 500 mm for cum_rain_7. Concerning downy mildew, with increasing values of doy, the probability of the class "inf" increased, until about doy 200, while decreasing after this threshold. For powdery mildew, the probability of the class "inf" markedly increased with ggd_7, until 1000, while the probability of the class "inf" for gray mold increased with ggd_jan_7, between about 1200 and 1600.

4. DISCUSSION

Results of the application of ML algorithms, trained on historical data, for the prediction of the appearance of symptoms of downy mildew, powdery mildew, and gray mold in grapevine, demonstrated a better performance of the algorithm C5.0 in comparison with the RF, in the test set ("test 1"), for all the three diseases. Similar results were found by Volpi et al. (2020), who applied ML algorithms for predicting the probability of infestation by *Bactrocera oleae* on olive trees, founding that C5.0 had a higher ROC compared to k-nearest neighbors (k-NN), Classification and Regression Trees (CART), Random Forest (RF) and Neural Network (NN).

The three datasets on grapevine diseases were unbalanced, since the observations in which the symptoms of diseases were recorded were a minority of the total observations, in particular for powdery mildew and gray mold (<20%). Class imbalance problems may lead to partial behaviour of the classifier towards the majority class and sampling methods are most commonly applied to balance the class distribution of the training data (Kaur et al., 2019). Moreover, the output of C5.0 classification for each observation is a probability between 0 and 1 of being classified as "inf" or "no" and the standard cut-off applied for classification is 0.5, which is not the most appropriate for imbalanced datasets (Zou et al., 2016). Therefore, the application of both the down-sampling technique and a cut-off for classification, optimized to improve the informedness of the model, increased the sensitivity of the model, thus increasing the amount of true positives and decreasing the amount of false negatives, which has a high cost for the prediction of plant diseases.

The final models achieved a good performance in predicting the presence of symptoms of the three diseases on "test 1", with a balanced accuracy of 0.8 for downy mildew, 0.7 for powdery mildew and 0.9 for gray mold, highlighting a lower occurrence of wrong classifications for the gray mold model.

The application of the models for downy mildew and powdery mildew on the two independent years (2018 and 2019) achieved a lower balanced accuracy than on "test 1", being, however, around 0.7 for the two diseases. This slightly lower performance of the ML model on unseen data may be due to the known bias-variance tradeoff of ML models, being complex models more subjected to high variance (Abu-Mostafa et al., 2012).

Differently to other ML techniques (i.e., Bayesian network) in which the causal relationships among the variables are linked to previous knowledge (Lu et al., 2020), the effect of the variables on the prediction in tree-based ML models is entirely data-driven. However, it is possible to interpret the C5.0 model by exploring the importance of variables in the modelling mechanism and the effect of variables on the prediction.

Indeed, it was possible to highlight, for all the diseases, a higher frequency in the top-ranking positions, in terms of importance, of indices related to precipitation rather than to air temperature. In particular, the cumulative precipitation from the beginning of April to 7 days before the day of observation was among the most important variables for the three diseases.

For downy mildew and gray mold, the probability of infection increased with increasing values of cumulative precipitation (approximately until 500 mm); while, for powdery mildew, the relationship was less clear. In particular, downy mildew is typically diffused in viticultural areas characterized by temperate climate and frequent precipitation during spring and summer (Lafon and Clerjeau, 1988), and precipitation was reported as a key driver for both primary and secondary infections (Rossi et al., 2008). Climate conditions at the end of spring, particularly precipitation, were found to be decisive for the development of downy mildew symptoms (Chen et al., 2020). Precipitation events have a positive effect in spreading the infection of powdery mildew (dispersing cleistothecia and releasing ascospores) and, though free water is detrimental to conidial germination, in rainy seasons the environmental conditions become favourable for the infection due to mild temperatures, limited direct sunlight, and high humidity (Gadoury et al., 2012). Furthermore, more severe gray mold epidemics were reported under wet growing seasons, since the wetness duration is a key factor for both the development of early season and late season infections (Ciliberti et al., 2015 a, b).

The frequency of symptoms observed in the previous year (the year before the one considered for ML application) was the most important variable in the modelling mechanism for the appearance of symptoms of the three diseases. In particular, the risk of symptom development in the current year increased with the occurrence of severe infection in the previous year. Severe infections may be a source of overwintering pathogens, potentially leading to new infections under optimal environmental conditions. Indeed, downy mildew is able to overwinter mainly on infected shoots, while powdery mildew in grapevine buds, and gray mold in grapevine debris (Pertot et al., 2017; Jaspers et al., 2013; Rügner et al., 2002).

Variables describing the progress of the season, such as doy for downy mildew and cumulative degree days for powdery mildew and gray mold, were among the most important variables for predicting the development of disease symptoms. In particular, the probability of infection increased for downy mildew from April to about mid-July and then decreased. Previous studies reported that the progress of disease relates to the phenological development of grapevine (Molitor et al., 2016; Carmichael et al., 2018; Bove et al., 2020). In addition, ggd_7 was a key variable for predicting the occurrence of powdery mildew symptoms; Carisse et al. (2009) used this variable to predict the proportion of seasonal airborne inoculum.

However, even if gdd or doy were among the most important variable in the modelling mechanism, the use of a multivariate approach through ML algorithms with respect to a univariate cumulative GDD index is recognized to be more suited to model non-linear patterns and variable interactions often characterizing real-world ecological patterns (Yo et al., 2017).

The effect of the number of chemical treatments was more important for powdery mildew than for the other diseases, since only for powdery mildew an index indicating the frequency of treatments was among the top variables. Further studies are needed to evaluate new approaches to include the effect of treatments in modelling predictions, considering the type of chemical and the mechanism of action.

Results from this work highlighted that a ML algorithm trained on historical data, may be efficiently used to predict the appearance of symptoms of downy mildew, powdery mildew, and gray mold in grapevine, providing an innovative control tool, even in association with traditional models. The simplicity of the approach requires, however, the availability of symptom records, which is the monitoring of disease occurrence. Massive datasets of disease symptoms or pest attacks may allow not only regional-level analyses, like in the present study, but also the recognition of specific and localized risk factors, which take into account additional variables, conferring susceptibility or resistance to a given disease or pest. The ML algorithms can be implemented with additional weather data that are used in other models for disease prediction (Rossi et al., 2008; Chen et al., 2020). Yet, climatic inputs can be further enriched to forecast the occurrence of downy mildew, powdery mildew, and gray mold under different climate scenarios and assess the future trajectories of these diseases.

The integration of ML models in decision support systems also represents a practical application to plan the reduction of fungicide treatments. In particular, the use of ML is a promising approach to implement early warning systems, identifying periods when climatic conditions are favourable to promote disease development and alerting on symptoms that are associated with high risk of infection (Caffi et al., 2010; Pellegrini et al., 2010). As future activity, the integration of mechanistic and ML models (e.g., in Bayesian networks) could be tested to evaluate the effect of including previous knowledge in the modelling mechanism.

5 CONCLUSION

The application of ML algorithms, trained on historical data, was proved useful for the prediction of the appearance of symptoms of downy mildew, powdery mildew, and gray mold in grapevine. The grape disease monitoring network enabled the observation of a wide range of symptoms. This, in combination with ERA5-Land dataset allowed the development of early detection algorithms to support the implementation of IPM in viticulture. Compared to ground weather stations, ERA5 data had the advantage of providing information for locations that are not covered by traditional agrometeorological networks. Nevertheless, for becoming fully operative, this approach needs an efficient monitoring system at the landscape scale and intensive field surveys at the local scale.

ACKNOWLEDGEMENTS

We thank the Phytosanitary Service of Regione Toscana.

REFERENCES

Abu-Mostafa Y. S., Magdon-Ismail M., Lin H.T., 2012. Learning From Data. AMLBook.

Allen C., 1976. A modified sine wave method for calculating degree days. Environmental Entomology, 5: 388–396.

Barka E. A., Gognies S., Nowak J., Audran J. C., Belarbi A. 2002. Inhibitory effect of endophyte bacteria on *Botrytis cinerea* and its influence to promote the grapevine growth. Biological Control, 24: 135-142.

Bove F., Savary S., Willocquet L., Rossi V., 2020. Designing a modelling structure for the grapevine downy mildew pathosystem. European Journal of Plant Pathology, 158: 599-614.

Buonassisi D., Colombo M., Migliaro D., Dolzani C., Peressotti E., Mizzotti C., Velasco R., Masiero S., Perazzolli M., Vezzulli S., 2017. Breeding for grapevine downy mildew resistance: a review of "omics" approaches. Euphytica, 213:1–21.

Caffi T., Rossi V., Bugiani R., 2010. Evaluation of a warning system for controlling primary infections of grapevine downy mildew. Plant Disease, 94: 709-716.

Caffi T., Rossi, V., Legler S. E., Bugiani R., 2011. A mechanistic model simulating ascosporic infections by *Erysiphe necator*, the powdery mildew fungus of grapevine. Plant Pathology, 60: 522-531.

Carmichael P. C., Siyoum N., Jongman M., Korsten L., 2018. Prevalence of *Botrytis cinerea* at different phenological stages of table grapes grown in the northern region of South Africa. Scientia Horticulturae, 239: 57-63.

Carisse O., Bacon R., Lefebvre A., Lessard K., 2009. A degree-day model to initiate fungicide spray programs for management of grape powdery mildew [Erysiphe necator]. Canadian Journal of Plant Pathology, 31: 186–194.

Chen M., Brun F., Raynal M., Makowski D. 2020. Forecasting severe grape downy mildew attacks using machine learning. Plos One, 15(3), e0230254

Ciliberti N., Fermaud M., Languasco L., Rossi V., 2015 (a). Influence of fungal strain, temperature, and wetness duration on infection of grapevine inflorescences and young berry clusters by Botrytis cinerea. Phytopathology, 105: 325–333.

Ciliberti N., Fermaud M., Roudet J., Rossi V., 2015 (b). Environmental conditions affect Botrytis cinerea infection of mature grape berries more than the strain or transposon genotype. Phytopathology, 105: 1090–1096.

Copernicus Climate Change Service (C3S) (2017): ERA5: Fifth generation of ECMWF atmospheric reanalyses of the global climate. Copernicus Climate Change Service Climate Data Store (CDS). https://cds.climate.copernicus.eu/cdsapp#!/home.

Elmer P.A.G., Michailides T.J., 2007. Epidemiology of Botrytis cinerea in orchard and vine crops. In: Elad Y, Williamson B, Tudzynski P, Delen N, editors. Botrytis: Biology, Pathology and Control. Springer Netherlands, pp. 243–272.

Gadoury D.M. and Pearson R. C., 1988. Initiation, development, dispersal, and survival of cleistothecia of Uncinula necator in New York vineyards. Phytopathology, 78:1413-1421.

Gadoury D.M., Seem R.C., Pearson R.C., Wilcox W.F., 2001. Effects of powdery mildew on vine growth, yield, and quality of Concord grapes. Plant Disease, 85:137–140.

Gadoury D.M., Cadle-Davidson L., Wilcox W.F., Dry I.B., Seem R.C., Milgroom M.G., 2012. Grapevine powdery mildew (*Erysiphe necator*): A fascinating system for the study of the biology, ecology and epidemiology of an obligate biotroph. Molecular Plant Pathology, 13: 1–16.

Gessler C., Pertot I., Perazzolli M., 2011. Plasmopara viticola: a review of knowledge on downy mildew of grapevine and effective disease management. Phytopathologia Mediterranea, 50:3–44.

González-Domínguez E. Caffi T., Ciliberti N. Rossi V. 2015. A mechanistic model of Botrytis cinerea on grapevines that includes weather, vine growth stage, and the main infection pathways. PLoS One, 10(10), e0140444.

Harrell F.E. Jr, 2019. Hmisc: Harrell Miscellaneous. R package version 4.2-0. https://CRAN.R-project.org/package=Hmisc.

Hijmans R.J., 2019 a. raster: Geographic Data Analysis and Modeling. R package version 2.8-19. https://CRAN.R-project.org/package=raster.

Hijmans R.J., 2019 b. geosphere: Spherical Trigonometry. R package version 1.5-10. https://CRAN.R-project.org/package=geosphere.

Hill G. N., Beresford R. M., Evans K. J., 2019. Automated analysis of aggregated datasets to identify climatic predictors of botrytis bunch rot in wine grapes. Phytopathology, 109: 84-95.

Jaspers M. V., Seyb A.M., Trought M.C.T., Balasubramaniam R., 2013. Overwintering grapevine debris as an important source of Botrytis cinerea inoculum. Plant Pathology, 62: 130–138.

John C.R., 2020. MLeval: Machine Learning Model Evaluation. R package version 0.3. https://cran.r-project.org/package=MLeval.

Kaur H., Pannu H.S., Malhi A.K., 2019. A systematic review on imbalanced data challenges in machine learning: Applications and solutions. ACM Computing Surveys, 52. Article 79.

Kuhn M., 2020. caret: Classification and Regression Training. R package version 6.0-85. https://CRAN.R-project.org/package=caret.

Lafon R., Clerjeau M., 1988. Downy mildew. In: Pearson, R.C., Goheen, A.C. (Eds.), Compendium of Grape Diseases. APS Press, St. Paul, Minnesota, USA, pp. 11–13.

Lee, D.S., Bae, Y.S., Byun, B.K., Lee, S., Park, J.K., Park, Y.S., 2019. Occurrence prediction of the citrus flatid planthopper (Metcalfa pruinosa (Say, 1830)) in South Korea using a random forest model. Forests, 10, 583.

Legler S.E., Caffi T., Rossi V., 2011. A non linear model for temperature-dependent development of Erysiphe necator chasmothecia on grapevine leaves. Plant Pathology, 61: 96-105.

Lu W., Newlands N. K., Carisse O., Atkinson D. E., Cannon A. J. 2020. Disease Risk Forecasting with

Bayesian Learning Networks: Application to Grape Powdery Mildew (Erysiphe necator) in Vineyards. Agronomy, 10(5), 622.

Marchi S., Guidotti D., Ricciolini M., Petacchi R., 2016. Towards understanding temporal and spatial dynamics of *Bactrocera oleae* (Rossi) infestations using decade-long agrometeorological time series. International Journal of Biometeorology, 60: 1681-1694.

Molitor D., Baus O., Hoffmann L., Beyer M., 2016. Meteorological conditions determine the thermal-temporal position of the annual Botrytis bunch rot epidemic on Vitis vinifera L. cv. Riesling grapes. Oeno One, 50: 231–244.

Muñoz-Sabater J., Dutra E., Agustí-Panareda A., Albergel C., Arduini G., Balsamo G., Boussetta S., Choulga M., Harrigan S., Hersbach H., Martens B., Miralles D., Piles M., Rodríguez-Fernández N., Zsoter E., Buontempo C., Thépaut J.N., 2021. ERA5-Land: A state-of-the-art global reanalysis dataset for land applications. Earth System Science Data Discussions [preprint], in review.

Orlandini S., Gozzini B., Rosa M., Egger E., Storchi P., Maracchi G., Miglietta F., 1993. PLASMO: a simulation model for control of Plasmopara viticola on grapevine 1. EPPO Bulletin, 23: 619-626.

Padulano R., Rianna G., Santini M., 2021. Datasets and approaches for the estimation of rainfall erosivity over Italy: A comprehensive comparison study and a new method. Journal of Hydrology: Regional Studies, 34: 100788.

Pellegrini A., Prodorutti D., Frizzi A., Gessler C., Pertot I., 2010. Development and evaluation of a warning model for the optimal use of copper in organic viticulture. Journal of Plant Pathology, 43-55.

Pertot I., Caffi T., Rossi V., Mugnai L., Hoffmann C., Grando M. S., Gary C., Lafond D., Duso C., Thiery D., Mazzoni V., Anfora G., 2017. A critical review of plant protection tools for reducing pesticide use on grapevine and new perspectives for the implementation of IPM in viticulture. Crop Protection, 97: 70-84.

R Core Team, 2020. R: A language and environment for statistical computing. R Foundation for Statistical Computing, Vienna, Austria. URL https://www.R-project.org/.

Rodríguez-Rajo F. J., Jato V., Fernández-González M., Aira M. J. 2010. The use of aerobiological methods for forecasting Botrytis spore concentrations in a vineyard. Grana, 49: 56-65.

Rossi V., Caffi T., Giosuè S., Bugiani R., 2008. A mechanistic model simulating primary infections of downy mildew in grapevine. Ecological Modelling, 212: 480–491.

Rossi V., Salinari F., Poni S., Caffi T., Bettati T. 2014. Addressing the implementation problem in agricultural decision support systems: the example of vite.net®. Computers and Electronics in Agriculture, 100: 88-99.

Rügner A., Rumbolz J., Huber B., Bleyer G., Gisi U., Kassemeyer H.H., Guggenheim R., 2002. Formation of overwintering structures of Uncinula necator and colonization of grapevine under field conditions. Plant Pathology, 51: 322–330.

Sperschneider J., 2019. Machine learning in plant–pathogen interactions: empowering biological predictions from field scale to genome scale. New Phytologist, 228: 35–41.

Thessen, A.E., 2016. Adoption of machine learning techniques in ecology and earth science. One Ecosystem 1, 1–38.

Valdés-Gómez H., Araya-Alman M., Pañitrur-De la Fuente C., Verdugo-Vásquez N., Lolas M., Acevedo-Opazo C., Gray C., Calonnec A., 2017. Evaluation of a decision support strategy for the control of powdery mildew, Erysiphe necator (Schw.) Burr., in grapevine in the central region of Chile. Pest Management Science, 73: 1813-1821.

Volpi I., Guidotti D., Mammini M., Petacchi R., Marchi S., 2020. Managing complex datasets to predict *Bactrocera oleae* infestation at the regional scale. Computers and Electronics in Agriculture, 179: 105867.

Yo M.A.R., Illig M.A.C.R., 2017. Statistically reinforced machine learning for nonlinear patterns and variable interactions. Ecosphere, 8: 1-16.

Zou Q., Xie S., Lin Z., Wu M., Ju Y., 2016. Finding the Best Classification Threshold in Imbalanced Classification. Big Data Research, 5: 2–8.

Table S1. Results of the application on the dataset "test 1" of the algorithm C5.0 trained with different subsampling techniques: down-sampling (down), up-sampling (up), Synthetic Minority Over-sampling Technique (SMOTE) and Random Over-Sampling Examples (ROSE).

	Downy mildew				Powdery mildew				Gray mold			
	down	up	SMOTE	ROSE	down	up	SMOTE	ROSE	down	up	SMOTE	ROSE
TP	758	657	748	706	236	155	170	256	77	47	63	55
FP	378	259	385	523	252	95	114	334	64	12	56	55
TN	1451	1570	1444	1306	1847	2004	1985	1765	912	964	920	921
FN	228	329	238	280	136	217	202	116	11	41	25	33
Sensitivity	0.77	0.66	0.76	0.72	0.63	0.42	0.46	0.69	0.87	0.53	0.72	0.62
Specificity	0.79	0.86	0.79	0.71	0.88	0.95	0.95	0.84	0.93	0.99	0.94	0.94
PPV	0.67	0.72	0.66	0.57	0.48	0.62	0.59	0.43	0.55	0.80	0.53	0.50
NPV	0.86	0.83	0.86	0.82	0.93	0.90	0.91	0.94	0.99	0.96	0.97	0.96
F1	0.71	0.69	0.71	0.64	0.55	0.50	0.52	0.53	0.67	0.64	0.61	0.56
Accuracy	0.78	0.79	0.78	0.71	0.84	0.87	0.87	0.82	0.93	0.95	0.92	0.92
Balanced accuracy	0.78	0.76	0.77	0.71	0.76	0.69	0.70	0.76	0.90	0.76	0.83	0.78

Link to a GitHub repository containing the R script for ML models and a subset of data as example: https://github.com/aeditsrl/grapevine_ML

Italian Journal of Agrometeorology
Rivista Italiana di Agrometeorologia

Firenze University Press
www.fupress.com/ijam

OPEN ACCESS

Citation: R. Bohovic, P. Hlavinka, M. Možný, D. Semerádová, J. Bálek, M. Trnka (2021) Earth observation method for an operational assessment of crop phenology metric "start of the season". *Italian Journal of Agrometeorology* (2): 71-80. doi: 10.36253/ijam-1075

Received: September 08, 2020

Accepted: November 05, 2021

Published: December 27, 2021

Data Availability Statement: All relevant data are within the paper and its Supporting Information files.

Competing Interests: The Author(s) declare(s) no conflict of interest.

ORCID:
RB: 0000-0003-2053-2410

Earth observation method for an operational assessment of crop phenology metric "start of the season"

Roman Bohovic[1,*], Petr Hlavinka[2,3], Martin Možný[4], Daniela Semerádová[2,3], Jan Bálek[2,3], Miroslav Trnka[2,3]

[1] *World from Space s.r.o., Pellicova 3, 60200 Brno, Czech Republic*
[2] *Global Change Research Institute, Bělidla 4a, 603 00 Brno, Czech Republic*
[3] *Institute of Agrosystems and Bioclimatology, Mendel University in Brno, Zemedělská 1, 613 00 Brno, Czech Republic*
[4] *Czech Hydrometeorological Institute, Na Šabatce 17, Praha, 143 06, Czech Republic*
*Corresponding author. E-mail: bohovic@worldfrom.space

Abstract. Vegetation phenology is one of the key indicators for assessing inter annual changes of ecosystems while crop phenology has crucial and practical importance for precise timing of farming practices of today's smart agriculture. The aim of this study is to develop and implement a procedure for filtering and processing daily satellite signals from Moderate Resolution Imaging Spectroradiometer (MODIS) satellites for the operational derivation of vegetation indices and land surface phenology (LSP) metrics. Second, this work investigates and selects precisely adjusted parameters for the calculation of a specific LSP metric – the SOS (start of the season). The SOS obtained from the satellite data was compared with available in situ ground measurements at 80 sites with records from 2000-2012 across the Czech Republic. The coefficients of determination, R^2, for the land surface phenology based on Earth observation and traditional ground phenology indicated differences between the two methods. However, the average R^2 at all sites for agricultural land was 0.31 for winter wheat onset of leaf sheath elongation; the R^2 exceeded 0.5 at 21 sites and was approximately 0.7 at some sites. The developed procedure proved suitable for operational monitoring of actual crop conditions and other influence factors that are important for drought monitoring.

Keywords: land surface phenology, vegetation, start of the season, MODIS, Czech Republic, drought.

1. INTRODUCTION

Phenology is the study of recurring biological life cycle stages and how these are influenced (Lieth, 1974) by seasonal and interannual variations in climate, as well as habitat factors (e.g. soil, site orientation) or agriculture practises and inputs (e.g. application of fertilizers, plant growth regulators, etc.). It is limited to vegetation in general and crops in particular within this study, with events studied in botany and agronomy. Vegetation dynamics play an important role in inter annual vegetation changes in terrestrial ecosystems and are key indicators of climate-vegetation interactions, land use/cover changes and year-to-year productivity (Zeng et al., 2020). Crop phenology has practical importance for precise timing of farming practices. Observation of vegetation conditions and stress are also used for indirect monitoring of drought (Liang et al., 2011; Trnka et al. 2020), even on a large scale (Lin et al., 2014).

The assessment of vegetation growth and condition changes and shifts in phenology are valuable signs. A range of methods for monitoring phases of plant species and their temporal development has emerged to address the relations between climate conditions and vegetation cover (Fraga et al., 2014; Xie et al., 2008). According to Cleland et al. (2007), these methods include: (1) species-level observations; (2) atmospheric monitoring of carbon dioxide concentrations as an indication of the timing of photosynthesis-driven carbon uptake; and (3) remote sensing of ecosystem production. The third approach was employed in this study. It is referred to as *land surface phenology* - LSP (Friedl et al., 2006) that differentiate Earth observation method from in-situ phenology. Remote sensing data record significant improvements regarding availability and temporal and spatial resolution; hence, the importance of using such data is growing. Known limitations are an abundance of noise that arises from various sources (such as atmospheric conditions) and agricultural land crop rotation practices for time series. Both limitations cause the persistent need for filtration of Earth observation data.

The most widely used vegetation index, derived from satellite measurements and closely related to vegetation activity, is known as the normalized difference vegetation index (NDVI) (Tucker, 1979). Zeng et al. (2020) summarise other indices used for LSP, such as physically based leaf area index (LAI). An NDVI time series may be used to estimate phenology metrics, such as the start of vegetation growth, especially on a regional and global scale (Reed at al., 1994; White et al., 2009).

The aim of this study was to develop a robust procedure for the near-real time filtering and processing of daily satellite signals that would otherwise include many missing or invalid values as a result of atmospheric conditions (mostly clouds) and to keep the procedure sufficiently sensitive to vegetation changes within agricultural landscapes. The second aim was to investigate the various settings for the proposed procedure and evaluate its impact. Last task was to identify the start of the season (SOS) with the procedure and compare the results with ground observations.

2. MATERIALS AND METHODS

2.1. Satellite data and ground observations

The NDVI was computed daily at a resolution of 250 x 250 m from red and near-infrared reflectance spectral bands of a Moderate Resolution Imaging Spectroradiometer (MODIS) time series. MODIS instruments are on-board Terra and Aqua satellites. A time series from 2000 to 2012 was used in this study. Although MODIS instruments are still operational long after their planned lifetime, the second dataset (the phenological observations see below) lasts only until 2012, when the ground observations were terminated. For the purpose of our calculations, the original 250 x 250 m resolution data were masked for land cover classes and aggregated to a 5 x 5 km grid; thus, we used only a reasonable fraction (e.g., agricultural land) of the 25 km^2 area that we assigned to a single grid cell. This in turn allowed masking of the annually changing crop composition that originates from altering crops on individual field blocks, while on the farm level, the crop mixture is usually stable. The MODIS product also offers a 16-day composite image that is often used; however, it is not possible to use for operational monitoring due to the time delay of production.

Corresponding phenological observations were taken from the PHENODATA database of the Czech Hydrometeorological Institute (CHMI). These data contain systematic phenological observations from 80 sites in the Czech Republic. The beginnings of phenophases were monitored according to the methodological instruction of the CHMI on selected individual plants. For that reason, we selected agricultural crops that are mostly grown as single-crop monocultures, which correspond to ground observation references. Two early spring phases of different cereals were analysed: the emergence of spring barley and the onset of leaf sheath elongation of winter wheat. Altogether, we identified 21 sites (the calibration set) with consistent observational data with a maximum of 2 missing values for each crop from 2000 to 2012. These sites are spread throughout the agricultural land of the Czech Republic.

2.2. Filtering method development

For the filtering of the remote sensing data, a new software utility called LINcoln (abbreviated as LIN) was developed, programmed and tested during a 2015 research study by the authors at the University of Nebraska–Lincoln. The core algorithm is described in the results (see Sec. 3.1) as its development was one of the main aims of this study. The utility enables the use of 3 parameters – the minimum threshold of the satellite data and the upper and lower coefficients of the standard deviation (see Sec. 3.1). For the comparison and testing of the LIN newly developed filtering method and to derive the SOS, alternate TIMESAT software (Eklundh and Jönsson, 2012) was used. For the TIMESAT settings, see Sec. 2.4.

2.3. LIN calibration phase

The correct setting of the adjustable parameters is crucial for the filtering method to function properly. The parameters have a considerable influence on the results, and it is particularly important to adjust the settings with respect to the region, vegetation type, land cover class and its structure, and spatial and temporal resolution. We also considered aspects of the production process and data availability after each satellite overpass due to the further use of filtered data in the monitoring system. Robust testing of the settings was performed at 21 agricultural testing locations in the Czech Republic (calibration dataset) with different conditions. Selection of the calibration sites was done due to availability of the sufficient phenology ground data for testing; thus, it covers winter wheat and spring barley observations. After visual evaluation, 14 combinations of reasonable settings were chosen. The considered values for the settings were as follows: a minimum threshold for NDVI values of 0.15, 0.2, 0.25, 0.275, 0.3, 0.325, 0.35; an upper coefficient of 0.3, 0.5, 1.0; and a lower coefficient of 1.0, 1.5, 2.0. The differences in the results of the aforementioned filtering settings are shown in Fig. 1.

2.4. TIMESAT software and the SOS

To evaluate the performance of the algorithm and the settings of the calibration phase, the time series was further processed with TIMESAT software (Jönsson and Eklundh, 2002, 2004). This software served two purposes in the study. The first was the additional smoothing of the utility output to assess the level of adaptation to the original data. Second, the software served to compute the start of the season (SOS).

Out of the available filters, the Savitzky-Golay filter (Chen at al., 2004) was applied for its ability to adapt to rapid changes in the NDVI course, which makes it favourable for the monitoring of drought events. As was done with our own algorithm, the time series at the testing sites was processed in TIMESAT with three different settings of the Savitzky-Golay filter. The first setting (in Table 1 referred to as set1) contains outputs of LIN with no significant changes generated by the TIMESAT software and was mainly utilized to calculate the SOS metric. Settings set2 and set3 exert additional smoothing on the time series, balancing the best fit for small changes and a rough NDVI course; noise values were also omitted.

For the calculation of the SOS, two approaches were adopted – absolute and relative threshold values. According to the former, the SOS is defined as the

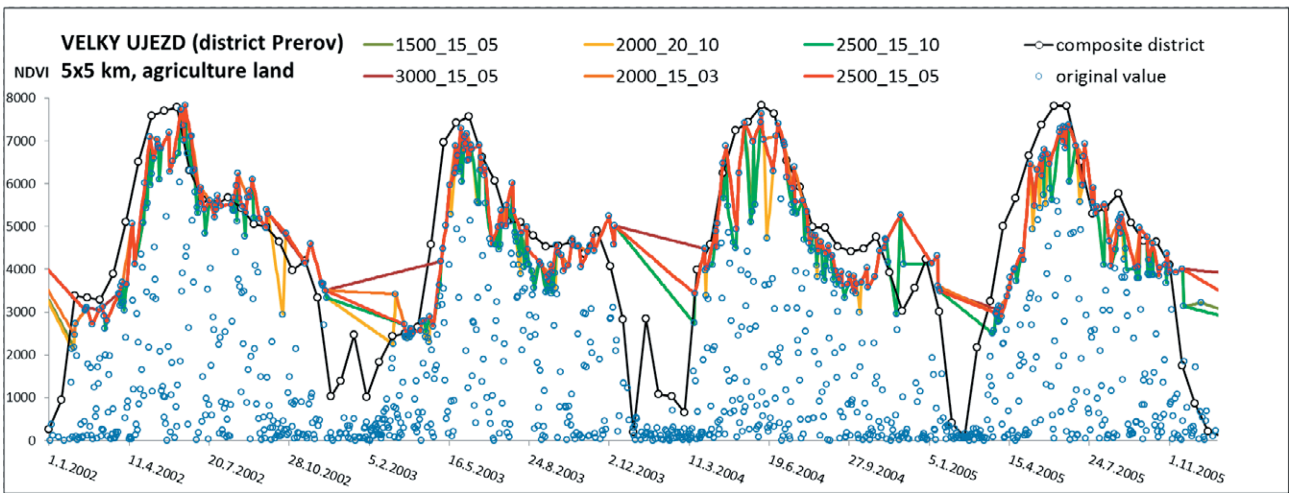

Fig. 1. Example of a MODIS NDVI time series from the Velký Újezd site (a 5 x 5 km area of agricultural land use) for the period from 2002 to 2005. Both the original NDVI satellite data (circles) and the effect of the newly developed filtering LIN method (colour lines) with different settings are shown (in order: minimum NDVI threshold_upper coefficient_lower coefficient). The 16-day composite product (as an average value target region - district Přerov) is depicted as a reference (all NDVI values are multiplied by 10000).

time of year when the threshold value of the NDVI is reached. The relative threshold is expressed as a certain ratio of the seasonal amplitude of the NDVI. The SOS was computed in TIMESAT for 4 different values of the absolute threshold (0.4, 0.45, 0.5 and 0.55) and 4 values of the relative threshold (0.25, 0.35, 0.45 and 0.5).

Different LIN software settings (14 combinations), TIMESAT settings (3 variants) and SOS derivation methods and values (8 cases) were used to compute the SOS at the testing sites. These were linearly correlated with ground observations of two phenological metrics available at the same locations - the emergence of spring barley and the onset of leaf sheath elongation of winter wheat. Matrices of the coefficients of determination (R^2), mean absolute difference and missing values averaged for the 21 testing sites were aggregated to evaluate the performance of the LIN algorithm, its settings and the SOS derivation parameters.

2.5. Correlation of satellite SOS and ground phenological observations

When optimal settings of the LIN filter and SOS derivation were chosen, the SOS for the entire Czech Republic and the whole data span was computed. To evaluate the performance of the LIN algorithm, the coefficients of determination for the linear correlation between the remotely sensed SOS results and the ground observations of phenology metrics were computed for different land cover classes (5x5 km) and for the original resolution (250x250 m) grids at 80 sites with observations. Six land cover classes were used: arable, agricultural, grass and mixed agricultural land; deciduous and conifer forest. This correlation was used to evaluate the performance of the new LSP algorithm and to compare both methods.

3. RESULTS

According to the aims of this study, the results are divided into three subchapters. The first deals with the method of filtering daily NDVI data and deriving the SOS. The procedure for operational processing was designed and implemented in a software utility called LIN. In the second subchapter, the robust testing of the settings for the procedure is evaluated and set. The third goal of this study was to calculate the SOS and evaluate its values compared to those from traditional ground phenology observations at ground sites. This is covered in the last subchapter.

3.1. Software utility - LIN filter

A three-step algorithm (called LIN) for the filtering of daily NDVI data was developed, implemented and tested. The procedure was designed with respect to further use as a simple operational method for MODIS data filtering, generating pixel-based time series and evaluating the SOS. The algorithm steps were constructed after inspection of a vast amount of spatially heterogeneous data values over time. After an erudite and creative algorithm design process, robust testing (this is part of 4.2) of the settings was performed. These are crucial for the performance of the utility for the given purpose and spatial extent.

The iterative steps of the LIN utility for filtering the time series are as follows:

1. Setting of a minimum NDVI value threshold (→ output is RAW1)
   - This setting filters mostly cloudy data and irrelevant values.
   - Values of original data (RAW) below a threshold value (several were tested) are neglected.

2. Adapting to higher values (from RAW1)
   - Assuming that the real vegetation change within 10 days is limited and considering that the highest values are more likely to represent a clear signal (real values)
   - For each day, the 1st, 2nd and 3rd highest values in a +/- 7 day window are selected. (For operational use, a 10-day backward window is applied.)
   - The weighted mean according to the time difference (actual day=100%, day±7=30%) is computed for the three highest values within the time window → RAW2.

3. Removing outliers
   - Calculating delta (the normalized difference between RAW & RAW2)
   - Computing the standard deviation of the calculated delta values in each pixel for the whole period
   - The buffer zone in each pixel is set as a multiplier of the upper and lower coefficients (LowCoef, UpCoef - several were tested) of standard deviation
   - Filtering values if delta is outside the buffer zone (-STDV*LowCoef > delta > STDV*UpCoef)
   - When delta is in the buffer zone, the RAW1 value is accepted → RAW3.

4. Daily linear interpolation of RAW3 → LIN output time series
   - Values for the filtered days are interpolated.

The final version of the software utility uses GeoTIFF files as a raster input of time series. It has the capacity to handle missing data and allows setting of different parameters - the threshold for the minimum NDVI value and the lower (LowCoef) and upper (UpCoef) buffer coefficients. An example of original and filtered NDVI outputs is depicted in Fig. 1 (note that only settings depicted with red line are used in final LIN utility).

3.2. Settings for the LIN filter and land surface phenology

The performance of the algorithm is considerably affected by the parameters that can be set (changed). Its proper tuning depends on local and regional conditions. For the calibration phase, different combinations of input parameters were examined, and the impact on the output was evaluated based on expert knowledge and testing of the credibility of the resulting time series for SOS derivation. Due to availability of consistent ground observations only two cereal crops were used for statistical testing in calibration phase, however same settings for LIN utility are expected within examined territory, weather and natural conditions on vegetated land cover.

To support a decision on the operational settings for LIN filters, the SOSs for crops in testing sites were derived with the use of different variations of settings. The outputs of SOS were correlated with ground observations. The robust correlation matrix for two crops (winter wheat and spring barley) was examined. It contained fourteen different options of the LIN utility in columns: three settings for TIMESAT and eight options for SOS derivation in 24 rows. Only a naturally reasonable time range within the year (the SOS between the 40^{th} and 170^{th} day of the year) was taken into account. Each cell represented an average of R^2 in 21 ground-observation sites for 13 vegetation seasons. The subsets (just the promising rows and columns) of matrices for winter wheat and spring barley are outlined in Table 1.

Investigation of the LIN utility outputs (see example Fig. 2) has shown that filtering is favourable for noisy daily MODIS NDVI data, except for the winter season, when data of the limited vegetation are often unreliable. In general, additional filtering with TIMESAT (set3) yielded slightly higher coefficients of determination for the SOS than when the LIN utility was used (set1). This is at a cost of higher generalization of the NDVI time series. The coefficients of determination for spring barley are generally lower than those for winter wheat. This could be caused by a problematic signal (many missing days due to the minimum threshold value). Additionally, a highly variable sowing date and the onset of suitable growing conditions caused by field accessibility (i.e., soil moisture) lead to inferior results compared to those of wheat. Satisfactory results were achieved for winter wheat, which was sowed during September or October of the previous year before the winter and began to grow according to the actual weather conditions; hence, the results were not influenced by the sowing date.

Table 1. R2 values for the SOS (derived from satellite data) and ground observations; the values are averages of 21 field stations and 13 vegetation seasons. The different settings of the LIN filter are in columns, and the SOS derivation with TIMESAT software are in rows (subset of the whole table).

SOS derivation	Winter wheat							Spring barley						
lower env.	0.5	0.3	0.5	1.0	0.5	1.0	0.5	0.5	0.3	0.5	1.0	0.5	1.0	0.5
upper env.	1.5	1.5	1.5	1.5	1.5	2.0	1.5	1.5	1.5	1.5	1.5	1.5	2.0	1.5
min. thresh.	0.15	0.2	0.25	0.25	0.3	0.3	0.35	0.15	0.2	0.25	0.25	0.3	0.3	0.35
set1, 35%	0.21	0.25	0.32	0.26	0.33	0.29	NA	0.12	0.12	0.12	0.12	0.10	0.15	0.11
set1, 45%	0.25	0.22	0.25	0.22	0.29	0.31	NA	0.11	0.12	0.12	0.14	0.12	0.22	0.19
set1, 0.4	0.25	0.31	0.32	0.26	0.33	0.35	0.17	0.14	0.17	0.20	0.14	0.15	0.19	0.22
set1, 0.45	0.29	0.37	0.38	0.35	0.38	0.38	0.27	0.13	0.14	0.15	0.11	0.16	0.11	0.15
set1, 0.5	0.30	0.32	0.36	0.33	0.35	0.37	0.43	0.12	0.13	0.15	0.14	0.15	0.14	0.16
set3, 50%	0.25	0.22	0.29	0.25	0.32	0.28	0.22	0.12	0.11	0.11	0.19	0.12	0.21	0.13
set3, 0.4	0.26	0.33	0.32	0.31	0.31	0.38	NA	0.18	0.23	0.16	0.18	0.22	0.22	0.28
set3, 0.45	0.30	0.36	0.38	0.30	0.39	0.37	0.27	0.13	0.15	0.14	0.16	0.18	0.15	0.12
set3, 0.55	0.35	0.34	0.37	0.35	0.34	0.37	0.23	0.08	0.11	0.12	0.15	0.11	0.13	0.14

set1=Savitzky-Golay filter (envelope iterations 1, adaptation strength 1, window size 1).
set3=Savitzky-Golay filter (envelope iterations 3, adaptation strength 5, window size 10).

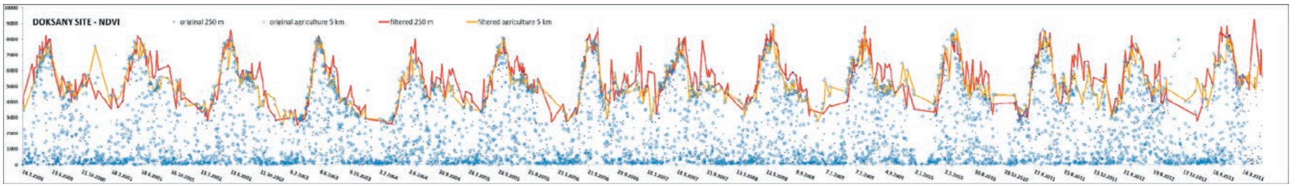

Fig. 2. Example of raw MODIS NDVI data values from the Doksany site in the original (250x250 m) and aggregated (5x5 km, only agriculture land) resolution accompanied by filtered time series (curves).

LIN itself proved to be suitable for data filtering. With respect to the correlation matrices and expert knowledge of site-specific phenology, the optimal minimum NDVI threshold was set to 0.25, the upper coefficient was set to 1.5 and the lower coefficient was set to 0.5 (see red line at Fig. 1 and 3rd column at Table 1). For these settings, R^2 is 0.38 on average, with values of approximately 0.7 at some sites (not shown). The start of the vegetation season (SOS) was set as the day in the year when the NDVI reached a threshold value of 0.45.

3.3. Land surface phenology - Start of the season

With the help of the LIN utility, the NDVI time series was filtered for each grid point in the Czech Republic, and the SOS was computed for the years 2000-2012. This is novel information for the Czech Republic. The SOS was compared to ground observations (two metrics were used) that were recorded during this period at field stations. Both datasets were correlated, and several conditions for the SOS were tested to understand similarities and differences between them. This included aggregation of the original data at a resolution of 250x250 for the 5x5 km grid according to the land cover classes.

See the example of the result for the Doksany site in Fig. 3. The SOS for neighbouring agricultural areas is quite consistent and in line with the observations. The coefficient of determination R^2 of the SOS with ground measurements for the corresponding location is 0.58, which shows the ability of land surface phenology to simulate traditional phenology observations in certain cases. Ideal conditions require homogeneous vegetation cover with single plants (monocultures).

The example of the Jaroměř observation site (see Fig. 4) shows differences among different land cover classes at the same 5x5 km aggregated grid. The computed results of the SOS correspond in general to the agricultural land cover class. A lower correlation is also observed for the 250x250 m resolution because there is no generalization effect of mixed signal and different crops at single pixel. Contrary, aggregation to 5x5 km grid proved to be more robust as it represents similar shares of various crops that differ at pixel level.

Tab. 2 shows the average R^2 at all sites in the Czech Republic with a minimum of 4 available pairs of ground- and satellite-based values. There are significant differences among the land cover classes and for the investigated ground observation metrics.

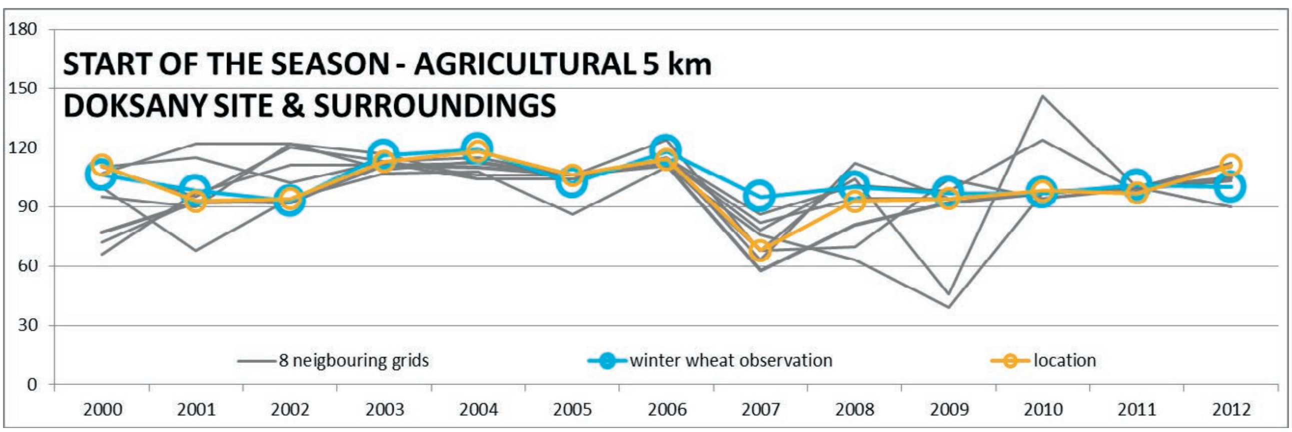

Fig. 3. Day of the year derived as the SOS for 9 neighbouring grid cells (5x5 km) around the ground observation site at Doksany (highlighted orange as "location") compared with ground observations for winter wheat (i.e., the onset of leaf sheath elongation in blue).

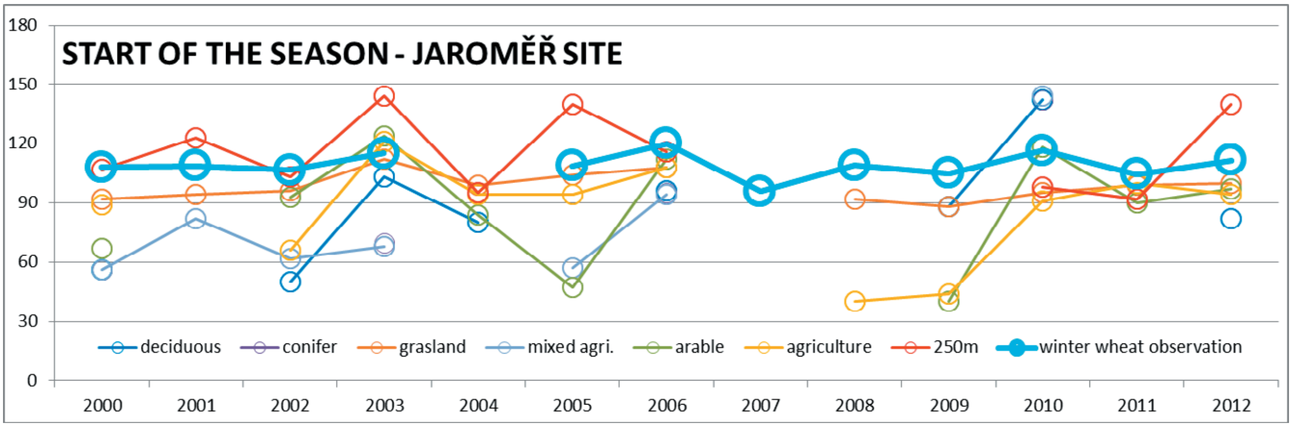

Fig. 4. SOS derived for the different land cover types (aggregated for 5x5 km) together with ground observations at the Jaroměř observation site. The red line shows the results for the SOS at the location using the original satellite data resolution (250x250 m).

Table 2. Correlation of the SOS with two phenological metrics. The table shows the average R2 at all ground stations (row count) with a minimum of 4 observations.

	winter wheat - beg. of leaf sheath elongation							spring barley - emergence						
	250 m	agric	arabl	conif	decid	grass	mixed	250 m	agric	arabl	conif	decid	grass	mixed
No. of ground stations	78	76	76	47	29	55	45	68	65	65	38	27	48	38
Average R^2	0.20	0.31	0.28	0.21	0.29	0.24	0.26	0.17	0.19	0.18	0.33	0.22	0.17	0.16

The correlation of the LSP SOS with the observations of the beginning of elongation of leaf sheath in winter wheat was shown in most tested sites across the Czech Republic (see Fig. 5). Good results are obtained for agricultural (0.31), arable (0.28) and deciduous (0.29) land cover classes; however, there are considerable differences from site to site (see map on Fig. 5). Promising results are obtained for the agricultural land cover class, where 21 out of 76 ground stations have R^2 values higher than 0.5. The R^2 values for winter wheat (0.20) and spring barley (only 0.17) at the original resolution of 250x250 m are, on average, much lower than the aggregated values for the arable and agricultural land cover classes (see Table 2). This might be due to contamination of the satellite signals by different surfaces. Inspection of possible patterns of higher R^2 values based on elevation, districts and primary agricultural production did not result in relevant findings.

The coefficients of determination of spring barley are generally lower than those of winter wheat, which could be caused by the non-crop winter signal (starting from bare land/snow values), the strong influence of the crop sowing date by farmers and a generally lower acreage within the agricultural landscape.

4. DISCUSSION

4.1. Filtering of the MODIS NDVI time series

Visual evaluation of the filtered time series together with the correlation with ground observations showed the suitability of the LIN filter to be used with daily data and produce time series with very good temporal resolution compared to composite MODIS NDVI products. However, the uncertainty of the winter signal needs to be considered in further studies.

Because the testing of the LIN utility showed the redundancy of the TIMESAT filter for additional smoothing, it would be possible to extend the use of our utility for raster data processing and deriving the SOS. To bring the LIN utility into operational use for monitoring vegetation conditions, the window size from the 2nd step of the abovementioned algorithm needs to be adapted to backward use only (as future values are not known in real-time operation). For this 10-day backward window was set, comparable results were derived, proving the hypothesis.

Using the NDVI for vegetation monitoring has known limitations during the vegetation peak when the index reaches saturation (Mutanga and Skidmore, 2004). Investigation of the enhanced vegetation index (EVI) in

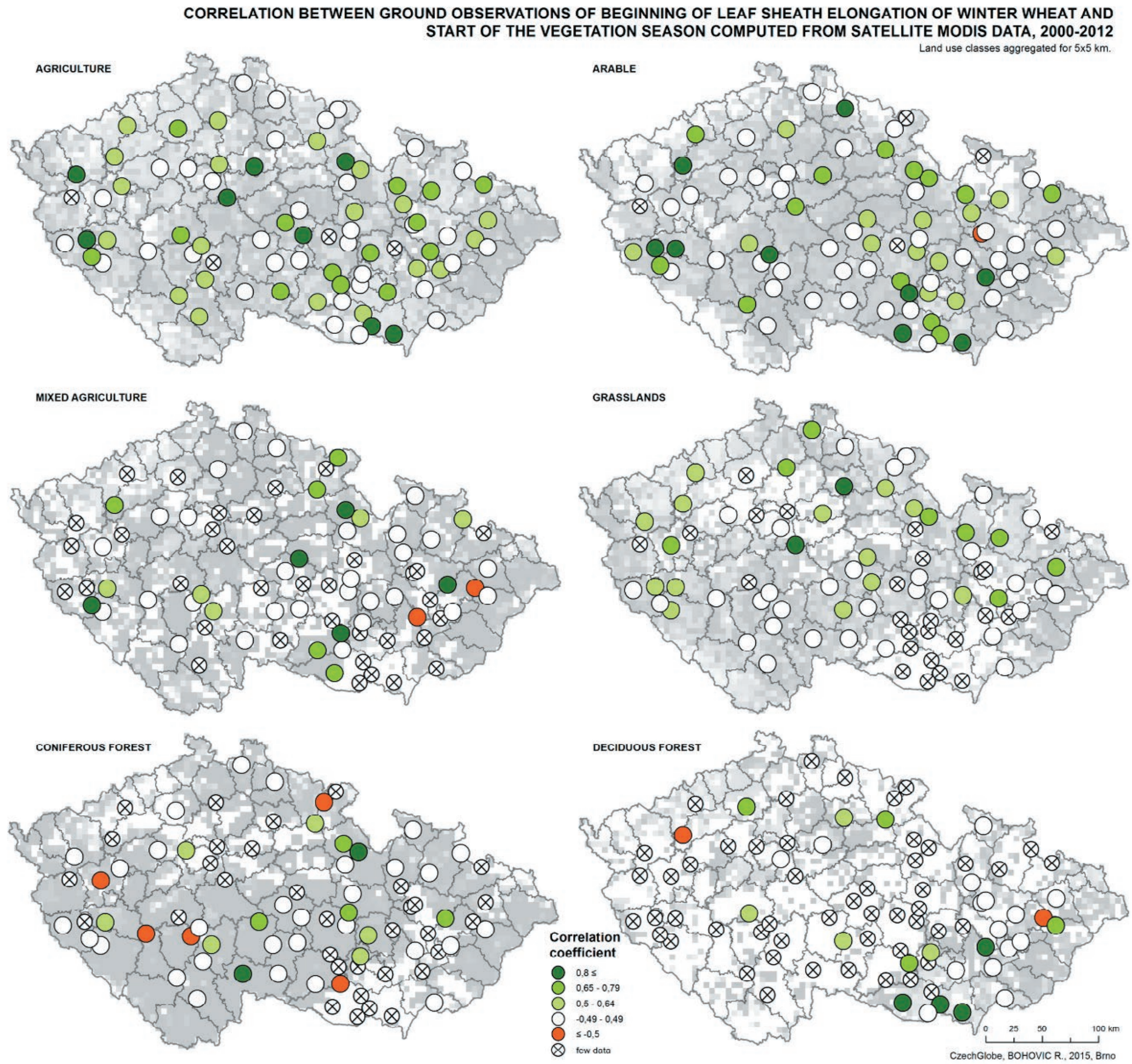

Fig. 5. Map of the correlation between ground observations of the beginning of leaf elongation of winter wheat and the SOS for different land cover classes.

the future is promising, as this is more sensitive to vegetation conditions before it reaches saturation.

The location of short drought events from satellite signals is still awaiting precise tuning.

4.2. Land surface phenology opportunity

The start of the season is the most often computed LSP metric with a wide range of uses. It is an input parameter of many scientific models related to vegetation, climate and climate change predictions. The results (see Sec. 3) of this study show that it cannot serve as an identical substitution for ground phenological measurements (Bohovic et al., 2016). These are species-related and differ significantly within the same ecotope. LSP is by its nature coupled with vegetation cover when the metric signals a certain phase (such as the start of the season) of the whole ecosystem. However, it offers a robust measure that can be obtained for large regions.

It is independent of ground infrastructure and is easily comparable across different regions with no observer-related constraints. LSP can serve as a valuable complement to ground measurements. When designed with the respect to its specifics, LSP can to some extend serve as an alternative to ground observations mainly at ecosystem level. This might be of much interest in the case of the Czech Republic, where a state-wide ground phenology observation network based on field stations was terminated in 2012. At the same time, study shows that species specific ground observations cannot be equally altered from earth observation. Necessity for calibration and evaluation of LSP makes in-situ observation still very valuable.

The average coefficients of determination between in-situ and LSP methods in the original satellite data resolution are quite low for both spring barley (0.17) and winter wheat (0.20). When we aggregate the signal for a larger area (serving as the area average) with respect to the corresponding land cover class (agriculture for crops), an average R^2 value of 0.31 is achieved in 76 stations (see Table 2). This study shows that the overlapping period of satellite data and in situ measurements can be successfully used for calibration of the SOS acquired by both methods.

4.3. Practical potential

The results of this study support two possible uses that can be implemented. The first is the use of the LIN filter and utility for operational filtering of the MODIS NDVI data. This was successfully applied as one of the data inputs for modelling (not part of this paper) in the national drought monitoring portal for agriculture in the Czech Republic called Czech Drought Monitor (Trnka et al., 2020; www.intersucho.cz). Such information is of high value not only for farmers but also for commodity brokers, public administration and state agriculture management. The use of LIN filter in agricultural insurance and compensation after natural disasters could also be considered. However, this requires operational experience for several seasons and is also subject to administrative settings.

The second opportunity for practical exploitation is the use of the LSP to estimate the start of the season as a substitution for ground phenology observations. Such a service could be run at a comparably lower cost than a system that requires a human observer to monitor individual plants in many locations (stations). If such observations were terminated, the LSP can substitute operational use cases where these data are used to support vegetation/agricultural-related decisions. Such transition would require adaptations to acknowledge important differences in the methods (mainly the resolution factor and plant-ecosystem aspect). At the same time, at least limited ground observation is necessary for calibration and validation purposes.

The Terra satellite has already surpassed its planned lifetime and is estimated to remain fully functional until the 2022 (limited science data are expected even further). This will provide a great opportunity for several years of data overlap with Sentinel-2 satellites that have been operational since 2015 (Sentinel-2A) and 2017 (Sentinel-2B).

5. CONCLUSION

The SOS was derived for the entire focus area, and these values were compared with ground phenological observations. Correlations between the LSP metrics and traditional observations have shown that methodological differences exist that prevent the full substitution of ground observations with Earth observation metrics (LSP). However, LSP can be adjusted in specific cases, such as the regionally specific phenology of monocultures. Regardless of the need to correlate LSP with traditional phenology, it can serve as a valuable measure of life phases of vegetation growth.

The main aim of this study, to develop and implement a procedure for filtering daily satellite signals for the operational derivation of a vegetation index and land surface phenology (LSP) metrics, was successfully achieved. A software utility called LIN was developed and was operationally deployed as one of the inputs in a drought monitoring system in the Czech Republic.

Settings considered optimal for the operational monitoring of drought using the LIN utility (a minimum threshold value of 0.25) and the SOS (an absolute NDVI threshold value of 0.45) have been chosen specifically with respect to agricultural land. This is subject to specific use and is also spatially relevant and thus cannot serve as a general conclusion. Other land cover classes would also require different settings, and these need to be investigated further.

ACKNOWLEDGEMENT

This study was undertaken within the project supported by project SustES - Adaptation strategies for sustainable ecosystem services and food security under adverse environmental conditions" (CZ.02.1.01/0.0/0.0/16_019/0000797)".

REFERENCES

Bohovic, R., Dobrovolny, P. and Klein, D., 2016. The spatial and temporal dynamics of remotely-sensed vegetation phenology in central Asia in the 1982–2011 period. European Journal of Remote Sensing, 49(1), 279-299.

Chen, J., Jönsson, P., Tamura, M., Gu, Z., Matsushita, B. and Eklundh, L., 2004. A simple method for reconstructing a high-quality NDVI time-series data set based on the Savitzky–Golay filter. Remote sensing of Environment, 91(3-4), 332-344.

Cleland, E.E., Chuine, I., Menzel, A., Mooney, H.A. and Schwartz, M.D., 2007. Shifting plant phenology in response to global change. Trends in ecology & evolution, 22(7), 357-365.

Eklundh, L. and Jönsson, P., 2012. TIMESAT 3.2 with parallel processing-Software Manual. Lund University, 52.

Fraga, H., Amraoui, M., Malheiro, A.C., Moutinho-Pereira, J., Eiras-Dias, J., Silvestre, J. and Santos, J.A., 2014. Examining the relationship between the Enhanced Vegetation Index and grapevine phenology. European Journal of Remote Sensing, 47(1), 753-771.

Friedl, M. H., Henebry, G. M., Reed, B. C., Huete, A., White, M. a, Morisette, J., Nemani, R. R., Zhang, X., Myneni, R. B. a Friedl, M., 2006. Land Surface Phenology. A community white paper requested by NASA, April 10.

Jönsson, P. and Eklundh, L., 2002. Seasonality extraction by function fitting to time-series of satellite sensor data. IEEE transactions on Geoscience and Remote Sensing, 40(8), 1824-1832.

Jönsson, P. and Eklundh, L., 2004. TIMESAT—a program for analyzing time-series of satellite sensor data. Computers & geosciences, 30(8), 833-845.

Liang, L., Schwartz, M.D. and Fei, S., 2011. Validating satellite phenology through intensive ground observation and landscape scaling in a mixed seasonal forest. Remote Sensing of Environment, 115(1), 143-157.

Lieth, H., 1974. Purposes of a phenology book. In Phenology and seasonality modelling, 3-19.

Lin, X., Hubbard, K.G., Mahmood, R. and Sassenrath, G.F., 2014. Assessing satellite-based start-of-season trends in the US High Plains. Environmental Research Letters, 9(10), 104016.

Mutanga, O. and Skidmore, A.K., 2004. Narrow band vegetation indices overcome the saturation problem in biomass estimation. International journal of remote sensing, 25(19), 3999-4014.

Reed, B.C., Brown, J.F., VanderZee, D., Loveland, T.R., Merchant, J.W. and Ohlen, D.O., 1994. Measuring phenological variability from satellite imagery. Journal of vegetation science, 5(5), 703-714.

Trnka, M., Hlavinka, P., Možný, M., Semerádová, D., Štěpánek, P., Balek, J., Bartošová, L., Zahradníček, P., Bláhová, M., Skalák, P. and Farda, A., 2020. Czech Drought Monitor System for Monitoring and Forecasting Agricultural Drought and Drought Impacts. International Journal of Climatology, 1-18.

Tucker, C.J., 1979. Red and photographic infrared linear combinations for monitoring vegetation. Remote sensing of Environment, 8(2), 127-150.

White, M.A., de Beurs, K.M., Didan, K., Inouye, D.W., Richardson, A.D., Jensen, O.P., O'KEEFE, J.O.H.N., Zhang, G., Nemani, R.R., van Leeuwen, W.J. and Brown, J.F., 2009. Intercomparison, interpretation, and assessment of spring phenology in North America estimated from remote sensing for 1982–2006. Global Change Biology, 15(10), 2335-2359.

Xie, Y., Sha, Z. and Yu, M., 2008. Remote sensing imagery in vegetation mapping: a review. Journal of plant ecology, 1(1), 9-23.

Zeng, L., Wardlow, B.D., Xiang, D., Hu, S., Li, D., 2020. A review of vegetation phenological metrics extraction using time-series, multispectral satellite data. Remote Sensing of Environment, 237, 111511.

Italian Journal of Agrometeorology
Rivista Italiana di Agrometeorologia

Firenze University Press
www.fupress.com/ijam

OPEN ACCESS

Citation: I.M. El–Metwally, H.S. Saudy, M. Tawfik Abdelhamid (2021) Efficacy of benzyladenine for compensating the reduction in soybean productivity under low water supply. *Italian Journal of Agrometeorology* (2): 81-90. doi: 10.36253/ijam-872

Received: March 09, 2020

Accepted: June 26, 2021

Published: December 27, 2021

Data Availability Statement: All relevant data are within the paper and its Supporting Information files.

Competing Interests: The Author(s) declare(s) no conflict of interest.

ORCID:
HSS: 0000–0002–6341–6156

Efficacy of benzyladenine for compensating the reduction in soybean productivity under low water supply

Ibrahim Mohamed El–Metwally[1], Hani Saber Saudy[2,*], Magdi Tawfik Abdelhamid[1]

[1] *Botany Department, National Research Centre, P.O. Box 12622–Dokki, El–Behos St. Dokki, Cairo, Egypt*
[2] *Agronomy Department, Faculty of Agriculture, Ain Shams University, P.O. Box 68–Hadayek Shoubra 11241, Cairo, Egypt*
*Corresponding author. E-mail: hani_saudy@agr.asu.edu.eg

Abstract. Undoubtedly, drought is a negative consequence of climate change. Farmers have to deal with this issue and may be forced to irrigate their crops with less water than required, however reduction in productivity is anticipated. Thus, two–year field trials were conducted to assess the impact of irrigation regimes (60, 80 and 100% of crop evapotranspiration, denoted ET_{60}, ET_{80}, and ET_{100}, respectively) and benzyladenine rates (0, 50, 100, 150 and 200 mg L^{-1}, symbolized as BA_0, BA_{50}, BA_{100}, BA_{150}, BA_{200}, respectively) on soybean. Findings clarified that the maximum increases in plant height and net assimilation rate were obtained with the interactions of ET_{100} or ET_{80} x BA_{200} or BA_{150} in both seasons. ET_{80} x BA_{200} (in both seasons) and ET_{100} x BA_{150} (in the first season) were as similar as ET_{100} x BA_{200} for enhancing pods number plant^{-1}. Irrigation water use efficiency progressively increased with decreasing irrigation water amount and increasing benzyladenine rate. In conclusion, the reduction in seed yield due to lowering water supply up to 80% of crop evapotranspiration (with saving 20% of irrigation water) could be compensated using benzyladenine, 150 mg L^{-1}, thus it should be involved in soybean irrigation programs.

Keywords: deficit water, growth promoters, relative growth rate, soybean oil.

INTRODUCTION

Soybean {*Glycine max* (L.) Merr.} occupies a prestigious position in the global economy, since its seeds are considered a major source of protein (approximately, 38–47%) and oil (approximately, 18–22%) (Nakagawa et al. 2020; Tian et al. 2020), besides its importance in sustainable agriculture. In water rationalization patterns, the increase of water use efficiency should be pursued in a sustainability prospective, increasing crop productivity per unit of water used (Oweis and Hachum 2003). In this respect, farmers are obligated to irrigate their crops using less water than required (El–Bially et al. 2018; Salem et al. 2021). However, soybean production is affected by abiotic pressures, i.e. water deficit. Water stress is a major factor in determining crop productivity, particularly in arid and semi–arid areas. In Egypt, based on the local farmers' irrigation practice for the soybean cropping system, the optimized water consumption is 550 mm/total growing period (Sheteiwy et al. 2021). Water deficit conditions affect the water potential and turgor pressure of the cells and this can disturb the normal plant physiological mechanisms inducing various impacts on growth and yield parameters of the crops (Reisdorph and Koster 1999; El-Metwally et al. 2021). Soybean under drought stress at beginning of pod, beginning of seed and full seed stages resulted in substantial yield losses (Dogan et al. 2007). The photosynthetic activity of soybean plants was severely decreased (Zhang et. al. 2016) and photoinhibition increased (Sofo et al. 2009) in drought conditions. Because of severe drought stress during flowering and pod-setting stage, losses in leaf area, dry matter and seed yield per soybean plant reached 61, 67 and 77%, respectively (Wei et al. 2018).

Due to application of plant growth regulators, alternations in metabolic and physiological processes in plants reflecting on flowering, fruiting, maturation, fruit drop, and defoliation were observed (Rademacher 2015). One of the most important plant growth promoters is cytokinins group which play a crucial role in plant differentiation and development (Yeh et al. 2015). In soybean, enhancement in yield was evident because of cytokinin foliar application (Soares et al. 2017). Borges et al. (2014) proved that benzyladenine as a compound of cytokinin can reduce pod abortion and improve yield of soybean. Moreover, application of benzyladenine significantly improved growth, yield, yield attributes and quality of soybean (Khaswa et al. 2014). Still, the knowledge about the potency of benzyladenine and its demeanor in soybean under drought is not sufficiently available.

Therefore, the objective of this study was to evaluate the efficacy of benzyladenina to alleviate the impacts of low water supply in soybean.

MATERIALS AND METHODS

Site attributes

The experiments were carried out under open field conditions during two years (2015 and 2016) at the experimental research and production station of National Research Centre, El–Nubaria region, Egypt (latitude 30°86'N, and longitude 31°16'E, and mean altitude 21 m above sea level). Location is typified as arid region having cool winters as well as hot dry summers with no rainfall. Mean values of weather status prevailing during soybean life cycle are provided in Table 1. Physical and chemical properties of the experimental soil are shown in Table 2.

Table 1. Averages of some weather data during life cycle of soybean grown at El–Nubaria region in 2015 and 2016 seasons.

Month	Air temperature (°c)		Wind speed (m sec^{-1})	Solar radiation (MJ m^{-2}day^{-1})
	Minimum	Maximum		
2015				
May	34.6	17.5	4.43	27.09
June	36.2	19.3	4.73	29.53
July	35.5	19.7	4.74	29.26
August	37.1	20.9	3.93	27.32
September	34.4	19.9	4.30	23.39
2016				
May	32.8	17.1	4.36	26.59
June	36.0	19.3	4.63	29.43
July	36.8	20.5	4.23	29.16
August	38.1	21.5	4.16	27.14
September	34.6	20.5	3.81	22.89

Table 2. Initial soil physical and chemical properties of El–Nubaria region.

Soil depth (cm)	Particle size distribution (%)			Texture class	Chemical properties			
	Coarse sand	Fine sand	Clay+ silt		Organic natter (%)	pH	EC (dS m^{-1})	$CaCO_3$ (%)
20	46.1	48.6	5.3	Sandy	0.70	8.5	0.32	6.56
40	54.2	39.1	6.7		0.45	8.7	0.30	2.51
60	56.2	37.0	6.8		0.30	9.1	0.42	4.75

Experimental set-up

Each experiment was established with a strip–plots design having four replicates. Three irrigation levels (60, 80 and 100% of crop evapotranspiration, ETc, denoted ET_{60}, ET_{80}, and ET_{100}, respectively) were practiced. As well, five benzyladenine (BA) rates (0, 50, 100, 150 and 200 mg L^{-1}, symbolized as BA_0, BA_{50}, BA_{100}, BA_{150}, BA_{200}, respectively) were sprayed twice at 45 and 60 days after sowing (DAS).

After harvesting the preceding crop (wheat), the experimental field was ploughed and ridged (60 cm width) before planting. During land preparation, single super–phosphate (15.5% P_2O_5) was applied at a rate of 357 kg ha^{-1}. Moreover, the field was divided into experimental units of about 3.5 m x 3.0 m each. Soybean seeds (cv Giza–111) were inoculated with the specific *Rhizobi-*

um strain and immediately sown in hills (2–3 seeds), 20 cm apart on both sides of the ridge. Sowing dates were May 18th and 25th in 2015 and 2016 seasons, respectively. At 20 and 35 DAS, all plots received 52.5 g ammonium nitrate (33.5 % N) and 157.5 g potassium sulphate (48% K_2O), respectively. Plants were watered through trickle irrigation system which comprised of emitters spaced 30.0 cm apart with discharge of 2.0 L h^{-1}.

Based on the information provided in Table 1, FAO Penman–Monteith equation (Allen et al. 1998) was exploited to estimate the daily reference evapotranspiration (ET_0) of soybean along the growing season. Thereafter, crop evapotranspiration (ETc) was calculated with the water budget and irrigation decision support model by FAO-56. Accordingly, the quantity of irrigation water requirement was computed as elucidated by Keller and Bliesner (1990). Seasonal irrigation water applied for 2015 and 2016 seasons are shown in Table 3.

Crop parameters

At 90 DAS, plant height was measured. Also, total chlorophyll content (SPAD value) of the 4th leaf was measured using chlorophyll meter (SPAD 502) according to Soil Plant Analysis Department Section, Minolta Camera Co., Osaka, Japan as reported by Minolta (1989). Moreover, ten plants were randomly selected from the inner rows of each plot at 60 (t_1) and 90 (t_2) DAS to determine relative growth rate (RGR) and net assimilation rate (NAR) as described by Hunt (1982) as follow:

$$RGR = \frac{\ln W_2 - \ln W_1}{t_2 - t_1} \text{ (g g}^{-1}\text{ week}^{-1}) \quad (1)$$

Where, ln = Natural log, W_1 = Dry weight of plant m^{-2} recorded at time t_1, W_2 = Dry weight of plant m^{-2} recorded at time t_2, t_1 and t_2 are the interval of time.

$$NAR = \frac{(W_2 - W_1)(\log LA_2 - \log A_1)}{(LA_2 - LA_1)(t_2 - t_1)} \text{ (g cm}^{-2}\text{ week}^{-1}) \quad (2)$$

Table 3. Seasonal irrigation water applied in soybean (m^3 ha^{-1}) in 2015 and 2016 seasons under various irrigation levels.

Irrigation level	2015 season	2016 season
ET_{60}	2394	2436
ET_{80}	3192	3248
ET_{100}	3990	4060

Note: ET_{60}, ET_{80}, and ET_{100}: irrigation level at 60, 80 and 100% of crop evapotranspiration, respectively.

Where: W_1 and W_2 are total plant dry weight as well as LA_1 and LA_2 are total leaf area at time t_1 and t_2 respectively.

At full maturity (29th September in 2015 and 6th October in 2016), plants of the experimental plots were harvested to assess pods number $plant^{-1}$, seed weight $plant^{-1}$ and seed yield ha^{-1}. According to AOAC (2012), seed oil and protein contents were estimated.

Irrigation water use efficiency and regression analysis

Depending on the computed irrigation water amounts for each irrigation level in 2015 and 2016 seasons (Table 3), irrigation water use efficiency (IWUE) for soybean crop was estimated as follow:

$$IWUE = \frac{\text{Seed yield}}{\text{Irrigation water amount}} \text{ (kg m}^{-3}) \quad (3)$$

Thereafter, simple regression analysis between IWUE (dependent variable) and benzyladenine rate (independent variable) under different irrigation water regimes was derived as explained by Draper and Smith (1998).

Statistical analysis

Data of each season were subjected to analysis of variance (ANOVA) according to Casella (2008), using Costat software program, Version 6.303 (2004). Means separation was performed only when the F–test indicated significant ($P<0.05$) differences among the treatments, according to the Fisher's protected LSD test.

RESULTS

Plant growth

Available results in Table 4 show the significant influence of each irrigation and benzyladenine on the investigated growth traits of soybean in 2015 and 2016 seasons. In this respect, with each increase in water amount, there were progressive increases in plant height, SPAD value, RGR and NAR. Application of ET_{100} recorded the maximum values of RGR and NAR surpassing ET_{80} or ET_{60}. The differences between ET_{100} and ET_{80} did not reach the $P<0.05$ level of significance for plant height and NAR in 2016 season as well as RGR in 2015 season. Moreover, the minimal values of such traits were obtained with ET_{60}.

Spraying soybean plants with benzyladenine (BA) caused significant increases in plant height, SPAD value, RGR and NAR (Table 4). With increasing BA rate up to 150 mg L^{-1}, all soybean growth traits progressively increased in both seasons, except RGR in 2015 season. In this respect, BA_{200} achieved the highest values significantly leveling with BA_{150}.

The significant interaction of irrigation level x benzyladenine rate presented in Table 5 revealed that the most effective combinations for enhancing plant height and NAR were ET_{100} or ET_{80} whether with BA_{200} or BA_{150} in both seasons. Also, ET_{100} x BA_{100} interaction statistically equaled the former remarkable interactions for plant height in 2016 season and NAR in both seasons.

Yield traits and oil and protein percentages

All yield traits of soybean statistically responded to irrigation and benzyladenine treatments in 2015 and 2016 seasons (Table 6). ET_{100} was the effective practice for producing higher values of pods number $plant^{-1}$, seed weight $plant^{-1}$, seed yield, oil % and protein %. There were no significant variations between ET_{100} and ET_{80} for seed yield (in 2015 seasons) and protein % (in 2016 season). Remarkable reductions in all crop traits were obviously obtained with ET_{60}.

Data presented in Table 6 show the significant increases in pods number $plant^{-1}$, seed weight $plant^{-1}$, seed yield, oil % and protein % with increasing BA rates from 0 to 200 mg L^{-1}. The highest values of all these traits were obtained from BA_{200} along with BA_{150}, except pods number $plant^{-1}$ in both seasons and oil % in the second season. The relative enhancements due to BA_{150} compared to untreated control (BA_0) reached 25.5% for seed weight $plant^{-1}$, 14.3% for seed yield, 9.2% for oil % and 7.2% for protein % (as averages of the two seasons).

Concerning the interaction of irrigation level x benzyladenine rate, the presented values in Table 7 clarify that under $ET_{100,}$ whether with BA_{200} or BA_{150} possessed the favorable effects on pods number $plant^{-1}$ and seed yield ha^{-1} in both growing seasons of 2015 and 2016. ET_{80} x BA_{200} (in both seasons) and ET_{100} x BA_{150} (in the first season) were as similar as ET_{100} x BA_{200} for enhancing pods number $plant^{-1}$. Moreover, in 2015 season, ET_{80} x BA_{150} or BA_{200} and ET_{100} x BA_{150} recorded seed yield values like that of ET_{100} x BA_{200}.

Irrigation water use efficiency and regression analysis

As depicted in Fig. 1, irrigation water use efficiency (IWUE) progressively increased with decreasing irrigation water amount and increasing benzyladenine rate. In this regard, the maximum values of IWUE were obtained with ET_{60} x BA_{200} in both seasons and ET_{60} x BA_{150} in

Table 4. Soybean growth parameters as affected by irrigation level and benzyladenine rate in 2015 and 2016 seasons.

Irrigation x BA	Plant height (cm)		SPAD value		RGR (g g^{-1} $week^{-1}$)		NAR (g cm^{-2} $week^{-1}$)	
	2015	2016	2015	2016	2015	2016	2015	2016
Irrigation								
ET_{60}	73.4^{c}	80.9^{b}	39.1^{c}	38.6^{c}	0.503^{b}	0.532^{b}	3.74^{c}	3.76^{b}
ET_{80}	85.4^{b}	84.7^{ab}	41.0^{b}	39.9^{b}	0.544^{a}	0.540^{b}	3.92^{b}	3.98^{a}
ET_{100}	88.4^{a}	86.6^{a}	42.4^{a}	41.8^{a}	0.578^{a}	0.576^{a}	4.08^{a}	4.16^{a}
Benzyladenine								
BA_0	74.7^{d}	80.9^{c}	38.1^{d}	38.1^{c}	0.530^{a}	0.480^{d}	3.70^{c}	3.60^{d}
BA_{50}	79.8^{c}	82.1^{bc}	39.8^{c}	39.1^{bc}	0.530^{a}	0.513^{c}	3.80^{bc}	3.81^{c}
BA_{100}	83.7^{b}	83.6^{b}	41.0^{bc}	39.7^{b}	0.546^{a}	0.556^{b}	3.90^{bc}	4.00^{b}
BA_{150}	86.4^{a}	86.6^{a}	42.3^{ab}	41.5^{a}	0.552^{a}	0.590^{a}	4.03^{ab}	4.16^{a}
BA_{200}	87.6^{a}	87.3^{a}	43.0^{a}	42.1^{a}	0.550^{a}	0.606^{a}	4.13^{a}	4.26^{a}

Note: ET_{60}, ET_{80}, and ET_{100}: irrigation level at 60, 80 and 100% of crop evapotranspiration, respectively; $B.A_0$, BA_{50}, BA_{100}, $BA_{150,}$ BA_{200}: benzyladenine rate of 0, 50, 100, 150 and 200 mg L^{-1}, respectively; SPAD: total leaf chlorophyll content; RGR: relative growth rate; NAR: net assimilation rate. Means followed by different letters in each column are significantly different (*P<0.05*).

Table 5. Plant height and net assimilation rate (NAR), of soybean as affected by irrigation level and benzyladenine rate interaction in 2015 and 2016 seasons.

Variable	Plant height (cm)			NAR (g cm^{-2} $week^{-1}$)		
	ET_{60}	ET_{80}	ET_{100}	ET_{60}	ET_{80}	ET_{100}
2015						
BA_0	66.7^{j}	75.0^{h}	82.3^{f}	3.50^{e}	3.70^{de}	3.90^{bcd}
BA_{50}	70.3^{i}	83.3^{ef}	85.7^{de}	3.70^{de}	3.80^{cde}	3.90^{bcd}
BA_{100}	75.0^{h}	87.0^{cd}	89.0^{bc}	3.80^{cde}	3.80^{cde}	4.10^{abc}
BA_{150}	77.0^{gh}	90.3^{ab}	92.0^{a}	3.80^{cde}	4.10^{abc}	4.20^{ab}
BA_{200}	78.0^{g}	91.7^{ab}	93.0^{a}	3.90^{bcd}	4.20^{ab}	4.30^{a}
2016						
BA_0	79.0^{f}	80.7^{def}	83.1^{cde}	3.50^{f}	3.60^{ef}	3.70^{def}
BA_{50}	79.3^{ef}	82.8^{cdef}	84.2^{bcd}	3.70^{def}	3.80^{def}	3.90^{cde}
BA_{100}	80.4^{def}	84.1^{bcd}	86.4^{abc}	3.70^{def}	4.00^{bcd}	4.30^{ab}
BA_{150}	83.0^{cde}	87.7^{ab}	89.2^{a}	3.90^{cde}	4.20^{abc}	4.40^{a}
BA_{200}	83.2^{cd}	88.5^{a}	90.1^{a}	4.00^{bcd}	4.30^{ab}	4.50^{a}

Note: ET_{60}, ET_{80}, and ET_{100}: irrigation level at 60, 80 and 100% of crop evapotranspiration, respectively; BA_0, BA_{50}, BA_{100}, $BA_{150,}$ BA_{200}: benzyladenine rate of 0, 50, 100, 150 and 200 mg L^{-1}, respectively; NAR: net assimilation rate. Means followed by different letters in each column are significantly different (*P<0.05*).

Table 6. Soybean yield traits, oil % and protein % as affected by irrigation level and benzyladenine rate in 2015 and 2016 seasons.

Irrigation x BA	Pods number plant^{-1}		Seed weight plant^{-1}		Seed yield (ton ha^{-1})		Oil %		Protein %	
	2015	2016	2015	2016	2015	2016	2015	2016	2015	2016
Irrigation										
ET_{60}	34.8^{c}	36.5^{c}	15.4^{c}	16.4^{c}	3.36^{b}	3.58^{c}	23.7^{c}	24.0^{c}	33.9^{c}	34.2^{b}
ET_{80}	41.3^{b}	41.8^{b}	17.2^{b}	18.2^{b}	3.92^{a}	3.95^{b}	25.3^{b}	25.5^{b}	35.5^{b}	36.0^{a}
ET_{100}	43.8^{a}	43.8^{a}	18.8^{a}	20.4^{a}	4.16^{a}	4.17^{a}	26.7^{a}	26.6^{a}	37.5^{a}	36.5^{a}
Benzyladenine										
BA_{0}	37.1^{d}	34.9^{e}	14.7^{d}	16.0^{d}	3.46^{d}	3.65^{d}	23.7^{e}	23.9^{d}	33.6^{d}	34.3^{c}
BA_{50}	38.6^{c}	37.8^{d}	16.0^{c}	17.0^{c}	3.66^{c}	3.76^{c}	24.5^{d}	24.7^{cd}	35.0^{c}	34.8^{c}
BA_{100}	40.8^{b}	41.2^{c}	17.1^{b}	18.5^{b}	3.83^{b}	3.86^{b}	25.4^{c}	25.5^{bc}	36.0^{b}	35.8^{b}
BA_{150}	40.9^{b}	44.2^{b}	18.7^{a}	19.8^{a}	4.00^{a}	4.12^{a}	26.0^{b}	26.2^{ab}	36.5^{ab}	36.3^{ab}
BA_{200}	42.4^{a}	45.4^{a}	19.4^{a}	20.4^{a}	4.11^{a}	4.13^{a}	26.4^{a}	26.7^{a}	37.2^{a}	36.7^{a}

Note: ET_{60}, ET_{80}, and ET_{100}: irrigation level at 60, 80 and 100% of crop evapotranspiration, respectively; BA_0, BA_{50}, BA_{100}, BA_{150}, BA_{200}: benzyladenine rate of 0, 50, 100, 150 and 200 mg L^{-1}, respectively. Means followed by different letters in each column are significantly different ($P<0.05$).

Table 7. Pods number plant^{-1} and seed yield of soybean as affected by irrigation level and benzyladenine rate interaction in 2015 and 2016 seasons.

Variable	Pods number plant^{-1}			Seed yield (ton ha^{-1})		
	ET_{60}	ET_{80}	ET_{100}	ET_{60}	ET_{80}	ET_{100}
2015						
BA_{0}	31.3^{i}	38.6^{ef}	41.4^{cd}	3.10^{i}	3.50^{fgh}	3.80^{cde}
BA_{50}	33.6^{h}	39.6^{de}	42.6^{bc}	3.30^{hi}	3.70^{def}	4.00^{bc}
BA_{100}	36.4^{g}	41.4^{cd}	44.5^{ab}	3.40^{gh}	3.90^{cd}	4.20^{ab}
BA_{150}	35.3^{gh}	42.2^{c}	45.3^{a}	3.40^{gh}	4.20^{ab}	4.40^{a}
BA_{200}	37.3^{fg}	44.6^{ab}	45.4^{a}	3.60^{efg}	4.30^{a}	4.40^{a}
2016						
BA_{0}	31.7^{g}	35.9^{ef}	37.1^{de}	3.40^{g}	3.70^{ef}	3.85^{cde}
BA_{50}	33.8^{fg}	39.0^{cde}	40.7^{c}	3.51^{g}	3.81^{cde}	3.97^{c}
BA_{100}	37.9^{cde}	41.0^{c}	44.8^{b}	3.54^{fg}	3.90^{cd}	4.14^{b}
BA_{150}	39.4^{cd}	45.8^{b}	47.3^{ab}	3.76^{de}	4.19^{b}	4.44^{a}
BA_{200}	40.0^{cd}	47.1^{ab}	49.1^{a}	3.72^{e}	4.19^{b}	4.45^{a}

Note: ET_{60}, ET_{80}, and ET_{100}: irrigation level at 60, 80 and 100% of crop evapotranspiration, respectively; BA_0, BA_{50}, BA_{100}, BA_{150}, BA_{200}: benzyladenine rate of 0, 50, 100, 150 and 200 mg L^{-1}, respectively. Means followed by different letters in each column are significantly different ($P<0.05$).

the second season, while ET_{100} x BA_0 or BA_{50} recorded the lowest value in both seasons. Despite the similarity of benzyladenine behavior under different irrigation regimes, its relationship strength with IWUE varied (Fig. 2). In this respect, regression analysis showed that benzyladenine rate was more correlated with IWUE under low water supply (ET_{60}), since R^2 value was higher compared to other irrigation regimes (ET_{80} or ET_{100}).

Fig. 1. Irrigation water use efficiency (IWUE) of soybean as influenced by irrigation level and benzyladenine rate. Note: ET_{60}, ET_{80}, and ET_{100}: irrigation level at 60, 80 and 100% of crop evapotranspiration, respectively; BA_0, BA_{50}, BA_{100}, BA_{150}, BA_{200}: benzyladenine rate of 0, 50, 100, 150 and 200 mg L^{-1}, respectively. Vertical bars represent means of 4 replications ± SE ($P\leq0.05$). Columns marked by different letters are significantly different

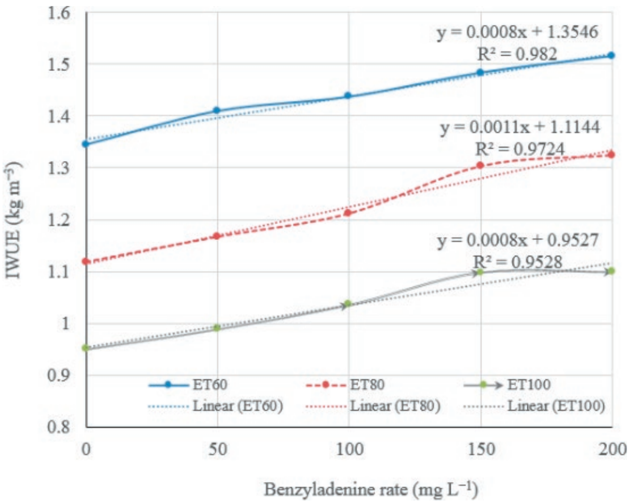

Fig. 2. Regression relationship between irrigation water use efficiency (IWUE) of soybean and benzyladenine rates under different irrigation levels. Note: ET_{60}, ET_{80}, and ET_{100}: irrigation level at 60, 80 and 100% of crop evapotranspiration, respectively.

DISCUSSION

As well known, supplying plants by water amounts less than required almost caused disorders in plant growth and development. Findings of the current research confirmed that reducing irrigation water by 40% in soybean mightily caused reduction in growth traits. Accordingly, irrigating soybean by 60% of crop evapotranspiration (ET_{60}) caused reductions (averages of the two seasons) could be amounted to 11.8% for plant height, 7.8% for SPAD value, 10.3% for RGR and 8.4% for NAR (Table 4). These results might be ascribed to that water stress causes changing in patterns of plant growth and development (Ouda et al. 2010) and disturbance of metabolites transportation within plant (Tayel and Sabreen, 2011). Also, subjecting plants to water amount less than needed may caused reduction in accumulation of assimilates in seeds leading to decreases in yield traits (Table 6). In this respect, De Souza et al. (1997) reported that water stress shortened the seed–filling period resulting 32 and 44% reductions in seed size and seed yield, respectively. Soybean plants exposed to water stress were characterized by significant decline in photosynthetic rate, stomatal conductance and transpiration rate (Ohashi et al. 2006). Excessive energy in reaction center of photosynthesis apparatus (PSII or PSI) can cause pigment bleaching in sun leaves, as well as can induce photoinhibition, thereby damaging pigments through oxidative stress (Kim et al. 2011; El-Metwally and Saudy 2021). Moreover, plants subjected to drought exhibit large reductions in relative water content of leaves (RWC) and water potential (Dekov et al. 2001; Nayyar and Gupta 2006), leading to dehydration of plant tissue as a result of high light intensity and soil water deficit (Nicolás et al. 2005). Additionally, Zhang et al. (2016) reported that stomata are sensitive to RWC and tend to close with decreasing RWC, which can result in lower stomatal conductance levels in drought–exposed plants. Stomatal closure primarily causes a decline in the photosynthesis rate (Mahajan and Tuteja 2005). Recent studies confirmed the adverse impacts of drought on crop growth and yields (Saudy and El-Metwally 2019; Saudy et al. 2020; Mubarak et al 2021; Saudy et al. 2021). Contrariwise, supplying soybean plants with adequate water requirement might enhance the plant to absorb a larger quantity of nutrients, which leads to increased vegetative growth of plants and increase the plant›s ability to intercept the radiation, hence increase the rate of photosynthesis (Tayel and Sabreen 2011, Gkaswa et al. 2014). Accordingly, yield and its attributes of soybean were enhanced by applying ET_{100} followed by ET_{80} (Table 6). Furthermore, the differences between ET_{100} and ET_{80} were slight and did not exceed 5.1% for pods number plant^{-1}, 9.6% for seed weight plant^{-1}, 5.4% for seed yield ha^{-1}, 4.6% for oil % and 3.3% for protein % (averages of the two seasons).

Motivational effect of benzyladenine toward growth and yield of soybean was more evident with elevating its concentration up to BA_{200} or BA_{150}, improving the performances (Tables 4 and 6). In this regard, BA plays a great role in cell division and cell differentiation, senescence, photosynthetic pigment (Sarwat and EL–Sherif 2007). Plant growth regulators can enhance the source–sink ratio and catalyze the translocation of photosynthesis assimilates, thereby helping in efficacious flower genesis, fruit and seed development and eventually boost crop productivity. Photosynthetic potentiality and effective partitioning of accumulated substances from source to sink were improved because of growth regulators application (Solamani et al. 2001). A correlation between endogenous levels of cytokinins and the degree of flower abortion and set was reported by Nooden et al. (1990). It is noted that cytokinins regulate flower and pod development in soybean, thus application of exogenous benzyladenine (individual of cytokinins) has been shown to prevent abortion of flowers and/or pods (Reese et al., 1995). The positive effect of benzyladenine spraying may be due to ability to adjust several biological processes owing their ability to influence almost all plant development and growth stages (Plihalova et al. 2016). benzyladenine substantially induced accumulation of total N and protein synthesis (Taiz and Zeiger 2006; Ayad and Gamal El–Din 2011).

Despite soybean plants differentiate plentiful floral buds, most of them fail to grow into pods and abort during development. Remarkable abortion of flowers and pods commonly occurs in soybean (Abernethy et al. 1997). Such phenomenon is exactly induced with presence of water stress. Seed abortion began earlier in stressed plants and the duration of the maturation period was significantly reduced, leading to accelerated senescence (Desclaux and Roumet 1996). Because of impairment of ovule function as result of water deficit, soybean flowers aborted (Kokubun et al. 2001). By examining the data in Tables 5 and 7, we can obtain that ET_{100} x BA_0 interaction (farmer common practice) is more effective for enhancing crop growth and yield traits than ET_{80} x BA_0 one. However, the values of plant height, NAR, pods number plant^{-1} and seed yield ha^{-1} due to ET_{80} x BA_{200} or BA_{150} treatments were higher than those of produced with common practice (ET_{100} x BA_0). Such finding refers to the beneficial impact of benzyladenine under low water supply conditions. Sharma and Walia (1996) reported that BA may be involved in the development of leaves and branches in plants under adverse conditions such as low drought. Exogenous application of plant hormones i.e. 6-benzyladenine (individual of cytokinins) have been used to improve vegetative growth and yields by foliar applications (Basuchaudhuri 2016). The improvements in plant growth under water stress as a result of benzyladenine application could be attributed to its importance for inducing the antioxidant compounds in treated plants. The application of cytokinins could raise the antioxidants such as phenolics and flavonoids levels (Rahneshan et al. 2018). The potential high antioxidant capacity in plants treated by BA was attributed to the high amounts of phenolics (Mangena 2020). Phenolics are highly potent antioxidants and free-radical scavengers owing to their capacity as strong reducing agents (Chandra et al. 2014). Similar result was obtained by Hassanein et al. (2005) and Ahmed et al. (2016).

Calculation of IWUE confirmed the beneficial effect of benzyladenine under severe stress, moderate stress or well–watered circumstance (Fig. 1), since its application regulate the ratio of soybean seed yield to applied water. In this situation, the increase in IWUE associated increasing benzyladenine rates refers to better exploiting each water drop to produce dry biomass. By comparing the efficiency of benzyladenine under different irrigation regimes, regression analysis (Fig. 2) forecasted that the more the rate of benzyladenine increases by one unit the more the IWUE increases by 0.0008, 0.0011 and 0.0008 units with ET_{60} ET_{80} ET_{100}, respectively. From R^2 value of each, it is noticed that the importance of benzyladenine is more evident in exhibiting changes in IWUE under severe stress (ET_{60}), since 98.2 % of these changes occurred. Accordingly, application of benzyladenine at a rate of 150 or 200 mg^{-1} is so useful under moderate water supply.

CONCLUSION

Our findings proved that benzyladenine had the potentiality to enhance crop growth and yield under severe drought (ET_{60}), moderate drought (ET_{80}) and non drought (ET_{100}) conditions. Moreover, the values of plant height, net assimilation rate, pods number plant^{-1} and seed yield ha^{-1} obtained with ET_{80} x BA_{200} or BA_{150} treatments were higher than those of produced with common farmers practice (ET_{100} x BA_0). As well, the reduction in seed yield due to lowering water supply by 20% (moderate drought) can be compensated using benzyladenine, 150 mg L^{-1}. Thus, benzyladenine should be involved in the various irrigation programs of soybean. Also, even if there is more available water in the area, farmers are exhorted to use moderately water–stressed plus benzyladenine pattern viz ET_{80} x BA_{150} treatment with saving 20% of irrigation water quantity which can be exploited for irrigating other lands. Hence, the treatment of ET_{80} x BA_{150} may consider an auspicious practice under areas suffering from water shortage for soybean crop production. However, several studies should be implemented to confirm the potency of benzyladenine in altering the physiological/biochemical response involving complex and variable metabolic pathways forming different metabolites in soybean.

ACKNOWLEDGEMENTS

Technical supports provided by the Faculty of Agriculture, Ain Shams University and National Research Centre, Egypt are acknowledged.

AUTHOR CONTRIBUTIONS

Conception and design of the study: Ibrahim Mohamed El–Metwally and Hani Saber Saudy. Acquisition of data for the study: Ibrahim Mohamed El–Metwally and Magdi Tawfik Abdelhamid. Analysis of data for the work: Hani Saber Saudy. Interpretation of data for the work: Ibrahim Mohamed El–Metwally and Magdi Tawfik Abdelhamid. Manuscript revision and approval: Ibrahim Mohamed El–Metwally, Magdi Tawfik Abdelhamid and Hani Saber Saudy.

REFERENCES

Abernethy R, Palmer, RG, Shibles RM, Anderson IC. 1997. Histological observations on abscising and retained soybean flowers. Cana. J Plant Sci. 57:713–716.

Ahmed MA, Bakhoum Gehan Sh, EL–Housini Ebtesam A, Badr Elham A. 2016. Alleviation of water stress on wheat by Benzyl adenine. Inter J PharmTech Res. 9:109–119.

Allen RG, Pereira LS, Raes D, Smith M. 1998. Crop evapotranspiration–guidelines for computing crop water requirements–FAO irrigation and drainage paper 56, Rome, Italy.

AOAC 2012. Official Method of Analysis: Association of Analytical Chemists. 19th Edition, Washington DC, USA.

Ayad HS, Gamal EL–Din, KM. 2011. Effect of atomic and Benzyl adenine on growth and some biochemical constituents of Lupine plant (*Lupinns termis* L). Amer–Euras J Agric Environ Sci. 10:519–524.

Basuchaudhuri P. 2016. Influences of plant growth regulators on yield of soybean. Ind J Plant Sci. 5:25–38.

Borges LP, Torres Junior HD, Neves TG, Cruvinel CKL, Santos PGF, Matos FS. 2014. Does benzyladenine application increase soybean productivity? Afr J Agric Res. 9:2799–2804.

Casella G (2008) Statistical Design. 1st ed. Springer, Gainesville, FL 32611–8545, USA.

Chandra S, Khan S, Avula B, Lata H, Yang MH, ElSohly MA, Khan IA. 2014. Assessment of total phenolic and flavonoid content, antioxidant properties, and yield of aeroponically and conventionally grown leafy vegetables and fruit crops: a comparative study. Evidence-Based Complem Alter Med. Article ID 253875, 9p. https://doi.org/10.1155/2014/253875

De Souza PI, Egli DB, Bruening WP. 1997. Water stress during seed filling and leaf senescence in soybean. Agron J. 89:807–812.

Dekov I, Tsonev T, Yordanov I. 2001. Effects of water stress and high–temperature stress on the structure and activity of photosynthetic apparatus of *Zea mays* and *Helianthus annuus*. Photosynth. 38:361–366.

Desclaux D, Roumet P. 1996. Impact of drought stress on the phenology of two soybean (*Glycine max* L. Merr) cultivars. Field Crops Res. 46:61–70.

Dogan E, Kirnak H, Copur O. 2007. Deficit irrigation during soybean reproductive stages and CRPGRO–soybean simulations under semi–arid climatic conditions. Field Crops Res. 103:154–159.

Draper NR, Smith H. 1998. Applied Regression Analysis, 3rd Ed. John Wiley & Sons, New York.

El–Bially MA, Saudy HS, El–Metwally IM, Shahin MG. 2018. Efficacy of ascorbic acid as a cofactor for alleviating water deficit impacts and enhancing sunflower yield and irrigation water–use efficiency. Agric Water Manage. 208: 132–139.

El-Metwally IM, Geries L, Saudy HS. 2021. Interactive effect of soil mulching and irrigation regime on yield, irrigation water use efficiency and weeds of trickle-irrigated onion. Archiv Agron Soil Sci <https://doi.org/10.1080/03650340.2020.1869723>

El-Metwally IM, Saudy HS. 2021. Interactional impacts of drought and weed stresses on nutritional status of seeds and water use efficiency of peanut plants grown in arid conditions. Gesunde Pflanzen 73:407-416 <https://doi.org/10.1007/s10343-021-00557-3>

Gkaswa SL, Dubey RK, Singh S, Tiwari RC. 2014. Growth, product and quality of soybean (*Glycine max* L.) under different levels and sources of phosphorus and plant growth regulators in sub humid Rajasthan. Afr J Agric Res. 9:1045–1051.

Hassanein RA, Khattab HKI, EL–Bassiouny HMS, Sadak MS. 2005. Increasing the active constituents of sepals of roselle (*Hibiscus sabdariffa* L.) plant by applying gibberellic acid and benzyladenine. J App Sci Res. 1:137–146.

Hunt R. 1982. Plant growth curves: The functional approach to plant growth analysis. London, Edward Arnold, p:14–46.

Keller J, Bliesner RD. 1990. Sprinkle and Trickle Irrigation. AVI Book. Van Nostrand Reinhold, New York.

Khaswa SL, Dubey RK, Singh S, Tiwari RC. 2014. Growth, productivity and quality of soybean (*Glycine max* (L.) Merr.) under different levels and sources of phosphorus and plant growth regulators in Subhumid Rajasthan. Afr J Agric Res. 9:1045–1051.

Kim SJ, Yu DJ, Kim TC, Lee HJ. 2011. Growth and photosynthetic characteristics of blueberry (*Vaccinium corymbosum* cv. Bluecrop) under various shade levels. Scientia Hort. 129:486–492.

Kokubun M, Shimada S, Takahashi M. 2001. Flower abortion caused by preanthesis water deficit is not attributed to impairment of pollen in soybean. Crop Sci. 41:1517–1521.

Mahajan S, Tuteja N. 2005. Cold, salinity and drought stresses: an overview. Arch Biochem Biophysics. 444:139–158.

Mangena P. 2020. Role of Benzyladenine Seed Priming on Growth and Physiological and Biochemical Response of Soybean Plants Grown under High Salinity Stress Condition. Int J Agron. Article ID 8847098, 5p. https://doi.org/10.1155/2020/8847098

Minolta. 1989. Chlorophyll meter SPAD–502. Instruction manual. Osaka: Minolta Co., Ltd., Radiometric Instruments Operations.

Mubarak M, Salem EMM, Kenawey MKM, Saudy HS. 2021. Changes in calcareous soil activity, nutrient availability, and corn productivity due to the integrated effect of straw mulch and irrigation regimes. J Soil Sci Plant Nutr 21:2020-2031. <https://doi.org/10.1007/s42729-021-00498-w>

Nakagawa ACS, Ario N, Tomita Y, Tanaka S, Murayama N, Mizuta C, Iwaya-Inoue M, Ishibashi Y 2020. High temperature during soybean seed development differentially alters lipid and protein metabolism, Plant Prod Sci. 23:504–512. DOI: 10.1080/1343943X.2020.1742581

Nayyar H, Gupta D. 2006. Differential sensitivity of C3 and C4 plants to water deficit stress: association with oxidative stress and antioxidants. Environ Exp Bot. 58:106–113.

Nicolás E, Torrecillas A, DellAmico J, Alarcón JJ. 2005. Sap flow, gas exchange, and hydraulic conductance of young apricot trees growing under a shading net and different water supplies. J Plant Physiol. 162:439–447.

Nooden ID, Santo KRS, Letham DS. 1990. Correlation of xylem sap cytokinin levels with monocarpic senescence in soybean. Plant Physiol. 93:33–39.

Ohashi Y, Nakayama N, Saneoka H, Fujita K. 2006. Effects of drought stress on photosynthetic gas exchange, chlorophyll fluorescence and stem diameter of soybean plants. Biol Planta. 50:138–141.

Ouda SA, Shreif MA, Abou Elenin R. 2010. Increasing water productivity of faba bean grown under deficit irrigation at middle Egypt. Fourteenth International Water Technology Conference, IWTC 14, Cairo, Egypt. pp:45–55.

Oweis T, Hachum AY. 2003. Improving water productivity in the dry areas of west Asia and North Africa. In KIJNE, J.W. BARKER, R. MOLDEN, D. (Eds.) Water productivity in agriculture: limits and opportunities for improvement. CAB International. pp:179–198.

Plihalova L, Vylicilova H, Dolezal K, Zahajska L, Zatloukal M, Strand M. 2016. Synthesis of aromatic cytokinins for plant biotechnology. New Tech. 33:614–624.

Rademacher W. 2015. Plant growth regulators: Backgrounds and uses in plant production. J Plant Growth Regul. 34:845–872.

Rahneshan Z, Nasibi F, Moghadam AA. 2018. Effects of salinity stress on some growth, physiological, biochemical parameters and nutrients in two pistachio (*Pistacia vera* L.) rootstocks. J Plant Interac. 13:73–82.

Reese RN, Dybing CD, White CA, Page SM, Larson JE. 1995. Expression of vegetative storage protein (VSP–β) in soybean raceme tissues in response to flower set. J Exp Bot. 46:957–964.

Reisdorph NA, Koster KI. 1999. Progressive loss of desiccation tolerance in germinating pea (*Pisum sativum*) seeds. Physiol Planta 105:266–271.

Sarwat MI, EL–Sherif MH. 2007. Increasing salt tolerance in some barley genotypes (*Hordeum vulgare*) by using kinetin and benzyl adenine. World J Agric Sci. 3:617–629.

Salem EMM, Kenawey MKM., Saudy HS, Mubarak M. 2021. Soil mulching and deficit irrigation effect on sustainability of nutrients availability and uptake, and productivity of maize grown in calcareous soils. Comm Soil Sci Plant Anal 52:1745-1761. <https://doi.org/10.1080/00103624.2021.1892733>

Saudy HS, El-Bially M, El-Metwally IM, Shahin MG. 2021. Physio-biochemical and agronomic response of ascorbic acid treated sunflower (Helianthus Annuus) grown at different sowing dates and under various irrigation regimes. Gesunde Pflanzen 73:169-179. <https://doi.org/10.1007/s10343-020-00535-1>

Saudy HS, El‑Metwally IM, Abd El‑Samad GA. 2020. Physio–biochemical and nutrient constituents of peanut plants under bentazone herbicide for broad–leaved weed control and water regimes in dry land areas. J Arid Land 12:630‑639. https://doi.org/10.1007/s40333–020–0020-y

Saudy HS, El‑Metwally IM. 2019. Nutrient utilization indices of NPK and drought management in groundnut under sandy soil conditions. Comm Soil Sci Plant Anal 50:1821‑1828. https://doi.org/10.1080/00103624.2019.1635147

Sharma K, Walia N. 1996. Growth and yield of soybean (*Glycine max* (L.) Merr.) as influenced by light and cytokinin. Environ Ecol. 14:307–310.

Sheteiwy MS, Ali DFI., Xiong YC, Brestic M, Skalicky M, Hamoud YA, Ulhassan Z, Shaghaleh H, AbdElgawad H, Farooq M, Sharma A, El-Sawah AM 2021. Physiological and biochemical responses of soybean plants inoculated with Arbuscular mycorrhizal fungi and *Bradyrhizobium* under drought stress. BMC Plant Biol **21,** 195. https://doi.org/10.1186/s12870-021-02949-z

Soares LH, Dourado Neto D, Fagan EB, Teixeira VF, Pereira IS. 2017. Physiological, phenometric and productive changes in soybean crop due to the use of kinetin. Pesquisa Agro Trop. 47:80–86.

Sofo A, Dichio B, Montanaro G, Xiloyannis C. 2009. Shade effect on photosynthesis and photoinhibition in olive during drought and rewatering. Agric Water Manage. 96:1201–1206.

Solamani A, Sivakumar C, Anbumani S, Suresh T, Arumugam K. 2001. Role of plant growth regulators on rice production: A Review. Agric Rev. 23:33–40.

Taiz L, Zeiger E. 2006. Plants physiology, 4th Ed. Sinauer Associates Inc. Publishers, Sunder land, Massachusetts, USA.

Tayel MY, Sabreen KhP. 2011. Effect of irrigation regimes and phosphorus level on two *Vica faba* varieties: 1– Growth characters. J App Sci Res. 7:1007–1015.

Tian X, Zhang K, Liu S, Sun X, Li X, Song J, Qi Z, Wang Y, Fang Y, Wang J, Jiang S, Yang C, Tian Z, Li W–X, Ning H 2020. Quantitative trait locus analysis of protein and oil content in response to planting density in soybean (*Glycine max* (L.) Merri.) seeds based on SNP linkage mapping. Front Genet. 11:563. doi: 10.3389/fgene.2020.00563

Wei Y, Jin J, Jiang S, Ning S, Liu L. 2018. Quantitative response of soybean development and yield to drought stress during different growth stages in the Huaibei Plain, China. Agron 8:97.

Yeh S, Chen H, Ng C, Lin C, Tseng T, Li W, Ku, MSB. 2015. Down–regulation of cytokinin oxidase 2 expression increases tiller number and improves rice yield. Rice. 8:1–13.

Zhang J, Liu J, Yang C, Du S, Yang W 2016. Photosynthetic performance of soybean plants to water deficit under high and low light intensity. South Afr J Bot 105:279–287.

Finito di stampare da
Logo s.r.l. – Borgoricco (PD) – Italia

RIGOROUS PEER REVIEW
Each submission to IJAm is subject to a rigorous quality control and peer-review evaluation process before receiving a decision. The initial in-house quality control check deals with issues such as competing interests; ethical requirements for studies involving human participants or animals; financial disclosures; full compliance with IJAm's data availability policy, etc.
Submissions may be returned to authors for queries, and will not be seen by our Editorial Board or peer reviewers until they pass this quality control check.
Each paper is subjected to critical evaluation and review by Field Editors with specific expertise in the different areas of interest and by the members of the international Editorial Board.

OPEN ACCESS POLICY
The Italian Journal of Agrometeorology provides immediate open access to its content. Our publisher, Firenze University Press at the University of Florence, complies with the Budapest Open Access Initiative definition of Open Access: By "open access", we mean the free availability on the public internet, the permission for all users to read, download, copy, distribute, print, search, or link to the full text of the articles, crawl them for indexing, pass them as data to software, or use them for any other lawful purpose, without financial, legal, or technical barriers other than those inseparable from gaining access to the internet itself. The only constraint on reproduction and distribution, and the only role for copyright in this domain is to guarantee the original authors with control over the integrity of their work and the right to be properly acknowledged and cited. We support a greater global exchange of knowledge by making the research published in our journal open to the public and reusable under the terms of a Creative Commons Attribution 4.0 International Public License (CC-BY-4.0). Furthermore, we encourage authors to post their pre-publication manuscript in institutional repositories or on their websites prior to and during the submission process and to post the Publisher's final formatted PDF version after publication without embargo. These practices benefit authors with productive exchanges as well as earlier and greater citation of published work.

COPYRIGHT NOTICE
Authors who publish with IJAm agree to the following terms:
Authors retain the copyright and grant the journal right of first publication with the work simultaneously licensed under a Creative Commons Attribution 4.0 International Public License (CC-BY-4.0) that allows others to share the work with an acknowledgment of the work's authorship and initial publication in IJAm.
Authors are able to enter into separate, additional contractual arrangements for the non-exclusive distribution of the journal's published version of the work (e.g., post it to an institutional repository or publish it in a book), with an acknowledgment of its initial publication in this journal.
Authors are allowed and encouraged to post their work online (e.g., in institutional repositories or on their website) prior to and during the submission process, as it can lead to productive exchanges, as well as earlier and greater citation of published work (See The Effect of Open Access).

PUBLICATION FEES
Unlike many open-access journals, the Italian Journal of Agrometeorology does not charge any publication fee.

WAIVER INFORMATION
Fee waivers do not apply at Firenze University Press because our funding does not rely on author charges.

PUBLICATION ETHICS
Responsibilities of IJAm's editors, reviewers, and authors concerning publication ethics and publication malpractice are described in IJAm's Guidelines on Publication Ethics.

CORRECTIONS AND RETRACTIONS
In accordance with the generally accepted standards of scholarly publishing, IJAm does not alter articles after publication: "Articles that have been published should remain extant, exact and unaltered to the maximum extent possible". In cases of serious errors or (suspected) misconduct IJAm publishes corrections and retractions (expressions of concern).

Corrections
In cases of serious errors that affect or significantly impair the reader's understanding or evaluation of the article, IJAm publishes a correction note that is linked to the published article. The published article will be left unchanged.

Retractions
In accordance with the "Retraction Guidelines" by the Committee on Publication Ethics (COPE) IJAm will retract a published article if:
- there is clear evidence that the findings are unreliable, either as a result of misconduct (e.g. data fabrication) or honest error (e.g. miscalculation)
- the findings have previously been published elsewhere without proper crossreferencing, permission or justification (i.e. cases of redundant publication)
- it turns out to be an act of plagiarism
- it reports unethical research.
- An article is retracted by publishing a retraction notice that is linked to or replaces the retracted article. IJAm will make any effort to clearly identify a retracted article as such.

If an investigation is underway that might result in the retraction of an article IJAm may choose to alert readers by publishing an expression of concern.

ARCHIVING
IJAm and Firenze University Press are experimenting a National legal deposition and long-term digital preservation service.

SUBMITTING TO IJAm
Submissions to IJAm are made using FUP website. Registration and access are available at: https://riviste.fupress.net/index.php/IJAm/submission
For more information about the journal and guidance on how to submit, please see https://riviste.fupress.net/index.php/IJAm/index

Principal Contact
Simone Orlandini, University of Florence
simone.orlandini@unifi.it

Support Contact
Alessandro Pierno, Firenze University Press
alessandro.pierno@unifi.it

GUIDE FOR AUTHORS
1. Manuscript should refer to original researches, not yet published except in strictly preliminary form.
2. Articles of original researches findings are published in Italian Journal of Agrometeorology (IJAm), subsequent to critical review and approval by the Editorial Board. External referees could be engaged for particular topics.
3. Three types of paper can be submitted: original paper, review, technical note. Manuscript must be written in English. All pages and lines of the manuscript should be numbered.
4. First Name, Last Name, position, affiliation, mail address, telephone and fax number of all the Co-Authors are required. Corresponding Authors should be clearly identified.
5. The abstract should be no longer than 12 typed lines.
6. Full stop, not comma, must be used as decimal mark (e.g. 4.33 and not 4,33).
7. Figures, tables, graphs, photos and relative captions should be attached in separate files. All images must be vector or at least 300 effective ppi/dpi to ensure quality reproduction.
8. Captions should be written as: Fig. x – Caption title, Tab. x – Caption title. Images should be referred to in the text as (Fig. x), (Tab. x).
9. Proof of the paper (formatted according to the Journal style) will be sent to the Corresponding Author for proof reading just one time. Corrections can be made only to typographical errors.
10. All the references in the text must be reported in the "References" section and vice-versa. In the text, only the Author(s) last name must be present, without the name or the first letter of the name (e.g. "Rossi, 2003" and not "Federico Rossi, 2003" or "F. Rossi, 2003"). If two authors are present, refer to them as: "Bianchi and Rossi, 2003" in the text (do not use "&" between the surnames). If more than two Authors are present, refer to them as: "Bianchi et al., 2003" in the text.
For journals, references must be in the following form:
Bianchi R., Colombo B., Ferretti N., 2003. Title. Journal name, number: pages.
For books:
Bianchi R., Colombo B., Ferretti N., 2003. Book title. Publisher, publishing location, total number of pages pp.
Manuscripts "in press" can be cited.

BECOME A REVIEWER
Peer review is an integral part of the scholarly publishing process. By registering as a reviewer, you are supporting the academic community by providing constructive feedback on new research, helping to ensure both the quality and integrity of published work in your field. Once registered, you may be asked to undertake reviews of scholarly articles that match your research interests. Reviewers always have the option to decline an invitation to review and we take care not to overburden our reviewers with excessive requests.
You must login before you can become a reviewer.
If you don't want to be a reviewer anymore, you can change your roles by editing your profile.

COMPETING INTERESTS
You should not accept a review assignment if you have a potential competing interest, including the following:
- Prior or current collaborations with the author(s)
- You are a direct competitor
- You may have a known history of antipathy with the author(s)
- You might profit financially from the work

Please inform the editors or journal staff and recuse yourself if you feel that you are unable to offer an impartial review.
When submitting your review, you must indicate whether or not you have any competing interests.

Italian Journal of Agrometeorology

Rivista Italiana di Agrometeorologia

n. 2 – 2021

Table of contents

Abayomi Eruola
Response of yam varieties to soil moisture regime in Southwestern Nigeria 3

Emre Topçu
Testing of Drought Exceedance Probability Index (DEPI) for Turkey using PERSIANN data for 2000-2021 period 15

Boutheina Douh, Amel Mguidiche, Massoud Jar Allah al-Marri, Mohamed Moussa, Hichem Rjeb
Assessment of deficit irrigation impact on agronomic parameters and water use efficiency of six chickpea (*Cicer Arietinum* L.) cultivars under Mediterranean semi-arid climate 29

Habibioallah Farrokhi, Ahmad Asgharzadeh, Malihe Kazemi Samadi
Yield and qualitative and biochemical characteristics of saffron (*Crocus sativus* L.) cultivated in different soil, water, and climate conditions 43

Iride Volpi, Diego Guidotti, Michele Mammini, Susanna Marchi
Predicting symptoms of downy mildew, powdery mildew, and gray mold diseases of grapevine through machine learning 57

Roman Bohovic, Petr Hlavinka, Martin Možný, Daniela Semerádová, Jan Bálek, Miroslav Trnka
Earth observation method for an operational assessment of crop phenology metric "start of the season" 71

Ibrahim Mohamed El–Metwally, Hani Saber Saudy, Magdi Tawfik Abdelhamid
Efficacy of benzyladenine for compensating the reduction in soybean productivity under low water supply 81